

UNCLASSIFIED

AD NUMBER
AD852998
NEW LIMITATION CHANGE
TO Approved for public release, distribution unlimited
FROM Distribution authorized to U.S. Gov't. agencies and their contractors; Administrative/Operational Use; Apr 1969. Other requests shall be referred to Director, Air Force Aero Propulsion Laboratory, Wright-Patterson AFB, OH 45433.
AUTHORITY
AFRPL ltr, 21 Sep 1971

THIS PAGE IS UNCLASSIFIED

AFAPL-TR-65-45

Part VIII



1.8

AD852998

ROTOR-BEARING DYNAMICS DESIGN TECHNOLOGY

Part VIII: Spiral Grooved Floating Ring Journal Bearing

J. Vohr
C. Chow

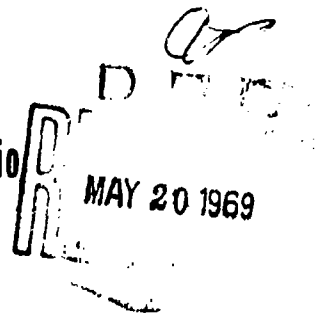
Mechanical Technology Incorporated

TECHNICAL REPORT AFAPL-TR-65-45, PART VIII

April 1969

This document is subject to special export controls and each transmittal to foreign governments or foreign national may be made only with prior approval of the Air Force Aero Propulsion Laboratory (APFL), Wright-Patterson Air Force Base, Ohio 45433.

Air Force Aero Propulsion Laboratory
Air Force Systems Command
Wright-Patterson Air Force Base, Ohio



AFAPL-TR-65-45

Part VIII

①

ROTOR-BEARING DYNAMICS DESIGN TECHNOLOGY

Part VIII: Spiral Grooved Floating Ring Journal Bearing

AD852998

J. Vohr
C. Chow

Mechanical Technology Incorporated

TECHNICAL REPORT AFAPL-TR-65-45, PART VIII

April 1969

This document is subject to special export controls and each transmittal to foreign governments or foreign national may be made only with prior approval of the Air Force Aero Propulsion Laboratory (APPL), Wright-Patterson Air Force Base, Ohio 45433.

Air Force Aero Propulsion Laboratory
Air Force Systems Command
Wright-Patterson Air Force Base, Ohio

MAY 20 1969

Best Available Copy

184

NOTICE

When Government drawings, specifications, or other data are used for any purpose other than in connection with a definitely related Government procurement operation the United States Government thereby incurs no responsibility nor any obligation whatsoever; and the fact that the Government may have formulated, furnished, or in any way supplied the said drawings, specifications, or other data, is not to be regarded by implication or otherwise as in any manner licensing the holder or any other person or corporation, or conveying any rights or permission to manufacture, use, or sell any patented invention that may in any way be related thereto.

ACCESSION NO.	
CFSTI	WHITE SECTION <input type="checkbox"/>
DDC	DIFF SECTION <input checked="" type="checkbox"/>
UNANNOUNCED	<input type="checkbox"/>
JUSTIFICATION	
BY	
DISTRIBUTION/AVAILABILITY CODES	
DIST.	AVAIL. AND OF SPECIAL
2	

Copies of this report should not be returned unless return is required by security considerations, contractual obligations, or notice on a specific document.

AFAPL-TR-65-45

Part VIII

ROTOR-BEARING DYNAMICS DESIGN TECHNOLOGY

Part VIII: Spiral Grooved Floating Ring Journal Bearing

**J. Vehr
C. Chow**

Mechanical Technology Incorporated

TECHNICAL REPORT AFAPL-TR-65-45, PART VIII

April 1969

This document is subject to special export controls and each transmittal to foreign governments or foreign national may be made only with prior approval of the Air Force Aero Propulsion Laboratory (APFL), Wright-Patterson Air Force Base, Ohio 45433.

**Air Force Aero Propulsion Laboratory
Air Force Systems Command
Wright-Patterson Air Force Base, Ohio**

FOREWORD

This report was prepared by Mechanical Technology Incorporated, 968 Albany-Shaker Road, Latham, New York 12110 under USAF Contract No. AF33(615)-3238. The contract was initiated under Project No. 3048, Task No. 304806. The work was administered under the direction of the Air Force Aero Propulsion Laboratory, with Mr. Michael R. Chasman (APFL) acting as project engineer.

This report covers work conducted from 1 May 1967 to 1 May 1968.

This report was submitted 31 July 1968. This report is Part VIII of final documentation issued in multiple parts.

This technical report has been reviewed and is approved.

Arthur V. Churchill
ARTHUR V. CHURCHILL, Chief

Fuels, Lubrication and Hazards Branch
Support Technology Division
Air Force Aero Propulsion Laboratory

ABSTRACT

In this volume is presented an analysis of the static and dynamic characteristics of the spiral-grooved journal bearing operating with incompressible lubricant in both laminar and turbulent regimes. Both single film and floating ring bearing configurations are considered. Extensive design data are presented giving load capacity, attitude angle, bearing torque, bearing flow rate, stiffness and damping coefficients and critical rotor mass for limit of stable operation. In addition, two computer programs accompany the volume, and instructions and listings of the programs are included. These programs may be used to obtain data for cases not covered by the presented design data.

This abstract is subject to special export controls and each transmittal to foreign governments or foreign nationals may be made only with prior approval of the Air Force Aero Propulsion Laboratory (APFL), Wright-Patterson Air Force Base, Ohio 45433.

TABLE OF CONTENTS

	<u>Page</u>
INTRODUCTION	1
DESCRIPTION OF SINGLE FILM AND FLOATING-RING SPIRAL GROOVED JOURNAL BEARINGS.....	3
ANALYSIS	7
RESULTS	27
SUMMARY AND CONCLUSIONS	39
TABLES	41
ILLUSTRATIONS	47
APPENDIX I: Derivation and Solution of Equation for Turbulent Spiral-Grooved Journal Bearing	89
APPENDIX II: Derivation of Relationships for Calculating Stiffness and Damping Coefficients	101
APPENDIX III: Computer Program PN 412 Performance of a Herringbone Journal Bearing Operated in the Turbulent Regime	107
APPENDIX IV: Computer Program PN 406 Static Performance of a Spiral-Grooved, Floating Ring Journal Bearing Operated in the Turbulent Regime ...	131
REFERENCES	175

ILLUSTRATIONS

<u>Figure</u>		<u>Page</u>
1	Schematic of Spiral-Grooved Journal Bearing -----	47
2	Various Configurations of Spiral-Grooved Journal Bearings -----	48
3	Coordinate System for Forces and Displacements -----	49
4	Geometry of Floating Ring Bearing -----	50
5	G_x and G_z vs. Local Reynolds Number R_h -----	51
6	Coefficient of Friction vs. Local Reynolds Number R_h -----	52
7	Load vs. Eccentricity, Single Film Bearing -----	53
8	Load vs. Eccentricity, Single Film Bearing -----	54
9	Load vs. Eccentricity, Single Film Bearing -----	55
10	Load vs. Eccentricity, Effect of Pressurization -----	56
11	Attitude Angle vs. Eccentricity, Single Film Bearing -----	57
12	Attitude Angle vs. Eccentricity, Single Film Bearing -----	58
13	Attitude Angle vs. Eccentricity, Single Film Bearing -----	59
14	Single Film Bearing Flow Due to Self Pumping Effect of Spiral Grooves -----	60
15	Single Film Bearing Flow Due to Pressurized Supply -----	61
16	Torque vs. Eccentricity, Single Film Bearing -----	62
17	Torque vs. Eccentricity, Single Film Bearing -----	63
18	Torque to Load Ratio vs. Reynolds Number, Single Film Bearing ----	64
19	Load vs. Inner Film Eccentricity Ratio, Floating Ring Bearing ----	65
20	Attitude Angle vs. Inner Film Eccentricity Ratio, Floating Ring Bearing -----	66
21	Attitude Angle vs. Inner Film Eccentricity Ratio, Floating Ring Bearing -----	67
22	Torque to Load Ratio vs. Inner Film Eccentricity, Floating Ring Bearing -----	68

Illustrations (Continued)

<u>Figure</u>		<u>Page</u>
23	Torque to Load Ratio, Comparison between Single Film and Floating Ring Bearing	69
24	Floating Ring Bearing Flow Due to Self-Pumping Effect of Spiral Grooves	70
25	Ring Speed Ratio vs. Inner Film Eccentricity Ratio, Floating Ring Bearing	71
26	Outer Film Eccentricity Ratio vs. Inner Film Eccentricity Ratio, Floating Ring Bearing	72
27	Stiffness Coefficients, Floating Ring Bearing	73
28	Damping Coefficients, Floating Ring Bearing	74
29	Stiffness Coefficients, Floating Ring Bearing	75
30	Damping Coefficients, Floating Ring Bearing	76
31	Stiffness Coefficients, Floating Ring Bearing	77
32	Damping Coefficients, Floating Ring Bearing	78
33	Critical Journal Mass, Floating Ring Bearing	79
34	Critical Journal Mass, Floating Ring Bearing	80
35	Critical Journal Mass, Comparison between Plain and Spiral-Grooved Floating Ring Bearings	81
36	Critical Journal Mass, Comparison between Plain and Spiral-Grooved Floating Ring Bearings	82
37	Critical Journal Mass, Comparison between Single Film and Floating Ring Spiral-Grooved Bearings	83
38	η and ξ Coordinates for Grooved Surface	84
39	Pressure Distribution around Spiral-Grooved Journal Bearing	85
40	Continuity of Mass Flow across Groove-Ridge Interface and Pressure Variation across Groove-Ridge Interface	86
41	Control Volume for Mass Flow Continuity Analysis	87

SYMBOLS

$B_{xx}, B_{xy},$ B_{yx}, B_{yy}	Bearing damping coefficients, lb-sec/in.
$\bar{B}_{xx}, \bar{B}_{xy}$ $\bar{B}_{yx}, \bar{B}_{yy}$	Dimensionless damping for overall floating ring bearing, $\bar{B}_{xx} = \frac{B_{xx} C_1}{\mu L D_1} \left(\frac{C_1}{R_1}\right)^2 \text{ etc.}$
$(\bar{B}_{xx})_1, (\bar{B}_{xy})_1$ $(\bar{B}_{yx})_1, (\bar{B}_{yy})_1$	Dimensionless damping for inner film, $(\bar{B}_{xx})_1 = 2\pi \frac{B_{xx1} C_1}{\mu L D_1} \left(\frac{C_1}{R_1}\right)^2 \text{ etc.}$
$(\bar{B}_{xx})_2, (\bar{B}_{xy})_2$ $(\bar{B}_{yx})_2, (\bar{B}_{yy})_2$	Dimensionless damping for outer film, $(\bar{B}_{xx})_2 = \frac{B_{xx2} C_2}{\mu L D_2} \left(\frac{C_2}{R_2}\right)^2 \text{ etc.}$
C	Bearing mean radial clearance, in.
D	Bearing diameter, in.
e	Eccentricity, in.
F_r	Radial component of bearing film force = $W \cos \phi$, lb.
F_t	Tangential component of bearing film force = $W \sin \phi$, lb.
F_x, F_y	Bearing film forces in x and y directions, lb.
\bar{F}_r	Dimensionless radial (cosine) component of bearing film force = $W \cos \phi C^2 / \mu (N_i + N_o) R^4$
\bar{F}_t	Dimensionless tangential (sin) component of bearing film force = $W \sin \phi C^2 / \mu (N_i + N_o) R^4$
G_x, G_z	Turbulent flow correction factors

SYMBOLS (continued)

h	Local film clearance, in.
h _g	Local film clearance in groove region, in.
h _r	Local film clearance in ridge region, in.
h'	Dimensionless clearance = h/C
K _{xx} , K _{xy} , K _{yx} , K _{yy}	Bearing stiffness coefficients, lb/in.
$\bar{K}_{xx}, \bar{K}_{xy},$ $\bar{K}_{yx}, \bar{K}_{yy}$	Dimensionless stiffness for overall floating ring bearing, $\bar{K}_{xx} = \frac{K_{xx} C_1}{\mu N_1 L D_1} \left(\frac{C_1}{R_1}\right)^2 \text{ etc.}$
$(\bar{K}_{xx})_1, (\bar{K}_{xy})_1,$ $(\bar{K}_{yx})_1, (\bar{K}_{yy})_1$	Dimensionless stiffnesses for inner film, $(\bar{K}_{xx})_1 = \frac{K_{xx1} C_1}{\mu (N_1 + N_2) L D_1} \left(\frac{C_1}{R_1}\right)^2 \text{ etc.}$
$(\bar{K}_{xx})_2, (\bar{K}_{xy})_2,$ $(\bar{K}_{yx})_2, (\bar{K}_{yy})_2$	Dimensionless stiffness for outer film, $(\bar{K}_{xx})_2 = \frac{K_{xx2} C_2}{\mu N_2 L D_2} \left(\frac{C_2}{R_2}\right)^2 \text{ etc.}$
L	Bearing length, in.
L ₁	Length of grooved region, in.
M	Shaft mass, lb.
M _c	Critical mass for threshold of whirl instability in floating ring bearing, lb.
M _{c1}	Inner film critical mass.
M _{c2}	Outer film critical mass.

SYMBOLS (continued)

M_r	Radial component of restoring moment, in-lb.
M_t	Tangential component of restoring moment, in-lb.
\bar{M}_c	Dimensionless critical mass = $\frac{M_c N_1 C_1^3}{\mu R_1^2 L D_1}$
\bar{M}_{c1}	Dimensionless critical mass = $\frac{M_{c1} (N_1 + N_2) C_1^3}{\mu R_1^2 L D_1}$
\bar{M}_{c2}	Dimensionless critical mass = $\frac{M_{c2} N_2 C_2^3}{\mu R_2^2 L D_2}$
\bar{M}_r	Dimensionless radial (cosine) component of bearing film force moment = $M_r C^2 / \mu (N_1 + N_o) R^5$
\bar{M}_t	Dimensionless tangential (sin) component of bearing film force moment = $M_t C^2 / \mu (N_1 + N_o) R^5$
m	Ring mass, lb.
N	Speed = $N_1 + N_2$, rps
N_1	Speed of journal, rps
N_2	Ring speed, rps
N_i	Speed of inner member, rps
N_o	Speed of outer member, rps
n	Ring speed ratio = N_2 / N_1
P	Pressure, lb/in ²
P_s	Supply pressure, lb/in ²

SYMBOLS (continued)

\bar{P}	Dimensionless pressure = $PR_1^2/\mu N_1 C_1^2$
\bar{P}	Smoothed, "overall" pressure distribution around spiral grooved journal, lb/in ²
\bar{P}_s	Dimensionless supply pressure = $P_s R_1^2/\mu N_1 C_1^2$
\bar{P}_{s1}	Dimensionless supply pressure, inner film = $P_s R_1^2/\mu(N_1 + N_2)C_1^2$
\bar{P}_{s2}	Dimensionless supply pressure, outer film = $P_s R_2^2/\mu N_2 C_2^2$
Q	Total lubricant flow rate, in ³ /sec.
Q _p	Lubricant flow due to self pumping of spiral grooves, in ³ /sec.
Q _s	Lubricant flow due to pressurization of supply, in ³ /sec.
\bar{Q}	Dimensionless total lubricant flow rate = $Q/k^2 C(N_1 + N_2)$
R	Bearing radius, in.
Re	Overall Reynolds number = $2\pi N_1 R_1 C_1/\nu$
R _h	Local Reynolds number = $2\pi(N_i - N_o)R_h/\nu$
Re ₁	Inner film Reynolds Number = $2\pi\rho(N_o - N_2)R_1 C_1/\mu$
Re ₂	Outer film Reynolds Number = $2\pi\rho N_2 R_2 C_2/\mu$
S	Overall Sommerfeld Number = $\frac{\mu N_1 D_1 L}{W} \left(\frac{R_1}{C_1}\right)^2$
S ₁	Inner film Sommerfeld Number = $\frac{\mu(N_1 + N_2)D_1 L}{W} \left(\frac{R_1}{C_1}\right)^2$
S ₂	Outer film Sommerfeld Number = $\frac{\mu N_2 D_2 L}{W} \left(\frac{R_2}{C_2}\right)^2$
T _B	Bearing torque, in-lb.

SYMBOLS (continued)

T_j	Journal Torque, in-lb.
\bar{T}_B	Dimensionless bearing torque = T_B/WC
\bar{T}_j	Dimensionless journal torque = T_j/WC
t	Time, sec.
U	Surface velocity of bearing, in/sec.
\bar{u}	Mean flow velocity in direction of rotation, in/sec.
\bar{u}_p	Mean flow velocity due to pressure gradient = $\bar{u} - V/2$, in/sec.
V	Surface speed of journal, in/sec.
W	Bearing load, lb.
W_x^E, W_y^E	Mass flow components, lb/(sec-in ²)
\bar{w}	Mean flow velocity in axial direction, in/sec.
x, y	Coordinates in direction of and normal to load vector, in.
\bar{Y}	Ratio of length of grooving to total length of bearing = L_1/L
Z_{xx}, Z_{xy}	Complex dimensionless bearing impedences
Z_{yx}, Z_{yy}	
Z'	Dimensionless Z coordinate = Z/L
<u>Greek</u>	
α	Ratio of groove width to groove plus land width = $a_g/(a_g + a_r)$
β	Groove angle, deg. (radians in equations)
Γ	Ratio of groove clearance to ridge clearance = h_g/h_r
γ	Missalignment angle, deg. (radians in equations)

SYMBOLS (continued)

$\bar{\nu}$	Whirl frequency ratio = ν/ω
e	Eccentricity ratio = e/C
η, ξ	Skewed coordinates
θ, z	Cylindrical coordinates
λ	Dimensionless parameter = $\frac{\mu RL}{\pi} (C/R)^2$
μ	Viscosity, lb-sec/in ²
ν	Kinematic viscosity, in ² /sec.
ν	Whirl frequency, radians/sec.
ρ	Density, lb/in ³
ϕ	Attitude angle, deg. (radians in equations)
ϕ'	Moment attitude angle, deg. (radians in equations)
ω	Total rotational speed = $(\omega_1 + \omega_2)$, radians/sec.
ω_1	Rotational speed journal, radians/sec.
ω_2	Rotational speed ring, radians/sec.

Subscripts

1	Refers to inner film
2	Refers to outer film

INTRODUCTION

In many applications of rotating machinery it is desirable to lubricate bearings with the process fluid in order to avoid the complication of a separate lube system with accompanying seal problems. In many instances, process fluids may have low kinematic viscosities which result in operation of the bearings in the turbulent flow regime.

Bearing power loss rises rapidly with Reynolds number in turbulent film bearings. In a number of prototype systems involving rotary machines operating in the turbulent regime, the bearing power loss has been an appreciable percentage of the net system output. In addition to the effect on system efficiency, high bearing power losses mean that large quantities of lubricant must be circulated through the bearing for cooling.

A very attractive bearing for use in applications where power loss is important is the floating ring bearing. This is a journal bearing in which a loose ring is fitted between the shaft and the bearing housing. This ring is free to rotate when the journal rotates, and by so doing, can reduce the rate of shear between adjacent bearing surfaces thereby reducing power loss.

In plain bearing form, the principal disadvantage of the floating ring bearing is the rather poor stability characteristics of plain journal bearings, particularly when lightly loaded. There are a variety of configurations of journal bearings which offer improved stability over plain journal bearings. These include the tilting pad journal bearing, the Rayleigh step journal bearing, multi-lobed journal bearings, and the spiral-grooved journal bearing. Of these, the most suitable for use in a floating ring configuration is the spiral-grooved bearing. In addition to improved stability characteristics over plain bearings, the spiral-grooved bearing also has several other attractive advantages. These include the ability to self-pump lubricant axially through the bearing film and the ability to operate without cavitation at high eccentricity ratios without using a pressurized lubricant supply.

Because of the potential advantages of spiral-grooved floating ring journal bearings for many applications, an analysis was performed of this bearing for both laminar and turbulent flow regimes. This analysis and the results obtained therefrom form the subject of this report. Extensive performance data are presented for both floating ring and single film configuration of the spiral-grooved bearing. These data include stiffness and damping coefficients and evaluations of critical mass for fractional frequency whirl instability.

DESCRIPTION OF SINGLE FILM AND FLOATING-RING SPIRAL GROOVED JOURNAL BEARINGS

A typical spiral-grooved journal bearing is shown schematically in Fig. 1. The configuration shown is that in which the grooving on the ends of the journal tends to pump inward, thereby pressurizing the interior of the bearing. Because of the symmetry of this configuration, there is no net flow of lubricant through the bearing.

Other possible configurations for the single film spiral-grooved bearing are shown in Fig. 2. Configuration 1 is as described above. Configuration 2 is an arrangement wherein spiral grooving is inscribed on one end of the bearing in a manner so as to pump fluid axially through the bearing toward the smooth or seal end. The axial flow of lubricant can remove heat from the bearing. The flow through the bearing can be increased by pressurizing the grooved end of the bearing to a supply pressure P_s as shown.

Configuration 3 shows a symmetrical arrangement wherein lubricant is pumped by spiral grooves outward from the center of the bearing. Lubricant may be supplied to the center of the bearing at an elevated pressure P_s . Configuration 3 consists, essentially, of two bearings of configuration 2 placed "back to back".

In all the configurations illustrated in Figs. 1 and 2, the spiral-grooving is shown inscribed on the journal which is considered to be the rotating member. One could, instead, inscribe the grooving on the stationary member and, for an incompressible lubricant, the performance of the bearing would be essentially the same. In this report, we shall only consider the case where the grooves are inscribed on the rotating member, this being the most common situation in practice.

The performance of a spiral-grooved bearing depends on the values of the groove parameters β (groove angle), α (ratio of groove width to total width), Γ (ratio of groove clearance to ridge clearance), and \bar{Y} (ratio of length of grooving to total length of bearing). These groove parameters are defined in Fig. 1. By a suitable choice of these parameters, one can optimize various performance characteristics of the bearing. In this report, we have chosen to present performance data for the case where the groove parameters are set at those values which yield maximum radial component of bearing stiffness at zero eccentricity.

The radial component of bearing stiffness at zero eccentricity is defined as the limiting value of $W \cos \phi / e$ as e approaches zero where W is bearing load, e is the journal displacement from the center of the bearing and ϕ is the attitude angle for the bearing (see Fig. 3). In determining the optimum values of groove parameters for maximum radial stiffness, it turned out that optimum values of α , β and \bar{Y} did not vary appreciably with Reynolds number or with L/D ratio in the range $0.5 \leq L/D \leq 1.0$. For simplicity, therefore, a fixed set of optimum values for these parameters was settled upon as valid for all Reynolds numbers and all L/D ratios between 0.5 and 1.0. The optimum value of groove depth ratio Γ however, did vary significantly with Reynolds number. Optimum values of α , β , \bar{Y} and Γ selected for configuration 1 and configuration 2 type bearings are given in Tables 1 and 2 below.

TABLE 1

OPTIMUM VALUES OF GROOVE PARAMETERS SELECTED FOR CONFIGURATION 1 BEARING

Reynolds No.	α	β	\bar{Y}	Γ
laminar, $Re < 500$	0.5	151.5°	0.75	2.1
1,000	"	"	"	2.7
5,000	"	"	"	3.0
9,000	"	"	"	3.0

TABLE 2

OPTIMUM VALUES OF GROOVE PARAMETERS SELECTED FOR CONFIGURATION 2 BEARING

Reynolds No.	α	β	\bar{Y}	Γ
laminar, $Re < 500$	0.55	149°	0.67	2.4
1,000	"	"	"	3.1
5,000	"	"	"	3.8
9,000	"	"	"	3.8

Fig. 4 shows a schematic drawing of a floating-ring bearing. A floating-ring bearing is a journal bearing in which there is a loose ring between the shaft and the bearing housing. In this way, the fluid film is separated into an inner film and an outer film. The quantities connected with the inner film are identified by subscript 1, whereas subscript 2 refers to the outer film. The floating-ring bearing shown in Fig. 4 is shown with spiral-grooving on the journal and on the outer surface of the floating ring. The configuration of the grooving is such as to pump lubricant outward from the axial midplane of the bearing. Lubricant is supplied to the two lubricant films at supply pressure P_s via supply holes in the bearing and in the floating ring. Circumferential grooves machined at the midplane of the journal and the floating ring distribute the lubricant at uniform pressure around the journal and around the outside of the floating ring. The ring is free to rotate, and under the influence of shear stress from the revolving journal, turns at some ring speed N_2 less than the speed N_1 of the journal. Since in journal bearings, load capacity is essentially proportional to $(N_1 + N_2)$ whereas power loss is roughly proportional to $(N_1 - N_2)$, it follows that rotation of the ring will improve the load capacity of the inner film while reducing the power loss. This is the principle of operation of the floating ring bearing.

Calculation of the performance characteristics of the floating ring bearing requires calculation and matching of the performance characteristics of the individual lubricant films. These individual performance characteristics depend on the values selected for the groove parameters, with the possibility of having different groove parameters for the inner and outer films. For the calculations presented in this report, the groove parameters were taken to be the same for the inner and outer film and were selected to be those which provide maximum radial component of bearing stiffness for each individual bearing film. (See Table 2).

A description of the analysis of the turbulent single film and floating ring spiral-grooved journal bearings is given in the next section.

ANALYSIS

Analysis of the performance characteristics of the turbulent, spiral-grooved, single film and floating-ring journal bearing is based on the concept of solving for the "overall", "smoothed" pressure distribution around the bearing, neglecting the local zig-zag details of the pressure profiles which arise due to the discontinuous groove-ridge geometry. The theoretical basis for this analytical approach is discussed in detail in Reference 1. Essentially, this analytical approach is valid in the limit as the number of grooves approaches an infinite number, but practically speaking, the analysis proves to be quite accurate when applied to bearings having a reasonable number of grooves. Experimental verification of this analytical approach has been provided by a number of investigations (References 2 and 3).

The differential equation that had been derived in Reference 1 for the smoothed, overall pressure distribution around a spiral-grooved journal bearing was re-derived in the present study to take account of the effects of turbulence in the bearing film. This derivation is presented in Appendix 1. The effects of turbulence in the bearing film are accounted for by means of the linearized turbulent lubrication theory developed by Ng and Fan (Reference 4). In this theory, which is based on the concept of a turbulent eddy viscosity, there are developed turbulent flow correction factors G_x and G_z which relate the mean pressure flow in the direction of rotation (x direction) and the axial direction (z direction) to the pressure gradients in these respective directions. The relationships developed are

$$u_p = - \frac{1}{\mu} G_x \frac{\partial p}{\partial x} \quad (1)$$

$$w = - \frac{1}{\mu} G_z \frac{\partial p}{\partial z} \quad (2)$$

where

$\bar{u}_p = \bar{u} - \frac{V}{2}$ = the mean flow velocity in the x direction minus 1/2 the surface velocity of rotation

\bar{w} = the mean flow velocity in the axial direction

h = local film clearance

μ = viscosity

In the generalized theory for turbulent fluid films developed by Elrod, Ng and Pan (Reference 5), G_x and G_z are functions of the pressure gradient in the film, the angle between the pressure gradient and the direction of rotation, and the Reynolds number based on rotational velocity. In the linearized theory of Ng and Pan, G_x and G_z are functions only of the local Reynolds number $R_h = \rho V h / \mu$. Values of G_x and G_z , plotted as a function of R_h , are shown in Figure 5.

A discussion of the theoretical basis of the linearized theory of turbulence is beyond the scope of this present report. For such a discussion, the reader can consult Reference 4. In this report, we have simply applied the results of this theory to derive the differential equation for a spiral-grooved journal bearing with turbulent, incompressible lubricant. This differential equation, obtained in Appendix I, is given below in dimensionless form.

$$\frac{\partial w^5}{\partial \theta} + \frac{\cos \beta}{R} \frac{\partial w^{\eta}}{\partial \theta} + \sin \beta \frac{\partial w^{\eta}}{\partial z} + \left(\frac{\partial}{\partial t} + \frac{V}{R} \frac{\partial}{\partial \theta} \right) \left\{ R \rho \sin \beta \left[\alpha h_g + (1-\alpha) h_r \right] \right\} = 0 \quad (3)$$

where

$$W^E = R \sin \beta \left\{ - \frac{\rho}{12\mu} h_r^3 \left[G_{1r} (\bar{A}_2 \frac{\partial \bar{P}}{\partial \xi} - \alpha \bar{B}_1 \frac{\partial \bar{P}}{\partial \eta} - \alpha \bar{B}_2) \right. \right. \\ \left. \left. + G_{2r} \frac{\partial \bar{P}}{\partial \eta} \right] + \rho h_r \frac{(U-V)}{2R} \right\}$$

$$W^\eta = R \sin \beta \frac{\rho}{12\mu} \left\{ \alpha h_g^3 \left[G_{3g} \frac{\partial \bar{P}}{\partial \eta} + G_{2g} (\bar{A}_2 \frac{\partial \bar{P}}{\partial \xi} - \alpha \bar{B}_1 \frac{\partial \bar{P}}{\partial \eta} - \alpha \bar{B}_2) \right] \right. \\ \left. + (1-\alpha) h_r^3 \left[G_{3r} \frac{\partial \bar{P}}{\partial \eta} + G_{2r} (\bar{A}_2 \frac{\partial \bar{P}}{\partial \xi} - \alpha \bar{B}_1 \frac{\partial \bar{P}}{\partial \eta} - \alpha \bar{B}_2) \right] \right\}$$

$$\frac{\partial \bar{P}}{\partial \eta} = \frac{\partial \bar{P}}{\partial \theta} \frac{\cos \beta}{R} + \frac{\partial \bar{P}}{\partial z} \sin \beta$$

$$\frac{\partial \bar{P}}{\partial \xi} = \frac{\partial \bar{P}}{\partial \theta}$$

$$A_1 = G_{1r} h_r^3$$

$$A_2 = - G_{1g} h_g^3$$

$$A_3 = A_2 - \alpha(A_2 + A_1)$$

$$B_1 = G_{2g} h_g^3 - G_{2r} h_r^3$$

$$h_2 = \frac{6\mu(h_r - h_o)}{R} (U-V)$$

$$\bar{A}_1 = A_1/A_3$$

$$\bar{A}_2 = A_2/A_3$$

$$\bar{B}_1 = B_1/A_3$$

$$\bar{B}_2 = B_2/A_3$$

and where G_{1r} , G_{1g} , G_{2r} , G_{2g} , etc. are lumped, turbulent flow correction factors defined by Eqs. (65), (66) and (67) in Appendix I.

Eq. (3) was solved numerically on a digital computer using the method of column-wise influence coefficients developed by Castelli and Shapiro (Ref. 6) and Castelli and Pirvic (Ref. 7). Two separate computer programs were developed, one to obtain results for the static and dynamic characteristics of a single film spiral-grooved bearing, and the second to calculate the overall static performance characteristics of a spiral-grooved floating-ring bearing.

Calculation of Performance of Single Film, Spiral-Grooved Journal Bearing

The computer program for calculating the performance characteristics of a single-film spiral-grooved journal bearing requires that the following quantities be specified. (Symbols are defined in the nomenclature).

Reynolds number based on mean radial clearance in the seal region of the bearing =
$$\frac{2\pi(N_i - N_o)RC}{\mu}$$

L/D ratio

C/R ratio

$$\text{Dimensionless pressure at both ends of the bearing} = \frac{p}{\mu(N_1 + N_0)} \left(\frac{C}{R}\right)^2$$

$$\text{Speed ratio factor} = \frac{N_0 - N_1}{N_1 + N_0}$$

$$\text{Dimensionless rate of change of eccentricity ratio} = \frac{\partial \epsilon}{\partial t} / 2\pi(N_1 + N_0)$$

$$\text{Dimensionless whirl speed ratio} = \frac{\partial \phi}{\partial t} / 2\pi(N_1 + N_0)$$

$$\text{Dimensionless rate of change of misalignment angle} = \frac{\partial \gamma}{\partial t} / 2\pi(N_1 + N_0)$$

Eccentricity ratio, ϵ

Angle of misalignment, γ

Groove geometry parameters $\alpha, \beta, \Gamma, \bar{Y}$

In addition, one must specify whether the bearing is of configuration 1 or configuration 2 (see Fig. 2). Subject to the above input conditions, Eq. (3) is solved by the computer program to determine the dimensionless pressure distribution \bar{P} . From this pressure distribution, the computer program then determines the following performance characteristics of the bearing.

Dimensionless tangential (sin) component of bearing film force,

$$\bar{F}_t = \frac{W \sin \phi}{\mu(N_1 + N_0)R^2} \left(\frac{C}{R}\right)^2 \quad (\text{see Fig. 3})$$

Dimensionless radial (cos) component of bearing film force,

$$\bar{F}_r = \frac{W \cos \phi}{\mu(N_1 + N_0)R^2} \left(\frac{C}{R}\right)^2 \quad (\text{see Fig. 3})$$

Dimensionless tangential (sin) component of the moment exerted by the bearing film force about an axis through the initial end of the bearing

$$\bar{M}_t = \frac{M \sin \phi}{\mu(N_1 + N_0)R^3} \left(\frac{C}{R}\right)^2$$

Dimensionless radial component of the moment exerted by the bearing film force about an axis through the initial end of the bearing,

$$\bar{M}_r = \frac{H \cos \phi'}{\mu(N_1 + N_0)R^3} \left(\frac{C}{R}\right)^2$$

Dimensionless flow through the journal, $\bar{Q} = \frac{Q}{R^2 C(N_1 + N_0)}$

Dimensionless bearing torque, $\bar{T}_B = \frac{T_B}{WC}$

Dimensionless journal torque, $\bar{T}_J = \frac{T_J}{WC}$

The problem of cavitation of the bearing film is handled by the approximate method of setting all sub-ambient fluid film pressure equal to zero before integrating for loads and flows. Experience with plain journal bearings indicates that this approach yields values for load which are on the order of 5% to 10% conservative when compared to a more exact treatment (Ref. 8). For spiral-grooved bearings, the extent of cavitation is much less than for plain bearings. Thus, one would expect that the error introduced by the approximate method of handling cavitation would not be significant in the case of spiral-grooved bearings.

In the calculation of bearing torque, it is assumed that regions of sub-ambient pressure are cavitated and therefore do not contribute to the shear stress on the journal or bearing.

The program for the single film bearing calculates values of the radial and tangential components of fluid film force F_r and F_t as functions of the steady state eccentricity of the journal, e , the instantaneous rate of change of eccentricity of the journal, $\partial e/\partial t$, and the instantaneous whirl velocity of the journal $\partial \phi/\partial t$. Let us now see how this program may be used to obtain

stiffness and damping coefficients for the bearing. Consider the reference axes x and y shown in Fig. 3 where x is taken as the direction of the steady state load, W , and y is normal to this. The stiffness and damping coefficients are defined by

$$\frac{dF_x}{dt} = -K_{xx} x - B_{xx} \frac{\partial x}{\partial t} - K_{xy} y - B_{xy} \frac{\partial y}{\partial t} \quad (4)$$

$$\frac{dF_y}{dt} = -K_{yx} x - B_{yx} \frac{\partial x}{\partial t} - K_{yy} y - B_{yy} \frac{\partial y}{\partial t} \quad (5)$$

It is shown in Appendix II that for bearings possessing rotational symmetry, K_{xx} , K_{yy} etc. may be determined from derivatives of F_r and F_t with respect to e and ϕ by means of the following expressions

$$K_{xx} = \frac{\partial F_r}{\partial e} \cos^2 \phi + \frac{\partial F_t}{\partial e} \cos \phi \sin \phi \quad (6)$$

$$B_{xx} = \frac{\partial F_r}{\partial \dot{e}} \cos^2 \phi + \frac{\partial F_t}{\partial \dot{e}} \cos \phi \sin \phi - \frac{\sin \phi}{e} \left[\cos \phi \frac{\partial F_r}{\partial \phi} + \sin \phi \frac{\partial F_t}{\partial \phi} \right] \quad (7)$$

$$K_{xy} = \frac{\partial F_t}{\partial e} \sin^2 \phi + \frac{\partial F_r}{\partial e} \cos \phi \sin \phi \quad (8)$$

$$B_{xy} = \frac{\partial F_t}{\partial \dot{e}} \sin^2 \phi + \frac{\partial F_r}{\partial \dot{e}} \cos \phi \sin \phi + \frac{\cos \phi}{e} \left[\cos \phi \frac{\partial F_r}{\partial \phi} + \sin \phi \frac{\partial F_t}{\partial \phi} \right] \quad (9)$$

$$K_{yx} = -\frac{\partial F_t}{\partial e} \cos^2 \phi + \frac{\partial F_r}{\partial e} \cos \phi \sin \phi - \frac{W}{e} \sin \phi \quad (10)$$

$$B_{yx} = -\frac{\partial F_t}{\partial \dot{e}} \cos^2 \phi + \frac{\partial F_r}{\partial \dot{e}} \cos \phi \sin \phi - \frac{\sin \phi}{e} \left[\sin \phi \frac{\partial F_r}{\partial \phi} - \cos \phi \frac{\partial F_t}{\partial \phi} \right] \quad (11)$$

$$K_{yy} = \frac{\partial F_r}{\partial e} \sin^2 \phi - \frac{\partial F_t}{\partial e} \cos \phi \sin \phi + \frac{W}{e} \cos \phi \quad (12)$$

$$B_{yy} = \frac{\partial F_r}{\partial \dot{e}} \sin^2 \phi - \frac{\partial F_t}{\partial \dot{e}} \cos \phi \sin \phi + \frac{\cos \phi}{e} \left[\sin \phi \frac{\partial F_r}{\partial \phi} - \cos \phi \frac{\partial F_t}{\partial \phi} \right] \quad (13)$$

where $\dot{e} = \frac{\partial e}{\partial t}$ is the instantaneous rate of change of eccentricity and $\dot{\phi} = \frac{\partial \phi}{\partial t}$ is the whirl velocity of the journal.

The determination of the derivatives $\partial F_r / \partial e$, $\partial F_r / \partial \dot{e}$ etc. from the single film program is tedious but essentially straight forward. Care must be taken, however, that the changes in e , \dot{e} and $\dot{\phi}$ used to evaluate these derivatives be chosen sufficiently small such that the results accurately apply to infinitesimally small amplitude motions of the journal center about a steady state position*. It is recommended that one keep $\Delta e / C < .05$, $\Delta \dot{e} / 2\pi(N_1 + N_0)C < .05$ and $e\dot{\phi} / 2\pi(N_1 + N_0)C < .05$ for evaluation of the above mentioned derivatives.

A detailed description of how to prepare input for the single film spiral-grooved journal bearing program is given in Appendix III together with a listing of the program.

Calculation of Steady State Performance of Floating Ring Bearing

The program for calculating the performance of a floating ring, spiral-grooved bearing consists, essentially, of two parts. The first part contains the program for a single film, spiral grooved journal bearing described above. This is used to calculate the individual performance characteristics of the inner and outer films of the floating ring bearing. The second part of the program consists of the logic required to determine the correct ring speed and eccentricity ratio of the outer film such that the load capacity of the outer film is equal to the load capacity of the inner film and the torque exerted by fluid shear stresses on the

*

The linear formulation represented by Eqs. (4) and (5) implicitly carries the assumption that the motions x , y , $\partial x / \partial t$, $\partial y / \partial t$ are vanishingly small.

inner surface of the ring is balanced by the fluid shear stresses on the outer surface of the ring. In detail, the computational procedure works as described below

1. To determine the overall performance of the floating ring bearing requires that the following quantities be specified as input to the program.

Radius ratio of ring and journal = R_2/R_1 where R_2 is the outside radius of the ring and R_1 is the radius of the journal.

Overall Reynolds number under which the bearing is to be operated

$$Re = 2\pi\phi N_1 R_1 C_1 / \mu$$

Eccentricity ratio of inner film to be examined = ϵ_1

Clearance to radius ratio for inner film = C_1/R_1

Clearance to radius ratio for outer film = C_2/R_2

Dimensionless supply pressure to center of bearing = $(P_0/\mu N_1) (C_1/R_1)^2$

Length to inner diameter ratio for bearing = L/D_1

Groove geometry parameters α , β , Γ and \bar{Y}

2. Given this input, the first thing the program does is to calculate and store in tabular form the following performance data for the inner and outer films of the floating ring bearing.

Inner film

$$\text{Sommerfeld No. } S_1 = \frac{\mu(N_1 + N_2)D_1 L}{W} \left(\frac{R_1}{C_1}\right)^2$$

$$\text{Dimensionless torque on journal } (\bar{T}_j)_1 = \frac{(T_j)_1}{WC_1}$$

$$\text{Dimensionless torque on inside of ring } (\bar{T}_B)_1 = \frac{(T_B)_1}{WC_1}$$

Attitude angle ϕ_1

Outer film

$$\text{Sommerfeld No. } S_2 = \frac{\mu N_2 D_2 L}{W} \left(\frac{R_2}{C_2}\right)^2$$

$$\text{Dimensionless torque on outside of ring } (\bar{T}_J)_2 = \frac{(T_J)_2}{WC_2}$$

$$\text{Dimensionless torque on inside of bearing } (\bar{T}_B)_2 = \frac{(T_B)_2}{WC_2}$$

Attitude angle ϕ_2

These performance data are stored in tables as functions of the eccentricity ratio and Reynolds number for the film concerned. Values are calculated for three predetermined values of eccentricity ratio and three predetermined values of Reynolds number. Thus, 9 separate calculations of performance characteristics must be made for each film (18 calculations altogether). The Reynolds number for the inner film is defined as

$$Re_1 = \frac{2\pi\rho(N_1 - N_2)R_1 C_1}{\mu} \quad (14)$$

while the Reynolds number for the outer film is defined as

$$Re_2 = \frac{2\pi\rho N_2 R_2 C_2}{\mu} \quad (15)$$

Note that since the overall Reynolds number Re is specified, Re_1 and Re_2 are determined uniquely by the ring speed ratio N_2/N_1 . Typically, the three values of Re_1 and Re_2 for which film characteristics are calculated are those corresponding to $N_2/N_1 = 0.25, 0.35$ and 0.45 . Typical values of eccentricity ratio for which the inner film characteristics are determined are $\epsilon_1 = 0.2, 0.3$ and 0.5 . The three values of ϵ_2 selected for calculation of outer film data are chosen in accordance with anticipated operating eccentricities of the outer film.

3. Once the tables of inner and outer film characteristics are prepared, the program next considers an initial guess for the ring speed ratio N_2/N_1 . This initial guess is read in as input to the program. From this ring speed ratio, the program then calculates a value for Re_1 . Corresponding to this value for Re_1 , and the value of ϵ_1 read into the program, there will be specific values of S_1 and $(\bar{T}_B)_1$ which the program will determine from the tabular data for the inner film characteristics. The program will interpolate within the tables if necessary.

4. The program next determines S_2 from the condition that the load capacities of the inner and outer film must be equal. This condition is expressed by

$$S_2 = S_1 \left(\frac{N_2}{N_1 + N_2} \right) \frac{R_2}{R_1} \left(\frac{R_2}{C_2} \right)^2 \left(\frac{C_1}{R_1} \right)^2 \quad (16)$$

The program also determines Re_2 corresponding to the guessed value of ring speed ratio.

5. With S_2 and Re_2 calculated, the program next determines the corresponding values of $(\bar{T}_J)_2$ and ϵ_2 from the tabular data for the outer film performance characteristics. The program then checks to see if

$$(\bar{T}_J)_2 = (\bar{T}_B)_1 \frac{C_1}{C_2} \quad (17)$$

i.e. the program checks to see if the torque on the outside of the floating ring matches the torque on the inside. If they match, the solution is complete. If the torque on the outside of the ring is lower (higher), then a slightly higher (lower) value for ring speed is guessed and the process is repeated until a convergent solution is obtained.

When a convergent solution is obtained for the floating ring bearing, the program prints out various performance data for the individual films and for the overall floating ring bearing. This output is described fully in Appendix IV. Detailed instructions for preparing the input for the floating ring program are also provided in this appendix along with a listing of the program.

Stiffness and Damping Coefficients for Floating Ring Bearing

In order to determine the overall stiffness and damping coefficients for the floating ring bearing, it is necessary to first determine the stiffness and damping coefficients for each individual bearing film. For each steady state solution for the floating ring bearing, the steady state operating conditions for each film are established. Stiffness and damping coefficients for each film can therefore be determined by the single-film, spiral-grooved journal bearing program as described earlier.

Let us denote the stiffness and damping coefficients for the inner film by the subscript 1 and those for the outer film by the subscript 2, i.e., K_{xx1} , K_{xx2} , etc. The overall stiffness and damping coefficients for the floating ring bearing are denoted simply as K_{xx} , K_{xy} , etc. Consider that the shaft moves in synchronous whirl with a frequency $\omega_1 = 2\pi N_1$ radians/sec. and with amplitude components $\bar{x}_1 e^{i\omega_1 t}$. The overall damping and stiffness coefficients are defined by the following relationships.

$$\frac{F_x e^{i\omega_1 t}}{W} = - \left(\frac{C_1 K_{xx}}{W} + i \frac{C_1 \omega_1 B_{xx}}{W} \right) \frac{\bar{x}_1}{C_1} e^{i\omega_1 t} - \left(\frac{C_1 K_{xy}}{W} + i \frac{C_1 \omega_1 B_{xy}}{W} \right) \frac{\bar{y}_1}{C_1} e^{i\omega_1 t} \quad (18)$$

$$\frac{\bar{y} e^{i\omega_1 t}}{W} = - \left(\frac{C_1 K}{W} + i \frac{C_1 \omega_1 B}{W} \right) \frac{\bar{x}_1}{C_1} e^{i\omega_1 t} - \left(\frac{C_1 K}{W} + i \frac{C_1 \omega_1 B}{W} \right) \frac{\bar{y}_1}{C_1} e^{i\omega_1 t}$$

(19)

or in short:

$$\begin{Bmatrix} \frac{F_x}{W} \\ \frac{F_y}{W} \end{Bmatrix} = - \begin{Bmatrix} Z_{xx} & Z_{xy} \\ Z_{yx} & Z_{yy} \end{Bmatrix} \begin{Bmatrix} x_1 \\ y_1 \end{Bmatrix}$$

(20)

where:

$$Z_{xx} = \frac{C_1 K}{W} + i \frac{C_1 \omega_1 B}{W} \quad (\text{analogous for } Z_{xy}, Z_{yx}, Z_{yy})$$

(21)

$$x_1 = \frac{\bar{x}_1}{C_1}$$

(22)

$$y_1 = \frac{\bar{y}_1}{C_1}$$

(23)

Let the center of the ring have whirl amplitudes $\bar{x}_2 e^{i\omega_1 t}$ and $\bar{y}_2 e^{i\omega_1 t}$ and let:

$$x_2 = \frac{\bar{x}_2}{C_1}$$

(24)

$$y_2 = \frac{\bar{y}_2}{C_1}$$

(25)

The dimensionless dynamic coefficients for the inner and outer film are obtained in the form:

Inner film:

$$\frac{C_1 K_{xx1}}{W}, \frac{C_1(\omega_1 + \omega_2)B_{xx1}}{W}, \text{ etc} \quad (26)$$

Outer film:

$$\frac{C_2 K_{xx2}}{W}, \frac{C_2 \omega_2 B_{xx2}}{W}, \text{ etc} \quad (27)$$

Define:

Inner film:

$$Z_{xx1} = \frac{C_1 K_{xx1}}{W} + i \frac{1}{1+n} \frac{C_1(\omega_1 + \omega_2)B_{xx1}}{W} \quad (28)$$

(similarly for $Z_{xy1}, Z_{yx1}, Z_{yy1}$)

Outer film:

$$Z_{xx2} = \frac{C_1}{C_2} \frac{C_2 K_{xx2}}{W} + i \frac{C_1}{C_2} \frac{1}{n} \frac{C_2 \omega_2 B_{xx2}}{W} \quad (29)$$

(similarly for $Z_{xy2}, Z_{yx2}, Z_{yy2}$)

where:

$$n = \frac{N_2}{N_1}$$

Hence, the dynamic forces acting on the shaft become:

$$\begin{Bmatrix} \frac{F_x}{W} \\ \frac{F_y}{W} \end{Bmatrix} = - \begin{Bmatrix} Z_{xx1} & Z_{xy1} \\ Z_{yx1} & Z_{yy1} \end{Bmatrix} \begin{Bmatrix} x_1 - x_2 \\ y_1 - y_2 \end{Bmatrix} \quad (30)$$

In order to bring Eq. (30) into the same form as Eq. (20) and thereby determine the overall dynamic coefficients it is necessary to eliminate x_2 and y_2 from the equations. This is done by setting up the equations of motion for the ring with mass m :

$$-\frac{C_1 m \omega_1^2}{W} \begin{Bmatrix} x_2 \\ y_2 \end{Bmatrix} = - \begin{Bmatrix} Z_{xx1} & Z_{xy1} \\ Z_{yx1} & Z_{yy1} \end{Bmatrix} \begin{Bmatrix} x_1 - x_2 \\ y_1 - y_2 \end{Bmatrix} - \begin{Bmatrix} Z_{xx2} & Z_{xy2} \\ Z_{yx2} & Z_{yy2} \end{Bmatrix} \begin{Bmatrix} x_2 \\ y_2 \end{Bmatrix} \quad (31)$$

or:

$$\begin{Bmatrix} (Z_{xx1} + Z_{xx2} - \frac{C_1 m \omega_1^2}{W}) & (Z_{xy1} + Z_{xy2}) \\ (Z_{yx1} + Z_{yx2}) & (Z_{yy1} + Z_{yy2} - \frac{C_1 m \omega_1^2}{W}) \end{Bmatrix} \begin{Bmatrix} x_1 - x_2 \\ y_1 - y_2 \end{Bmatrix} = \begin{Bmatrix} (Z_{xx2} - \frac{C_1 m \omega_1^2}{W}) & Z_{xy2} \\ Z_{yx2} & (Z_{yy2} - \frac{C_1 m \omega_1^2}{W}) \end{Bmatrix} \begin{Bmatrix} x_2 \\ y_2 \end{Bmatrix} \quad (32)$$

Substitute Eq. (32) into Eq. (30) and compare with Eq. (20) to get:

$$\begin{Bmatrix} Z_{xx} & Z_{xy} \\ Z_{yx} & Z_{yy} \end{Bmatrix} = \begin{Bmatrix} Z_{xx1} & Z_{xy1} \\ Z_{yx1} & Z_{yy1} \end{Bmatrix} \begin{Bmatrix} (Z_{xx1} + Z_{xx2} - \frac{C_1 m \omega_1^2}{W}) & (Z_{xy1} + Z_{xy2}) \\ (Z_{yx1} + Z_{yx2}) & (Z_{yy1} + Z_{yy2} - \frac{C_1 m \omega_1^2}{W}) \end{Bmatrix}^{-1} \begin{Bmatrix} (Z_{xx2} - \frac{C_1 m \omega_1^2}{W}) & Z_{xy2} \\ Z_{yx2} & (Z_{yy2} - \frac{C_1 m \omega_1^2}{W}) \end{Bmatrix} \quad (33)$$

Solving for Z_{xx} , Z_{xy} , etc. and using Eq. (21) yields the overall dynamic coefficients for the floating-ring bearing.

In general the mass of the ring is relatively small such that:

$$\frac{C_1 \omega_1^2}{W} \ll \frac{C_2 K_{xx}}{W}$$

in which case it can be ignored in the calculations. This condition applies to all the numerical results given in the present report.

Stability Calculation for Floating Ring Bearing

The overall stability of the floating ring journal bearing to self-excited whirl may be calculated from the overall dynamic coefficients described above. In this present study, the stability calculations were performed by means of the computer program developed under USAF contract No. AF 33(615)-3238 and described in part V of the final documentation issued under this contract (Ref. 9). A brief description of the analysis upon which the stability calculations are based is provided below.

At any given rotor speed and with a known static load on the bearing, the journal center occupies a certain unique equilibrium position relative to the bearing center. When the journal whirls around this equilibrium in a small orbit, the dynamic forces F_x and F_y generated in the bearing fluid film can be expressed in linearized form as:

$$F_x = -K_{xx} x - B_{xx} \frac{dx}{dt} - K_{xy} y - B_{xy} \frac{dy}{dt} \quad (34)$$

$$F_y = -K_{yx} x - B_{yx} \frac{dx}{dt} - K_{yy} y - B_{yy} \frac{dy}{dt} \quad (35)$$

where x and y are the whirl amplitudes measured from the static equilibrium position, t is time, and the four spring coefficients (the K - coefficients) and the four damping coefficients (the B - coefficients) would be determined for the floating ring bearing from the analysis described above. For a given bearing geometry and known lubricant properties, the 8 coefficients are functions of the bearing load and the rotor speed and, if the lubricant is compressible like a gas, they are also functions of the whirl frequency. In the latter case, Eqs. (34) and (35) are only valid for harmonic motions such that:

$$x = x_c \cos(\nu t) - x_s \sin(\nu t) \quad (36)$$

$$y = y_c \cos(\nu t) - y_s \sin(\nu t) \quad (37)$$

where ν is the angular whirl frequency. These equations can also be written:

$$x = \operatorname{Re} \left\{ (x_c + ix_s) e^{i\nu t} \right\} \quad (38)$$

$$y = \operatorname{Re} \left\{ (y_c + iy_s) e^{i\nu t} \right\} \quad (39)$$

where $i = \sqrt{-1}$ and " $\operatorname{Re} \{ \}$ " means that only the real part of the bracketed expression applies. For convenience the " $\operatorname{Re} \{ \}$ " and the $e^{i\nu t}$ are dropped whereby Eqs. (38) and (39) are written

$$x = x_c + ix_s \quad (40)$$

$$y = y_c + iy_s \quad (41)$$

When these equations are used in the analysis their complete meaning is defined through Eqs. (38) and (39).

With this notation Eqs. (34) and (35) can be written:

$$F_x = -\bar{Z}_{xx} x - \bar{Z}_{xy} y \quad (42)$$

$$F_y = -\bar{Z}_{yx} x - \bar{Z}_{yy} y \quad (43)$$

where:

$$\bar{Z}_{xx} = K_{xx} + i \left(\frac{\nu}{\omega}\right) \omega B_{xx} = K_{xx} + i\gamma \omega B_{xx} \quad (44)$$

$$\bar{\gamma} = \frac{\nu}{\omega} \quad (45)$$

and similarly for \bar{Z}_{xy} , \bar{Z}_{yx} and \bar{Z}_{yy} . Here, ω is the angular speed of rotation and $\bar{\gamma}$ gives the ratio between the whirl frequency and the rotational frequency. In this form, the equations are equally valid for an incompressible and a compressible lubricant.

To illustrate the procedure for calculating the threshold of instability, assume for simplicity that the rotor is rigid and symmetric such that the two bearings support an equal mass M which equals half the mass of the rotor. Then the equations of motion for a journal become:

$$\begin{aligned} M \frac{d^2 x}{dt^2} &= F_x \\ M \frac{d^2 y}{dt^2} &= F_y \end{aligned} \quad (46)$$

By substitution from Eqs. (41) through (43), these equations can be written in matrix form:

$$\begin{pmatrix} (\bar{z}_{xx} - Mv^2) & \bar{z}_{xy} \\ \bar{z}_{yx} & (\bar{z}_{yy} - Mv^2) \end{pmatrix} \begin{pmatrix} x \\ y \end{pmatrix} = 0 \quad (47)$$

At the threshold of instability, a non-zero solution of x and y must exist which means that the determinant Δ of the matrix should be zero:

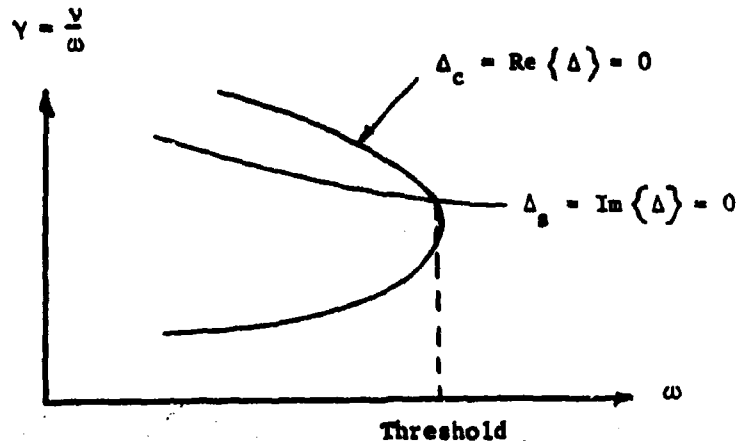
$$\Delta = \Delta_c + i\Delta_s = (\bar{z}_{xx} - Mv^2)(\bar{z}_{yy} - Mv^2) - \bar{z}_{xy}\bar{z}_{yx} = 0 \quad (48)$$

or

$$\Delta_c = R_e\{\Delta\} = (K_{xx} - \bar{\gamma}^2 M\omega^2)(K_{yy} - \bar{\gamma}^2 M\omega^2) - K_{xy}K_{yx} - \bar{\gamma}^2 \left[\omega B_{xx} \omega B_{yy} - \omega B_{xy} \omega B_{yx} \right] = 0 \quad (49)$$

$$\Delta_s = \text{Im}\{\Delta\} = \bar{\gamma} \left[(K_{xx} - \bar{\gamma}^2 M\omega^2)\omega B_{yy} + (K_{yy} - \bar{\gamma}^2 M\omega^2)\omega B_{xx} - K_{xy}\omega B_{yx} - K_{yx}\omega B_{xy} \right] = 0 \quad (50)$$

These two equations must be satisfied simultaneously at the threshold of instability. They contain two unknowns, namely the whirl frequency ratio, $\bar{\gamma}$, and the angular speed of rotation, ω . In the general case, the 8 dynamic fluid film coefficients are functions of both $\bar{\gamma}$ and ω , making a closed form solution impossible, and the solution is most conveniently obtained graphically. For any fixed value of ω , Δ_c and Δ_s can be plotted as functions of $\bar{\gamma}$ to find their zero points. With $\bar{\gamma} > 0$ it is seen that Δ_s has one zero point and Δ_c has up to two zero points (only true in this simple case). The calculation is repeated for several values of ω and the results may be plotted as shown:



The intersection of the two curves define the speed at which instability sets in.

RESULTS

Single Film Bearing

Results of calculations of the performance of single film spiral-grooved journal bearings are shown in Figs. 7 through 18. In all cases, the results shown are for bearings having groove geometry optimized for maximum radial component of stiffness at $\epsilon = 0$. These optimum values of groove geometry parameters are given in Tables 1 and 2 presented earlier in the text.

Load capacity of the single film spiral-grooved journal bearing is shown in Figs. 7, 8, 9 and 10, in terms of dimensionless load $W/\mu N_1 LD (C/R)^2$ vs. eccentricity ratio ϵ . Fig. 7 shows results for a bearing of configuration 1 i.e. a bearing having no flow-through of lubricant (see Fig. 2). L/D ratio is taken to be 1.0. It is assumed that only the grooved journal is rotating. In this figure, it can be noted that the existence of turbulence does not significantly effect the linearity of the load vs. eccentricity curve, but only serves to increase the load capacity over that which would be obtained if flow remained laminar.

In Fig. 8 are shown load vs. eccentricity curves for a bearing of configuration 2 with $L/D = 1.0$, in which there is net flow of lubricant pumped through the bearing entirely by action of the spiral grooving ($P_s = 0$). The load capacity of this bearing is seen to be slightly less than that for the configuration 1 bearing. On the other hand, the through-flow of lubricant is useful in removing heat from the bearing.

Fig. 9 shows load capacity of a configuration 2 type bearing with $L/D = 0.5$. As can be seen, unit load capacity, W/LD , decreases significantly with decrease in L/D ratio. As a rough guide, it is found that in the range $0.5 \leq L/D \leq 2.0$, unit load capacity is very nearly proportional to L/D ratio.

To provide a greater flow of lubricant through a configuration 2 bearing, one can supply the lubricant to the grooved end at an elevated pressure P_s . The effect of this on load capacity is relatively slight as shown by the curves in

Fig. 10. The results are shown for $Re = 5000$ but are typical of those obtained at all values of Reynolds number. The degree of pressurization considered is indicated by the dimensionless parameter $\bar{P}_s G_z D/L$ where \bar{P}_s is the dimensionless supply pressure defined as $\bar{P}_s = [P_s / \mu(N_1 + N_0)]^{1/2} (C/R)^2$ and G_z is a turbulent viscosity correction factor corresponding to the mean Reynolds No. (G_z is obtained from Fig. 5). When the supply pressure parameter $\bar{P}_s G_z (D/L)$ is maintained at 0.35, the net flow of lubricant through the bearing due to pressurization is approximately equal to that due to self-pumping of the grooves, independent of Reynolds number. When this parameter doubles, flow due to pressurization doubles.

In general one may conclude that for values of $\bar{P}_s G_z (D/L)$ less than 0.7, the effect of pressurization on load capacity may be neglected. In any case, it is conservative to do so since pressurization tends to increase load capacity*.

Figs. 11, 12, and 13 show curves of attitude angle ϕ vs. eccentricity ratio for configuration 1 and configuration 2 bearings at different Reynolds numbers and L/D ratios. The effect of pressurization on attitude angle is also shown by the dashed curves in Figs. 12 and 13.

Referring to Fig. 11, which gives attitude angle for a configuration 1 bearing, we see that for laminar flow ϕ decreases slightly with eccentricity ratio. This decrease is mostly due to effects of cavitation in the bearing film. At higher values of Reynolds number, very little or no cavitation occurs in the bearing film out to $\epsilon = 0.7$ and, as a consequence, attitude angle shows very little dependence on ϵ . The extent of cavitation that does occur in the bearing will be discussed later in connection with predicted bearing torque.

 * Pressurization of the grooved end of a spiral-grooved journal bearing produces hydrostatic load capacity whether the journal is rotating or not. Such pressurization will help to promote rotation of the ring in a spiral-grooved floating ring bearing. Getting the ring to rotate can be somewhat of a problem in plain, cylindrical floating ring bearings. Whether this is true for spiral-grooved floating ring bearings remains to be seen.

For configuration 2 bearings, we find again that for laminar flow, ϕ decreases with ϵ due to cavitation whereas this effect is less pronounced at higher values of Reynolds number. We also find that pressurization tends to decrease attitude angle. In most instances, this effect is not great, although for laminar flow and $L/D = 0.5$, a pressurization of $\bar{P}_s G_z D/L = 0.7$ produces approximately a 10 degree reduction in attitude angle.

Comparing Figs. 11 and 12, we see that a configuration 2 bearing of $L/D = 1.0$ has a slightly higher attitude angle than a configuration 1 bearing of the same L/D ratio. Comparing Figs. 12 and 13 we see that for configuration 2 spiral-grooved journal bearings, attitude angle decreases quite substantially as L/D ratio is decreased from 1.0 to 0.5. This latter effect does not occur in plain cylindrical bearings.

In general, we can observe that development of turbulence in spiral-grooved journal bearings reduces the attitude angle by a significant amount i.e. approximately 10 degrees at low eccentricity ratios for both configuration 1 and configuration 2 geometries.

The bearing through-flow, Q_p , that is generated by the self-pumping of spiral grooving is shown in Fig. 14. Results are plotted in terms of $Q_p/R^2 C(N_1 - N_0)$ vs. ϵ . The results shown were obtained neglecting effects of cavitation. This was done because the way in which cavitation is handled in the present analysis does not provide an accurate calculation of flow rate when cavitation appears. This is not a serious deficiency since spiral-grooved bearings usually operate with a full fluid film.

As Fig. 14 indicates, the "self-pumping" flow of an optimized bearing increases as turbulence develops in the bearing film. This is probably due to the fact that the optimum value of groove depth increases as turbulence develops. When turbulence is fully developed ($Re = 5000$) both flow and optimum pocket depth approach asymptotic values.

It should be kept in mind that the results shown in Fig. 14 pertain to a bearing

with $\bar{Y} = 0.67$ i.e. a bearing with grooving on 67% of its length. Flow through the bearing can be increased by increasing \bar{Y} slightly with very little penalty paid in terms of loss of load.

The flow of lubricant, Q_g , through a spiral-grooved bearing that results from pressurizing either end of the bearing is directly proportional to $P_g C^3 G_z / \mu (D/L)$ for any given eccentricity ratio and Reynolds number. Curves of dimensionless pressure flow, $Q_g \mu / G_z C^3 (L/D)$ are plotted vs. ϵ in Fig. 15. Use of the turbulent viscosity correction factor G_z in forming this dimensionless flow takes account of the influence of Reynolds number quite well, although some slight dependence on Reynolds number still remains.

The dimensionless torque, $T_j C / \mu N_1 R^3 L$, on the journal of a spiral-grooved bearing is plotted in Fig. 16 for a configuration 1 bearing and in Fig. 17 for a configuration 2 bearing. The solid lines show the torque for a bearing with a complete fluid film while the dashed curve shows the torque taking account of cavitation that would be expected to occur. Cavitation is accounted for by assuming that all regions of subambient pressure are cavitated and that shear stresses in these regions are negligible. The discrepancies between the dashed and solid curves in Figs. 16 and 17 provide an indication of the extent of cavitation that develops as eccentricity increases.

Looking at Fig. 16, we see that for a configuration 1 bearing, cavitation does not set in until $\epsilon \approx 0.3$ for laminar flow, until $\epsilon \approx 0.5$ for $Re = 1000$, and does not occur at all below $\epsilon = 0.7$ for $Re = 5000$ and 9000 . For an unpressurized configuration 2 bearing (Fig. 17), cavitation occurs at lower values of ϵ than for a configuration 1 bearing and does occur at $Re = 5000$ and 9000 . Cavitation can easily be eliminated, however, by modest pressurizing of the bearing.

The solid curves shown in Fig. 17 also apply with reasonable accuracy to bearings with $L/D = 0.5$. The dashed curves do not, however, because there is less tendency for a spiral-grooved bearing to cavitate as L/D ratio is decreased. For configuration 2 bearings with $L/D = 0.3$, no cavitation occurs for $Re > 1000$ and $\epsilon < 0.7$.

An important quantity to consider is how the dimensionless ratio of friction torque to load, T_j/WC , varies with Reynolds number. This is shown in Fig. 18 for $\epsilon = 0.2, 0.5$ and $\epsilon = 0.7$. As can be seen, torque increases more rapidly than does load when turbulence develops in the bearing film. One can note at this point that one of the advantages of the floating ring bearing is that the Reynolds number in each separate bearing film is less than the Reynolds number that would be obtained if the bearing had only a single film. Hence, due to this effect alone, the floating ring bearing can operate with a more favorable torque to load ratio than an equivalent bearing with only a single film.

Floating Ring Bearing

The floating ring configuration chosen for analysis was one having an overall length to diameter ratio of $L/D = 1.0$. (See Figure 4). This means that each half of the floating ring bearing had an effective length to diameter ratio of 0.5. Grooving parameters for each half of the floating ring bearing were those presented in Table 2. Grooving on the outside surface of the ring was the same as that on the shaft.

Two values of the ratio of inner clearance to outer clearance were considered i.e. $C_2/C_1 = 1.2$ and 0.8. Results were obtained for no pressurization of the bearing ($\bar{P}_s = 0$) and for a degree of pressurization corresponding to $\bar{P}_s G_z D/L = 0.35$.

The static performance data for the floating ring journal bearing are given in Table 3. Dynamic performance data are given in Tables 4 and 5. Much of this data is presented in graphical form in Figs. 19 through 36. These figures are discussed below.

Curves of dimensionless load, \bar{W} , vs the eccentricity ratio of the inner film ϵ , are presented in Fig. 19. The curves are for $C_2/C_1 = 1.2$ although they apply within a few percent accuracy to the case of $C_2/C_1 = 0.8$. As can be seen the degree of pressurization considered for the floating ring bearing (dashed curves) results in a substantial increase in load capacity over the

unpressurized case (solid curves). For the single film bearing, the same apparent degree of pressurization resulted in only a slight increase in load capacity (See Figure 10). The reasons for the greater apparent effect of pressurization on the floating ring bearing are as follows.

First, the parameter $\bar{P}_s G_z D_1/L$ for the floating ring bearing is based on the overall L/D_1 . The effective value of this parameter for each half of the floating ring bearing is actually twice the overall value. Second, the value for G_z used in establishing the parameters $\bar{P}_s G_z D_1/L$ is based on the overall Reynolds number $Re = 2\pi N_1 R_1 C_1/\nu$. Because of rotation of the ring, the individual Reynolds numbers for the inner and outer films are each less than the overall. Hence, the effect of pressurization of each film is greater than is indicated by the parameter $\bar{P}_s G_z D_1/L$ because, in turbulent flow, the lower the Reynolds number the greater the amount of flow for a given supply pressure. Third, the dimensionless supply pressure \bar{P}_s is based on the shaft speed N_1 . For spiral-grooved bearings, it turns out that rotation of the ring decreases rather than increases the load capacity of the inner film. Hence pressurization of the inner film becomes relatively more significant with respect to load capacity of the film.

Roughly speaking, the increase in load capacity resulting from pressurization of a floating ring bearing is linearly proportional to the gauge supply pressure. One can therefore linearly interpolate between the curves shown in Fig. 19 to determine load capacity at supply pressures different from that considered.

Curves of overall attitude angle ϕ of the floating ring bearing are shown in Figs. 20 and 21. Overall attitude angle is defined in Fig. 4. Values for the attitude angles of the inner and outer films are given in Table 3. Due to rotation of the ring, which decreases the spiral-grooved pumping effect in the inner film, attitude angles for the inner film are considerably greater than for the outer film.

Values of dimensionless journal torque, $\bar{T}_j = T_j/WC$, are given in Fig. 22 for a floating ring bearing with $C_2/C_1 = 1.2$. Similar curves for a bearing with $C_2/C_1 = 0.8$ would run about 7% higher.

One of the primary advantages of the floating ring bearing is that, for a given eccentricity of the inner film, the ratio of torque to load is much lower than for a comparable single film bearing. This is particularly true for plain bearings for which load capacity of the inner film is proportional to the sum of the speeds of the shaft and ring. In spiral grooved bearings, however, the pumping effect of the grooves is proportional to the difference in speed between the shaft and ring. Load capacity of these bearings is due partly to this pumping effect and partly to the usual hydrodynamic effect which is proportional to the sum of the shaft and ring speed. The net effect is that as ring speed increases, load capacity of the inner film for a spiral-grooved bearing decreases slightly. Consequently, spiral-grooved floating ring bearings do not enjoy the same torque to load advantage possessed by plain floating ring bearings. Nonetheless, the spiral-grooved floating ring bearing does have a torque to load ratio better than that of a single film bearing operating at the same eccentricity ratio. This is evidenced by the curves shown in Fig. 23. The single film bearing used for comparison in this figure is a configuration 2 bearing with $L/D = 0.5$. This provides a fair comparison because each side of the centrally fed floating ring configuration we are considering consists, essentially, of an isolated bearing with $L/D = 0.5$.

Total flow pumped through the floating ring bearing by the self-pumping effect of the spiral grooves is plotted in Fig. 24. The increase in lubricant flow that would result from pressurization of the bearing can be calculated from the single film curves plotted in Fig. 15. These single film curves can be applied directly to each individual film of the floating ring bearing on either side of the central feeding groove. In applying these curves to calculate pressure flow, one must be careful to use the appropriate Reynolds number and L/D ratio corresponding to the individual film being considered. The pressure flow that is calculated can be added directly to the self-pumping flow calculated from Fig. 24.

Ring speed ratio, N_2/N_1 , is plotted as a function of inner film eccentricity e_1 in Figs. 25a and 25b. Results for laminar flow and $Re = 9000$ are shown. Results for $Re = 5000$ are nearly the same as for $Re = 9000$ while results for $Re = 1000$

lie between the $Re = 9000$ and laminar curves. Ring speed ratio for laminar flow tends to decrease with ϵ_1 while, for turbulent flow, ring speed ratio remains relatively constant with eccentricity. Note that ring speed ratio is not strongly affected by the clearance ratio C_2/C_1 .

ϵ_2 , the eccentricity ratio for the outer film, is plotted as a function of ϵ_1 in Fig. 25. In general, ϵ_2 increases approximately linearly with ϵ_1 . As would be expected, ϵ_2 is considerably greater than ϵ_1 for $C_2/C_1 = 1.2$ and more nearly equal to ϵ_1 for $C_2/C_1 = 0.8$.

Dynamic data for the floating ring bearing are given in Tables 4 and 5. These data consist mostly of stiffness and damping coefficients for the individual bearing films and for the overall bearing. The data also include values of the dimensionless critical mass for the threshold of whirl instability.

Data for the individual bearing films are given in Table 4. Stiffness and damping for the inner film pertain to the fluid film forces that develop in the inner film due to relative motion between the shaft and the ring. Stiffness and damping for the outer film pertain to fluid film forces developed in that film due to relative motion between the ring and the outer bearing.

Stiffness and damping coefficients for the overall floating ring bearing are given in Table 5. These pertain to the forces developed on the shaft due to a relative motion between the shaft and the outer bearing including the effect of motion of the ring.

Overall stiffness and damping coefficients for the floating ring bearing are plotted vs. ϵ_1 for a number of representative situations in Figs. 27 through 32. Qualitatively, the behavior of the overall stiffness and damping coefficients as eccentricity ratio increases is similar to that for single film bearings.

The stiffness and damping coefficients presented in Tables 4 and 5 may be used to calculate a critical mass at the threshold of whirl instability. The critical masses determined from the inner or outer film damping and stiffness coefficients,

while not of great physical significance, are still of interest to calculate. The critical mass M_{c1} , determined from the inner film coefficients, is the critical mass of the shaft within the rotating ring assuming that the ring were restricted from any translational motion i.e. assuming that the outer film were infinitely stiff. M_{c2} , the critical mass calculated from the outer film coefficients, is the critical mass for the ring rotating within the bearing neglecting any effect of the inner bearing film. Essentially, M_{c2} represents the critical mass for a single film bearing operating at Reynolds number Re_2 and eccentricity ratio ϵ_2 .

M_c , the critical mass determined from the stiffness and damping coefficients for the overall floating ring bearing, represents the critical mass for the shaft rotating within the composite floating ring structure. It is the appropriate value of critical mass for the shaft of the floating ring bearing.

The critical masses M_{c1} , M_{c2} and M_c are presented in Tables 4 and 5 in the dimensionless form

$$\bar{M}_{c1} = \frac{M_{c1} C_1 (N_1 + N_2)}{\mu (R_1/C_1)^2 LD_1}$$

$$\bar{M}_{c2} = \frac{M_{c2} C_2 N_2}{\mu (R_2/C_2)^2 LD_2}$$

$$\bar{M}_c = \frac{M_c C_1 N_1}{\mu (R_1/C_1)^2 LD_1}$$

In attempting to compare the critical masses in these tables one should keep in mind that each is made non-dimensional on a slightly different basis.

Values of overall critical mass vs. ϵ_1 are plotted in Figs. 33 and 34 for

$C_2/C_1 = 1.2$ and 0.8 respectively. In general, critical mass for hydrodynamic bearings increases with eccentricity ratio. However, when operating in the turbulent regime, spiral-grooved bearings exhibit the anomalous characteristic that critical mass decreases with eccentricity in certain ranges. This characteristic may be related to the fact that the attitude angle of spiral-grooved bearings sometimes increases with eccentricity ratio in the turbulent regime. This increase in attitude angle can be qualitatively explained on the basis that as eccentricity increases, the usual plain-bearing-type of hydrodynamic action becomes relatively more significant compared with the self-pressurizing hydrodynamic action of the spiral grooves, particularly in turbulent flow. Hence, there is a tendency for attitude angle to increase with eccentricity in spiral-grooved bearings.

It is interesting to note in Figs. 33 and 34 that pressurization of the floating ring bearing has a more significant effect on bearing stability than it does on bearing load capacity. It is obvious that pressure feeding of the bearings is an effective means of stabilization.

An important point to investigate is whether the spiral-grooved, floating ring bearing configuration is more or less stable than an equivalent spiral-grooved, single film bearing. Comparisons of the critical masses of the floating ring and single film configurations are shown in Figs. 35 and 36 for laminar and turbulent flow respectively. The single film values of critical mass were taken from the values for M_{c2} calculated for the outer film. The L/D ratio of the outer film is about 20% less than that for the inner film but this fact should not greatly effect the comparison.

For laminar flow, the single film bearing is more stable than the floating ring bearing with $C_2/C_1 = 0.8$ and, at low eccentricities, is also more stable than the floating ring bearing with $C_2/C_1 = 1.2$. However, at high eccentricities, the critical mass for the floating ring bearing with $C_2/C_1 = 1.2$ exceeds that of the single film bearing.

For turbulent flow, the stability of the single film configuration is clearly

superior to that of the floating ring bearing.

The floating ring configuration of spiral-grooved bearings suffers in regard to stability for the following reason. The good stability of spiral-grooved bearings is due principally to the self-pressurizing effect of the spiral grooves. This self-pressurizing effect is proportional to the difference in speeds, $(N_1 - N_2)$. Consequently, in a floating ring configuration, rotation of the ring reduces this self-pressurizing effect in the inner film and, hence, reduces the stability of the inner film. The stability of the overall bearing suffers as a consequence.

Stability of the spiral-grooved configuration is compared with the stability of a plain floating ring bearing in Fig. 37. At low eccentricities, stability of the spiral-grooved configuration is better but, at high eccentricity, stability of the plain bearing increases rapidly due to the effect of cavitation and begins to surpass that of the spiral-grooved bearing.

An important point to keep in mind when comparing the stability of plain and spiral-grooved bearings is that the plain bearings achieves stability only as a result of cavitation in the bearing film. A plain bearing operating with a full fluid film is inherently unstable for any speed or mass. Often, particularly with liquid metals as lubricants, it is undesirable to operate with cavitated bearing films because of the problem of cavitation damage. If a pressurized supply is used with plain bearings to suppress cavitation, the stability of the bearings suffers drastically.

On the other hand, spiral-grooved bearings, even when unpressurized, operate without cavitation in the bearing film out to quite large eccentricity ratios due to the self-pressurizing action of the spiral grooves. Stability of these bearings is achieved through this self-pressurizing action. Moreover, use of a pressurized lubricant supply further enhances the stability of these bearings as is evidenced by the performance charts presented in this report.

SUMMARY AND CONCLUSIONS

An analysis has been performed of the turbulent, spiral-grooved, journal bearing with incompressible lubricant. Optimum values of groove parameters have been determined to provide maximum radial stiffness. Performance charts are presented for load capacity, attitude angle, lubricant flow rate and bearing frictional torque for both single film and floating ring configurations of the spiral-grooved journal bearing. In addition, stiffness and damping coefficients are presented for the floating ring configuration and values of the critical mass for threshold of whirl instability are determined. Performance data are presented for bearings operating with and without a pressurized supply of lubricant.

The following general conclusions can be drawn concerning the performance of spiral-grooved single film and floating ring journal bearings:

- 1) Compared with plain, cylindrical journal bearings, spiral-grooved bearings offer the following advantages: (a) They possess greater stability under lightly loaded conditions. (b) They tend to operate without cavitation due to the self-pressurizing effect of the spiral-grooving. (This is an important consideration when operating the bearing with liquid metal lubricants where the problem of cavitation damage is significant.) (c) The spiral grooving provides self-pumping of lubricant through the bearing eliminating the need for a pressurized supply. (d) All performance characteristics of spiral-grooved bearings can be easily enhanced by use of a pressurized supply of lubricant.
- 2) The floating ring configuration of spiral-grooved bearing operates with lower torque to load ratio than is achieved with a similarly loaded single film bearing. On the other hand, stability of the single film spiral-grooved bearing is generally better than that for the floating ring bearing.
- 3) In spiral-grooved bearings, development of turbulence results in an increase in frictional torque, an increase in load capacity, an increase in stability and a decrease in attitude angle. In general, the ratio of frictional torque to load capacity increases with development of turbulence.

TABLE 3 STATIC PERFORMANCE DATA FOR THE FLOATING RING JOURNAL BEARING

C_2/C_1	ω	H_0	e_1	e_2	e	N_2/N_1	N_{s1}	N_{s2}	μ	μ_1	μ_2	H_L/HC_1	μ_{s1}	μ_{s2}	θ_1	θ_2	θ	ϕ_1	ϕ_2	
0.8	0	LAM	.2	.254	.220	.396	LAM	LAM	1.87	2.45	1.58	21.7	0	0	52.7	29.8	41.2	4.22	2.12	4.00
			.3	.383	.331	.300	LAM	LAM	1.19	1.55	.965	14.0	0	0	51.3	29.5	40.3	4.20	2.18	3.94
			.5	.640	.560	.257			.628	.791	.437	7.72	0	0	45.8	29.5	37.6	4.13	2.39	3.78
0.8	0	1000	.2	.231	.210	.369	631	354	1.66	2.27	1.65	28.4	0	0	46.9	24.3	36.0	6.12	2.78	5.47
			.3	.349	.316	.366	634	351	1.07	1.46	1.06	18.8	0	0	46.7	24.7	36.1	6.07	2.79	5.47
			.5	.629	.551	.338	662	324	.575	.769	.524	10.7	0	0	45.0	27.7	36.3	5.90	2.93	5.09
0.8	0	5000	.2	.225	.207	.385	3071	1851	.912	1.26	.949	37.1	0	0	42.4	18.9	31.3	8.80	3.76	8.06
			.3	.344	.313	.385	3076	1846	.582	.806	.605	24.0	0	0	41.2	19.2	30.7	8.68	3.74	7.88
			.5	.576	.525	.381	3093	1830	.328	.451	.336	14.0	0	0	41.4	20.7	31.5	8.38	3.70	7.44
0.8	0	9000	.2	.209	.200	.392	5472	3386	.673	.938	.713	40.2	0	0	42.4	18.1	31.3	9.36	3.94	8.60
			.3	.314	.300	.391	5477	3381	.436	.606	.460	26.3	0	0	42.3	18.2	31.3	9.22	3.90	8.46
			.5	.547	.511	.386	5519	3341	.234	.324	.244	14.6	0	0	41.5	19.1	31.0	8.86	3.80	8.00
0.8	4.20	LAM	.2	.241	.216	.312	LAM	LAM	1.48	1.94	1.24	16.6	3.20	5.99	33.4	18.0	25.9	25.1	13.7	19.5
			.3	.356	.322	.309	LAM	LAM	.948	1.24	.791	11.0	3.21	6.04	33.6	18.2	26.1	26.2	14.4	20.7
			.5	.578	.530	.300	LAM	LAM	.503	.654	.407	6.68	3.23	6.23	34.5	19.5	27.2	29.7	16.3	24.6
0.8	5.13	1000	.2	.235	.214	.366	634	351	1.15	1.57	1.13	19.0	3.76	6.23	26.8	14.2	20.7	32.0	16.6	22.0
			.3	.355	.322	.362	638	348	.748	1.02	.731	12.7	3.77	6.30	27.2	14.8	21.2	33.0	17.1	23.1
			.5	.607	.545	.349	651	335	.420	.567	.396	7.83	3.80	6.52	28.9	17.2	23.1	36.4	18.8	27.4
0.8	10.0	5000	.2	.233	.213	.382	3085	1837	.618	.855	.639	24.1	7.23	11.6	24.5	11.2	18.1	40.6	20.0	29.4
			.3	.362	.326	.381	3093	1830	.388	.537	.400	15.3	7.24	11.6	23.6	11.6	17.7	42.0	20.6	30.4
			.5	.601	.542	.378	3106	1817	.223	.307	.226	9.23	7.25	11.7	24.6	13.3	19.1	45.6	22.4	33.4
0.8	14.2	9000	.2	.218	.206	.389	5498	3361	.460	.639	.483	26.2	10.2	16.2	24.8	11.0	18.4	43.8	21.6	30.6
			.3	.327	.309	.388	5502	3357	.299	.416	.314	17.3	10.2	16.2	25.0	11.2	18.6	44.6	21.8	31.8
			.5	.563	.525	.385	5531	3329	.163	.226	.170	9.87	10.2	16.3	25.2	12.3	19.1	47.2	22.0	35.0

TABLE 3 (continued)

C_2/C_1	$\bar{P}_0 = \frac{PC_1^2}{HN_1R_1^2}$	$Re = \frac{2xN_1R_1C_1}{v}$	e_1	e_2	e	N_2/N_1	$Re_1 = \frac{2x(N_1 - N_2)R_1C_1}{v}$	$Re_2 = \frac{2xN_2R_2C_2}{v}$	$\theta = \frac{10 \mu N_1 R_1^2}{VC_1^2}$	$\theta_1 = \frac{10 \mu (N_1 + N_2) R_1^2}{VC_1^2}$	$\theta_2 = \frac{10 \mu N_2 R_2^2}{VC_2^2}$	τ_1/NO_1	$\bar{P}_{01} = \frac{PC_1^2}{\mu(N_1 + N_2)R_1^2}$	$\bar{P}_{02} = \frac{PC_2^2}{\mu N_2 R_2^2}$	d_1	d_2	δ	$Ol = \frac{O}{P_1^2 C_1^2 N_1}$	$Ol_1 = \frac{O_1}{P_1^2 C_1^2 (N_1 + N_2)}$	$Ol_2 = \frac{O_2}{P_2^2 C_2^2 N_2}$
1.2	0	LAM	.2	.409	.306	.391	LAM	LAM	1.08	2.61	.881	19.3	0	0	57.4	29.4	37.4	5.13	1.78	3.53
			.3	.587	.447	.354	LAM	LAM	1.21	1.64	.514	12.6	0	0	54.3	29.1	36.6	4.96	1.84	3.42
			.5	.870	.694	.289	LAM	LAM	.639	.824	.222	7.41	0	0	47.1	28.9	34.8	4.76	2.24	3.73
1.2	0	1000	.2	.370	.286	.406	594	504	1.71	2.41	.634	26.9	0	0	49.5	23.1	31.2	7.62	2.54	5.73
			.3	.540	.420	.397	603	572	1.10	1.54	.525	18.0	0	0	49.0	24.2	32.0	7.40	2.57	5.51
			.5	.929	.729	.340	659	491	.577	.773	.236	10.6	0	0	45.0	30.0	34.7	6.98	2.91	5.20
1.2	0	5000	.2	.340	.270	.408	2960	2938	.946	1.33	.463	36.3	0	0	44.1	18.5	26.8	10.8	3.57	8.21
			.3	.507	.405	.405	2977	2913	.605	.849	.294	23.6	0	0	42.9	19.1	26.9	10.6	3.57	7.91
			.5	.831	.673	.393	3135	2829	.333	.464	.157	13.8	0	0	42.3	23.6	29.8	10.0	3.60	7.31
1.2	0	9000	.2	.332	.266	.408	5327	5288	.690	.972	.338	39.4	0	0	43.4	17.8	26.3	11.5	3.80	11.74
			.3	.483	.392	.406	5342	5267	.444	.625	.217	25.7	0	0	43.0	18.1	26.5	11.2	3.74	8.44
			.5	.821	.661	.395	5448	5115	.237	.331	.112	14.5	0	0	42.0	22.1	28.8	10.4	3.74	7.64
1.2	4.2	LAM	.2	.336	.270	.399	LAM	LAM	1.47	2.06	.705	14.3	3.0	10.5	35.2	13.1	20.4	42.4	14.2	32.8
			.3	.485	.395	.388	LAM	LAM	.947	1.32	.441	9.71	3.0	10.8	35.3	13.7	21.0	45.4	14.8	37.0
			.5	.795	.655	.329	LAM	LAM	.504	.669	.199	6.42	3.16	12.8	35.1	18.0	23.9	54.0	16.5	56.6
1.2	5.13	1000	.2	.320	.263	.406	594	585	1.16	1.63	.567	17.3	3.65	12.6	27.2	10.1	16.0	50.3	15.9	37.8
			.3	.480	.390	.401	599	578	.759	1.06	.396	11.7	3.66	12.8	27.7	10.9	16.7	53.2	17.5	41.4
			.5	.870	.700	.356	644	512	.422	.572	.180	7.74	3.78	14.4	29.0	18.0	21.5	64.4	18.9	63.0
1.2	10.0	5000	.2	.307	.256	.408	2958	2938	.631	.889	.309	22.9	7.10	24.5	24.8	8.7	14.4	60.6	20.5	45.0
			.3	.467	.388	.405	2974	2917	.400	.562	.195	14.7	7.11	24.7	24.1	9.1	14.3	63.9	20.9	49.3
			.5	.796	.655	.394	3032	2834	.226	.316	.107	6.97	7.18	25.4	24.9	12.7	16.9	72.8	22.9	60.1
1.2	14.2	9000	.2	.303	.254	.408	5332	5282	.445	.654	.227	25.0	10.1	34.8	26.8	8.6	14.3	64.8	22.1	47.9
			.3	.446	.376	.407	5356	5275	.300	.423	.147	16.4	10.1	34.9	24.7	8.9	14.6	66.1	22.3	49.4
			.5	.758	.637	.398	5417	5159	.165	.231	.079	9.40	10.2	35.7	23.3	11.7	16.5	71.8	23.2	57.3

TABLE 4 DYNAMIC PERFORMANCE DATA FOR THE FLOATING RING JOURNAL BEARING

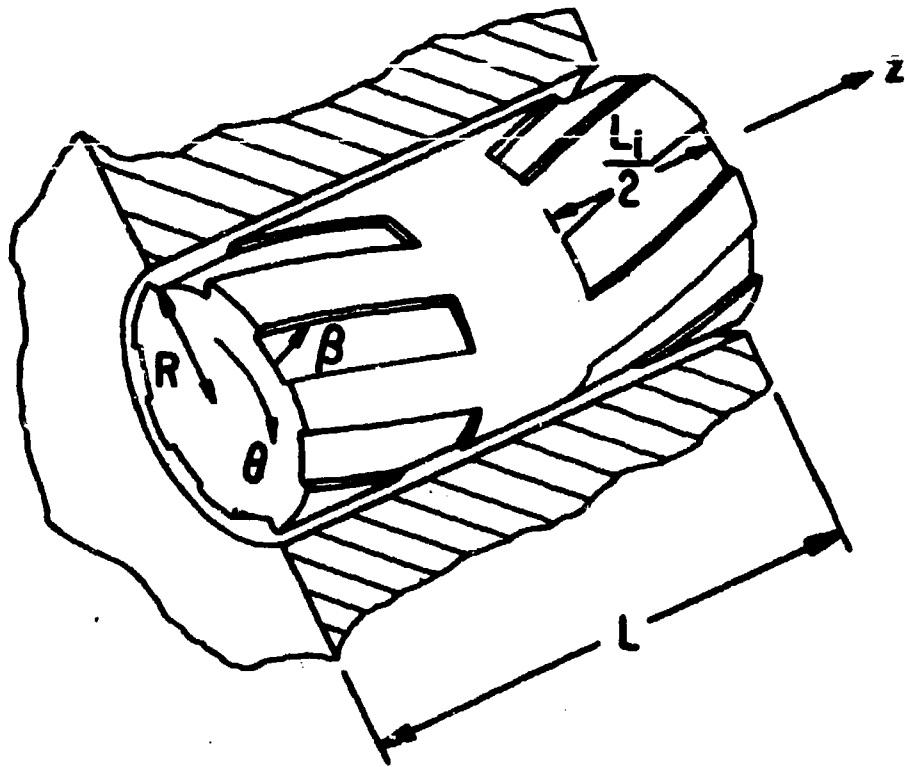
C_2/C_1	$\frac{P}{W} = \frac{PC_1}{HN_1R_1^2}$	$R_0 = \frac{2N_1R_1C_1}{\sqrt{L}}$	e_1	\bar{R}_{xx1}	\bar{R}_{yy1}	\bar{R}_{xz1}	\bar{R}_{yx1}	\bar{R}_{xy1}	\bar{R}_{yz1}	\bar{R}_{zy1}	\bar{R}_{xx2}	\bar{R}_{yy2}	\bar{R}_{xz2}	\bar{R}_{yx2}	\bar{R}_{xy2}	\bar{R}_{yz2}	\bar{R}_{zy2}	$(M_c)_1 = \frac{M_c(N_1+N_2)C_1}{2L}$	$(M_c)_2 = \frac{M_c(N_1+N_2)C_2}{2L}$			
1.2	0	LAM	.2	1.10	1.07	1.72	-1.58	1.07	3.19	.165	-0.15	3.27	3.45	1.94	-1.32	2.43	3.08	.377	.225	2.65	.109	.258
			.3	1.30	1.36	1.81	-1.52	1.36	3.14	.453	.321	3.36	5.15	2.90	-1.70	2.85	4.43	.925	.670	3.28	.129	.363
			.5	2.45	2.07	2.64	-1.38	2.07	3.93	1.32	1.05	3.46	17.5	9.69	-2.55	4.53	21.0	8.29	8.37	7.34	.181	1.24
1.2	0	1000	.2	1.43	1.34	1.67	-1.58	1.34	3.13	.174	-0.23	3.14	3.54	1.51	-1.37	2.94	2.68	.220	.063	2.38	.134	.266
			.3	1.50	1.39	1.84	-1.65	1.39	3.32	.292	-0.64	3.34	4.20	1.90	-1.83	3.00	3.49	.507	.282	2.70	.143	.270
			.5	2.36	2.01	2.37	-1.63	2.01	4.02	.95	.620	3.78	31.8	17.5	-2.81	4.39	81.6	40.3	46.8	28.2	.211	1.59
1.2	0	5000	.2	2.86	2.72	2.75	-2.60	2.72	5.18	.253	-0.61	5.17	7.16	2.44	-1.93	5.95	4.16	.240	.014	3.81	.272	.605
			.3	3.23	2.92	3.07	-2.56	2.92	5.44	.404	.048	5.40	7.76	2.67	-2.65	6.21	5.00	.479	.173	4.09	.299	.557
			.5	3.85	3.09	3.55	-3.01	3.09	6.45	.991	.492	6.26	13.8	5.93	-4.89	6.26	14.9	3.47	3.06	5.68	.341	.869
1.2	0	9000	.2	4.15	3.97	3.97	-3.28	3.97	7.09	.315	-0.55	7.06	9.30	2.97	-2.98	8.44	5.81	.342	.062	5.22	.403	.789
			.3	4.42	3.96	3.96	-3.76	3.97	7.58	.680	.167	7.48	11.3	3.72	-3.41	8.93	6.90	.624	.239	5.66	.415	.880
			.5	6.30	5.67	5.67	-4.16	4.34	9.07	1.47	.829	8.76	17.4	7.10	-6.11	9.34	16.5	3.55	3.18	7.84	.471	1.22
1.2	4.2	LAM	.2	2.14	1.96	1.51	-1.42	1.96	3.28	.172	-0.16	3.19	5.00	1.15	-1.09	4.08	2.85	.169	.025	2.41	.259	.748
			.3	2.42	2.03	1.71	-1.51	2.03	3.59	.318	.129	3.39	6.31	1.53	-1.52	4.44	3.72	.316	.126	2.67	.271	.895
			.5	3.51	2.26	2.47	-1.97	2.26	4.82	.916	.593	4.12	11.1	3.60	-5.54	4.85	11.2	2.4	1.90	4.50	.314	.750
1.2	5.13	1000	.2	2.83	2.69	1.46	-1.44	2.69	3.18	.157	-0.40	3.09	5.91	1.04	-1.13	5.41	2.57	.115	-.027	2.28	.331	.756
			.3	3.00	2.70	1.57	-1.57	2.70	3.43	.254	-0.26	3.21	6.46	1.24	-1.58	5.56	3.18	.217	.023	2.46	.331	.675
			.5	3.66	2.80	2.02	-2.14	2.80	4.48	.668	.331	3.76	15.6	5.34	-4.74	5.27	20.9	4.80	4.96	4.66	.333	1.28
1.2	10.0	5000	.2	5.38	5.12	2.45	-2.38	5.12	5.24	.227	-0.87	5.11	11.3	1.76	-1.75	10.2	4.07	.154	-.060	3.74	.618	1.47
			.3	6.25	5.33	2.87	-2.26	5.33	5.57	.344	-0.11	5.27	12.2	1.94	-2.39	10.9	4.79	.262	-.019	3.93	.687	1.29
			.5	6.47	5.44	3.03	-3.34	5.44	6.85	.801	.302	5.85	13.0	2.91	-7.31	10.5	12.0	1.74	1.22	5.32	.619	.937
1.2	14.2	9000	.2	8.00	6.99	3.75	-2.82	6.99	7.17	.282	-0.89	6.99	15.1	2.22	-2.49	14.6	5.69	.212	-.051	5.12	.932	1.02
			.3	7.73	7.33	3.41	-3.62	7.33	7.79	.506	-0.63	7.25	19.7	3.09	-3.12	14.8	6.64	.359	.012	5.39	.987	1.22
			.5	10.5	7.42	4.98	-4.44	7.42	9.65	1.19	.551	8.12	18.9	3.86	-6.00	15.5	13.2	1.58	.905	6.91	.902	1.40

TABLE 5 DYNAMIC PERFORMANCE DATA FOR THE FLOATING RING JOURNAL BEARING

C_2/C_1	$\frac{P}{\mu} = \frac{P C_1^2}{\mu N L D_1}$	$Re = \frac{2\pi N R_1 C_1}{\nu}$	ϵ_1	K_{xx}	K_{xy}	K_{yx}	K_{yy}	B_{xx}	B_{yy}	B_{yx}	B_{yy}	$\frac{M C_1^2}{L D_1} \left(\frac{C_1}{R_1} \right)^2$	$(\nu/\omega)_c$
1.2	0	LAN	.2	.785	.762	-.616	.637	1.32	.629	0	1.41	.084	.50
			.3	1.00	.928	-.653	.745	1.52	.990	.123	1.64	.102	.50
			.5	2.69	2.05	-.33	1.28	2.09	2.61	.833	2.23	.530	.29
1.2	0	1000	.2	.909	.652	-.592	.782	1.29	.541	-.041	1.31	.106	.48
			.3	1.06	.790	-.676	.799	1.51	.743	.020	1.46	.113	.49
			.5	3.18	2.42	.006	1.58	.199	2.82	.859	2.43	.174	.57
1.2	0	5000	.2	1.81	1.04	-.928	1.58	2.10	.842	-.087	2.16	.223	.46
			.3	1.97	1.15	-.985	1.62	2.40	1.03	-.021	2.28	.244	.45
			.5	3.44	2.07	-1.27	1.71	3.84	2.40	.555	2.92	.356	.44
1.2	0	9000	.2	2.44	1.38	-1.19	2.23	2.97	1.09	-.089	2.93	.337	.43
			.3	2.85	1.58	-1.45	2.34	3.33	1.40	-.016	3.20	.336	.46
			.5	4.88	2.91	-1.72	2.49	5.38	3.15	.697	4.10	.538	.42
1.2	4.2	LAN	.2	1.26	.528	-.492	1.06	1.44	.431	-.039	1.36	.243	.36
			.3	1.51	.655	-.588	1.11	1.73	.607	.004	1.48	.258	.37
			.5	2.72	1.34	-.965	1.20	3.30	1.60	.417	2.19	.453	.33
1.2	5.13	1000	.2	1.54	.473	-.482	1.42	1.38	.392	-.051	1.31	.315	.35
			.3	1.68	.542	-.582	1.44	1.62	.506	-.038	1.39	.308	.36
			.5	3.71	1.47	-.688	1.44	3.18	1.96	.514	1.98	-1.33	.21
1.2	10	5000	.2	2.97	.802	-.784	2.74	2.25	.637	-.097	2.18	.595	.35
			.3	3.17	.869	-.814	2.76	2.53	.744	-.063	2.20	.649	.34
			.5	4.11	1.32	-1.63	2.80	4.83	1.65	.312	2.88	.693	.36
1.2	14.2	9000	.2	4.00	1.08	-.938	3.69	3.10	.808	-.098	2.88	.907	.33
			.3	4.84	1.28	-1.34	3.99	3.51	1.14	-.067	3.18	.830	.37
			.5	5.77	1.80	-2.05	3.95	6.18	2.09	.261	3.77	.999	.35

TABLE 5 (continued)

Q_2/c_1	\bar{z}	H_c	ϵ_1	K_{xx}	K_{xy}	K_{yx}	K_{yy}	B_{xx}	B_{xy}	B_{yx}	B_{yy}	H_c	$(v/w)_c$
0.8	0	LAN	.2	1.21	1.31	-1.15	1.09	2.04	.794	-.096	2.25	.105	.57
			.3	1.39	1.43	-1.12	1.24	2.18	1.08	.016	2.46	.127	.56
			.5	2.43	2.12	-1.07	1.77	2.88	2.26	.572	2.79	.179	.57
0.8	0	1000	.2	1.41	1.19	-1.13	1.31	1.94	.799	-.120	2.11	.122	.58
			.3	1.56	1.32	-1.18	1.33	2.08	.956	-.067	2.23	.127	.58
			.5	2.16	1.77	-1.21	1.62	2.76	1.82	.294	2.72	.178	.55
0.8	0	5000	.2	2.67	1.82	-1.73	2.52	3.11	1.19	-.179	3.33	.241	.55
			.3	3.03	2.06	-1.54	2.72	3.42	1.50	-.105	3.49	.301	.52
			.5	3.53	2.44	-2.15	2.65	4.14	2.09	.148	4.00	.278	.57
0.8	0	9000	.2	3.59	2.45	-2.38	3.48	4.24	1.44	-.201	4.49	.322	.55
			.3	4.31	2.91	-2.27	3.77	4.67	1.92	-.125	4.78	.382	.54
			.5	5.06	3.37	-3.01	3.71	5.58	2.73	.243	5.44	.376	.58
0.8	4.2	LAN	.2	1.90	1.03	-.95	1.71	2.28	.781	-.138	2.31	.266	.43
			.3	2.18	1.19	-1.03	1.77	2.52	.982	-.075	2.44	.278	.44
			.5	3.15	1.79	-1.40	1.90	3.46	1.74	.202	2.95	.318	.47
0.8	5.13	1000	.2	2.35	.946	-.939	2.21	2.19	.794	-.153	2.20	.337	.43
			.3	2.51	1.03	-1.03	2.23	2.40	.925	-.123	2.28	.335	.44
			.5	3.06	1.38	-1.47	2.22	3.20	1.45	.048	2.66	.328	.47
0.8	10.0	5000	.2	4.32	1.48	-1.45	4.11	3.43	1.16	-.210	3.44	.615	.43
			.3	4.94	1.68	-1.33	4.25	3.87	1.41	-.147	3.56	.781	.39
			.5	5.26	1.92	-2.19	4.27	4.88	1.95	-.025	3.97	.614	.46
0.8	14.2	9000	.2	6.14	2.16	-1.98	5.60	4.50	1.62	-.255	4.69	.781	.45
			.3	6.86	2.39	-1.90	5.87	5.26	1.82	-.180	4.83	.990	.41
			.5	7.34	2.64	-2.97	5.97	6.43	2.51	-.003	5.36	.819	.47



$$e = \frac{a_g}{a_j + a_r}$$

$$\Gamma = \frac{h_g}{h_r}$$

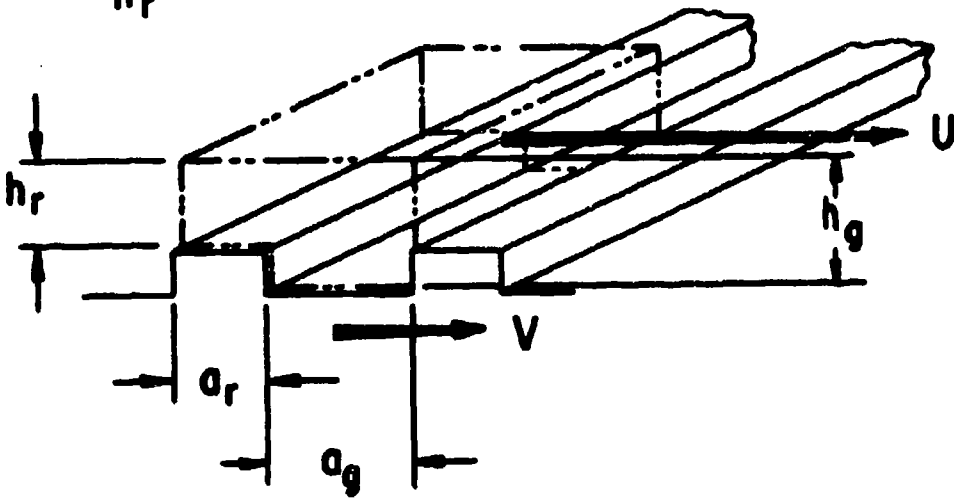


Figure 1. Schematic of Spiral-Grooved Journal Bearing

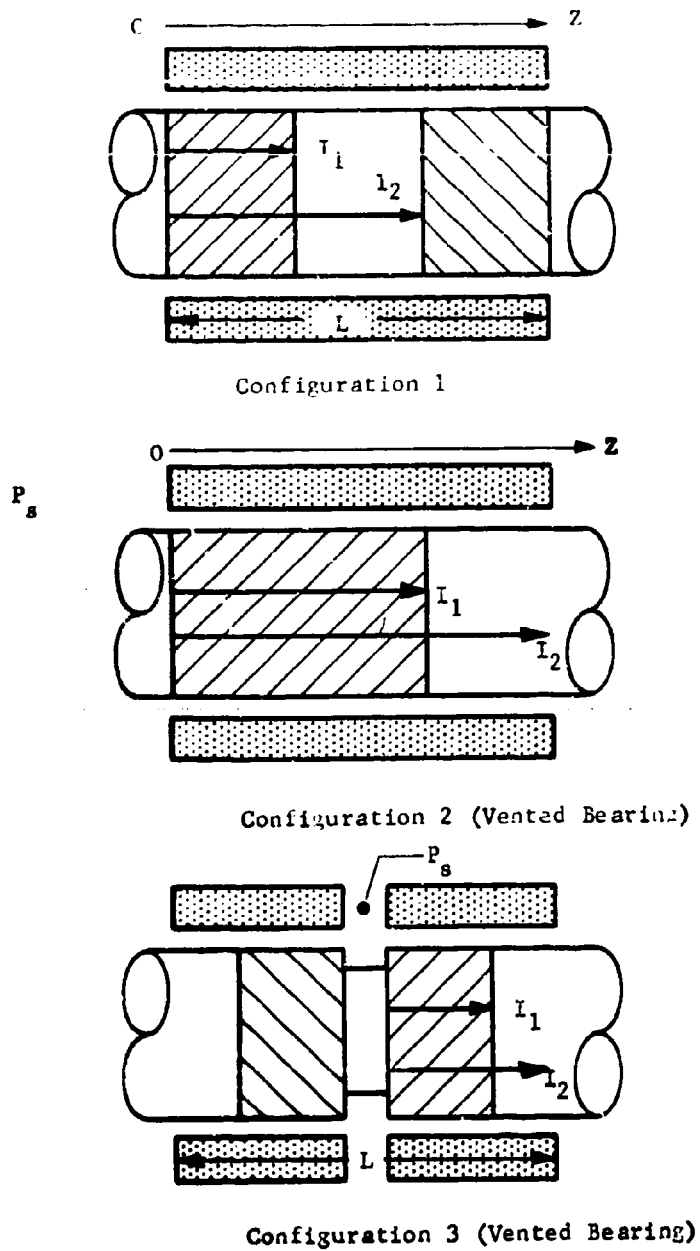


Figure 2. Various Configurations of Spiral-Grooved Journal Bearings

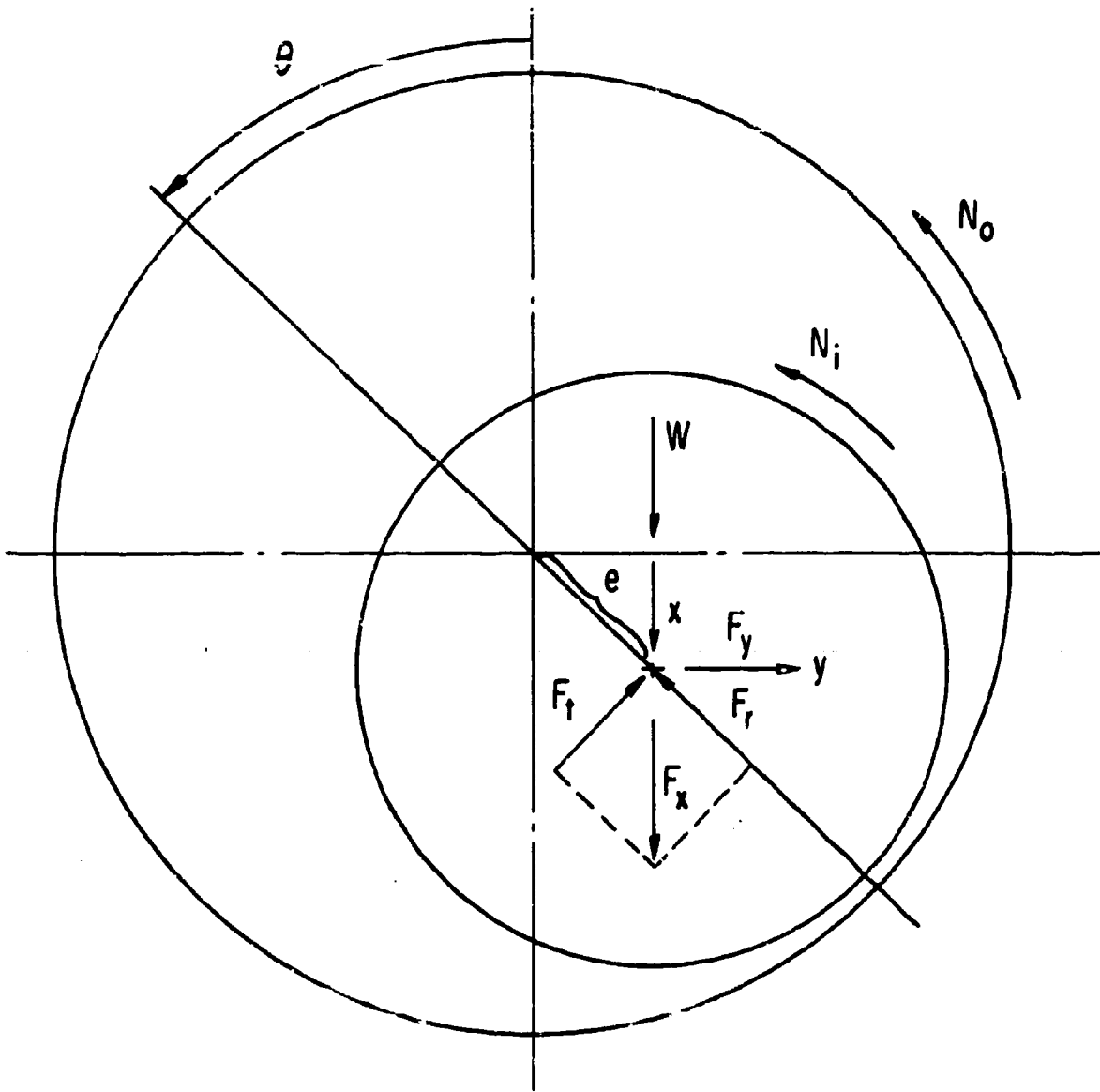


Figure 3. Coordinate System for Forces and Displacements

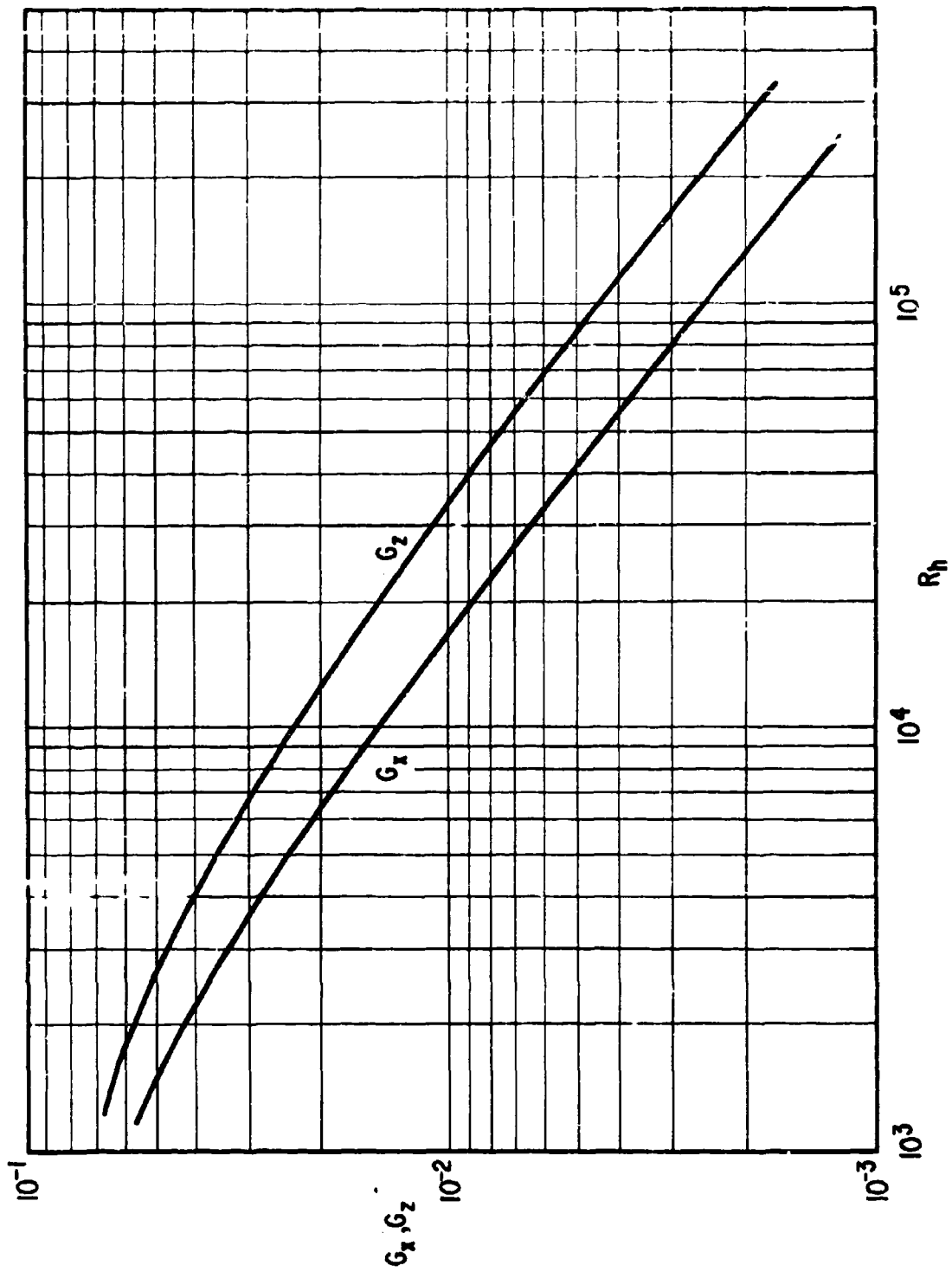


Figure 5. G_x and G_z vs. Local Reynolds Number R_h

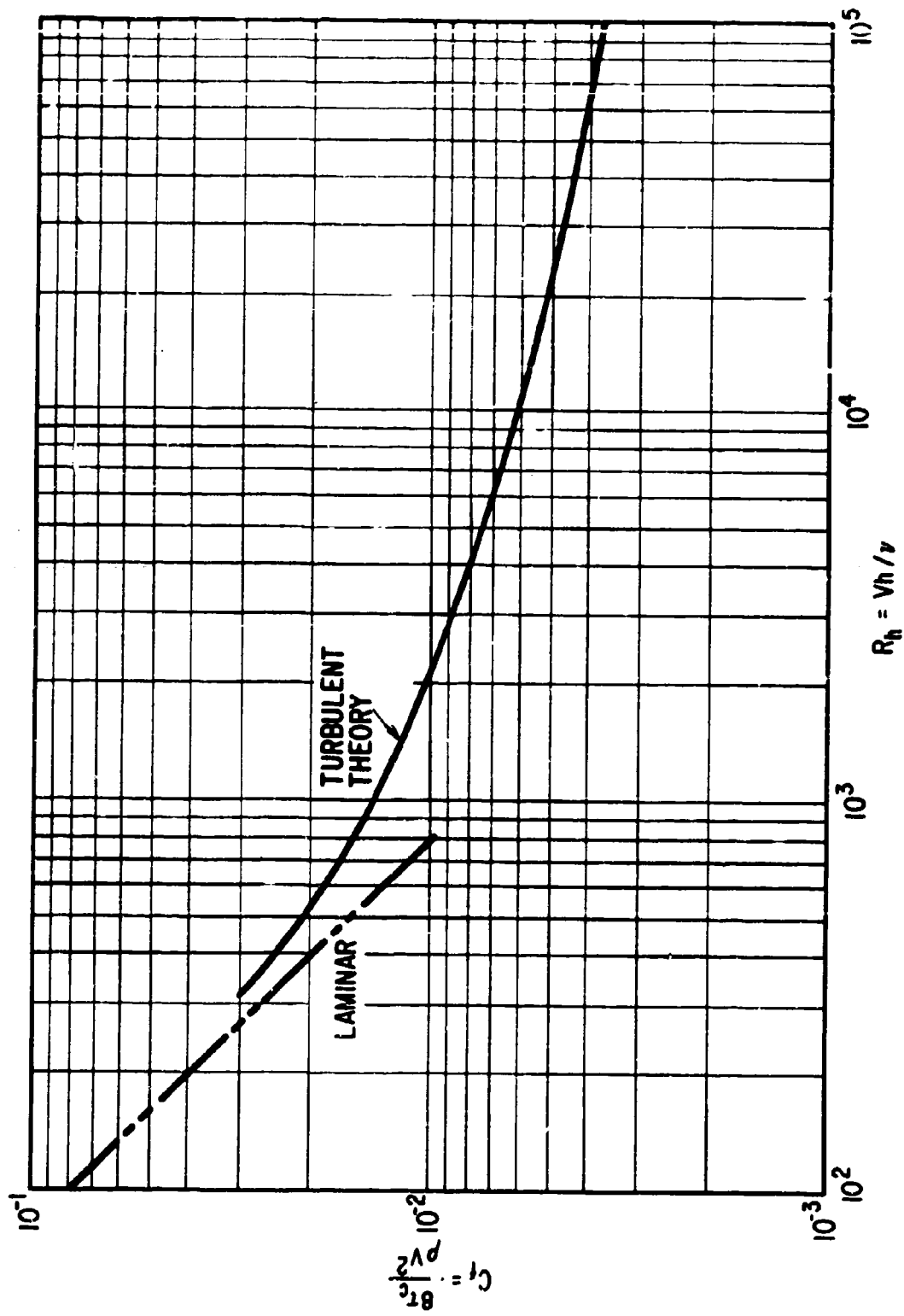


Figure 6. Coefficient of Friction vs. Local Reynolds Number R_h

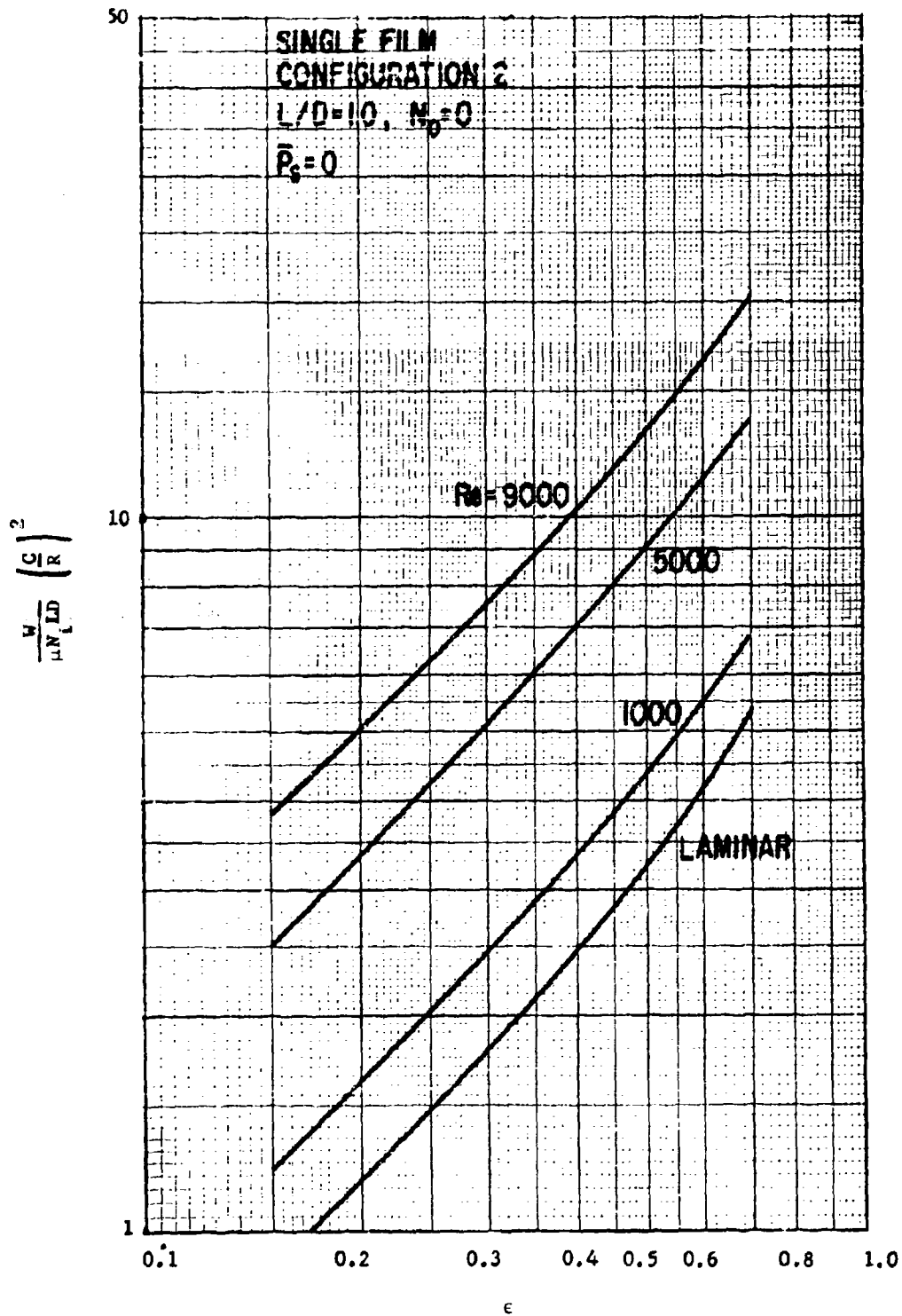


Figure 7. Load vs. Eccentricity, Single Film Bearing

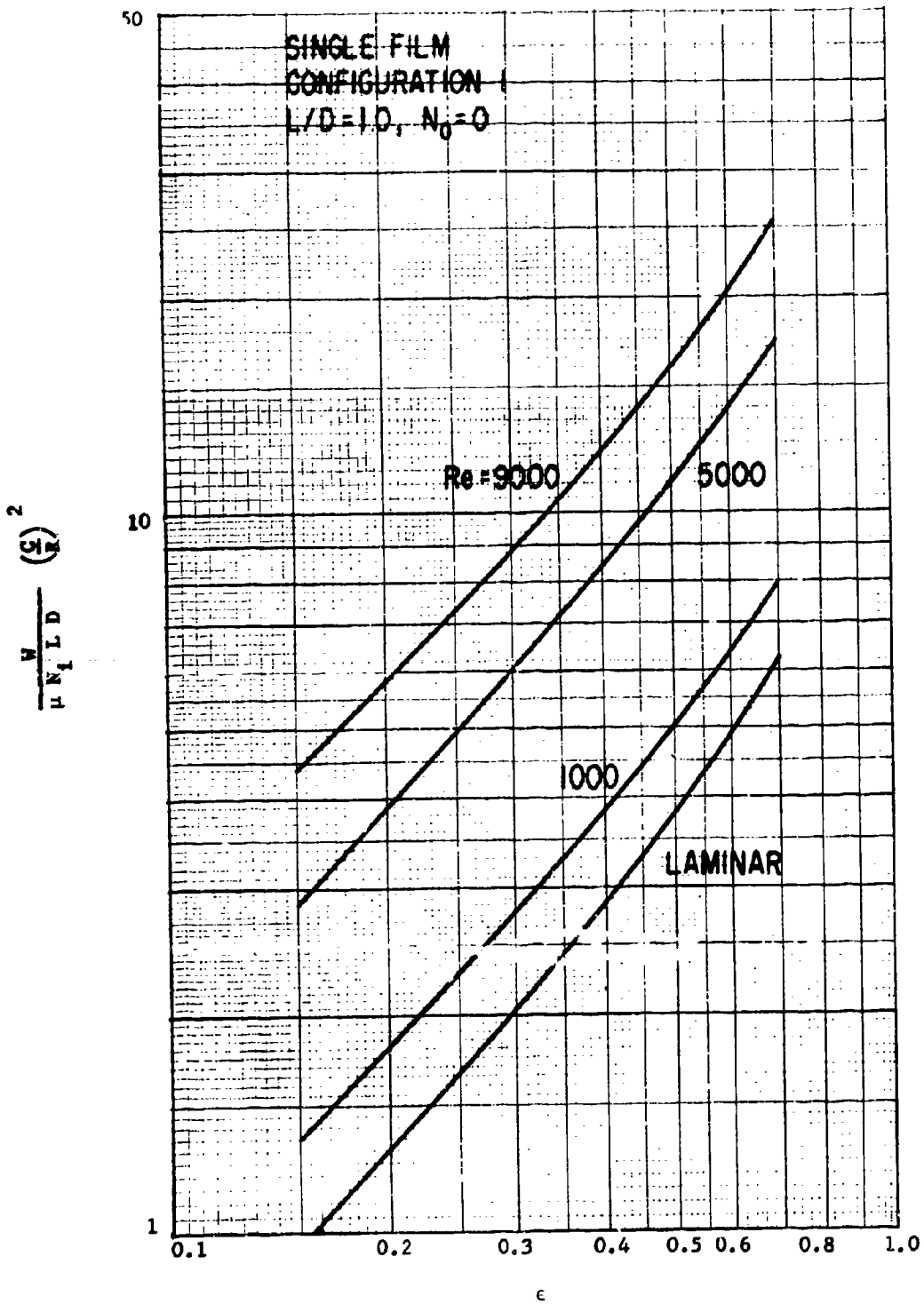


Figure 8. Load vs. Eccentricity, Single Film Bearing

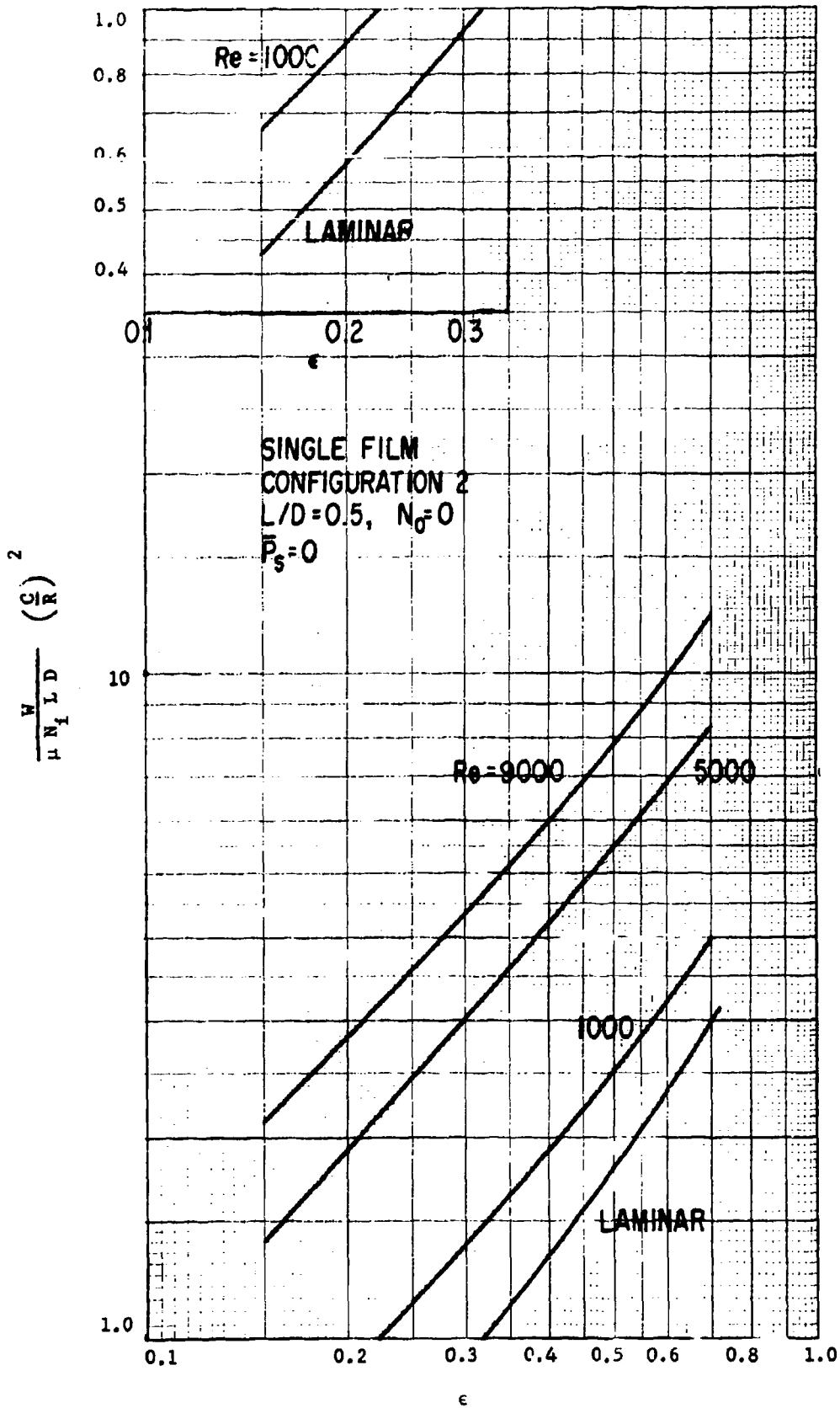


Figure 9. Load vs. Eccentricity, Single Film Bearing

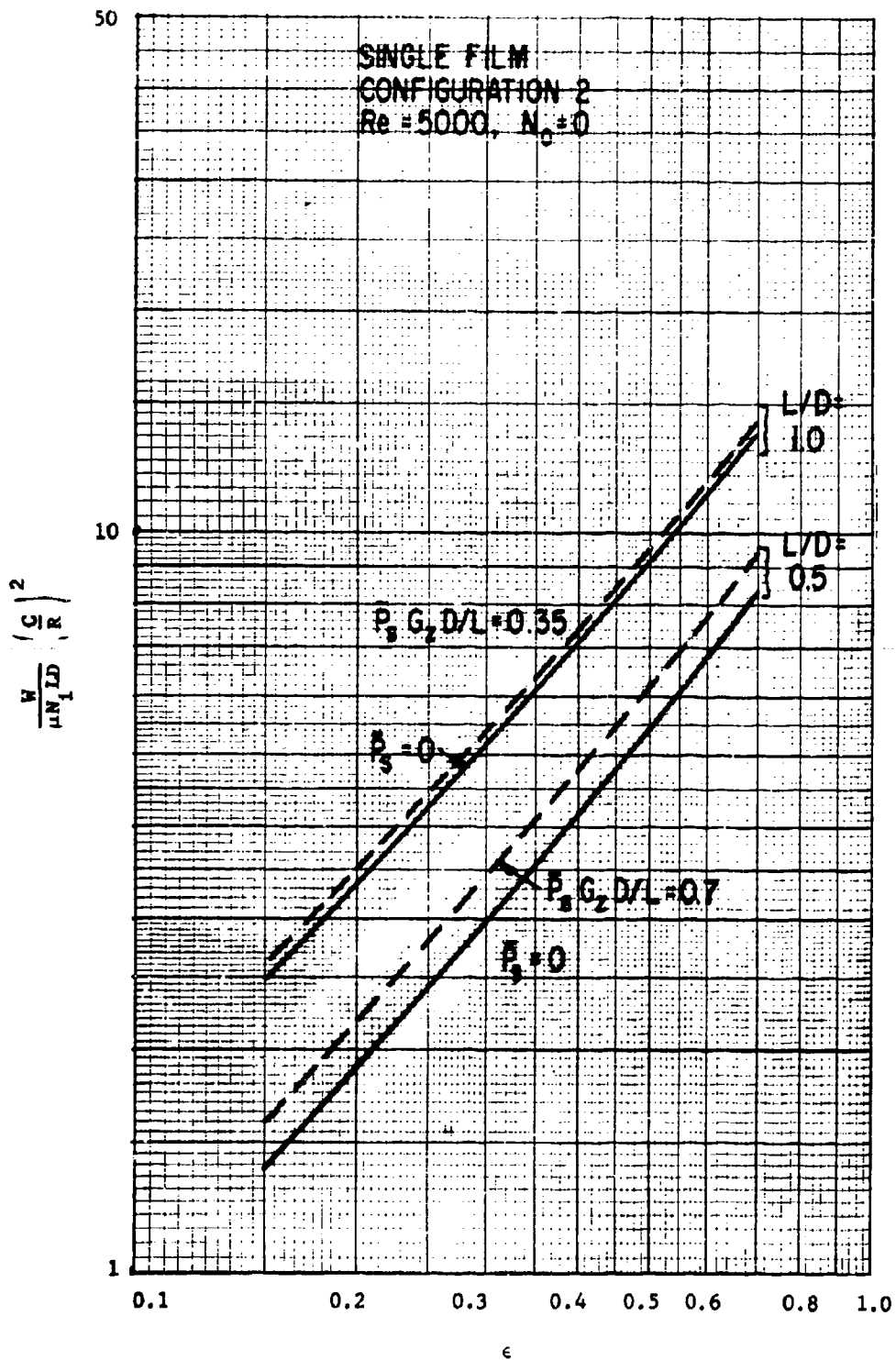


Figure 10. Load vs. Eccentricity, Effect of Pressurization

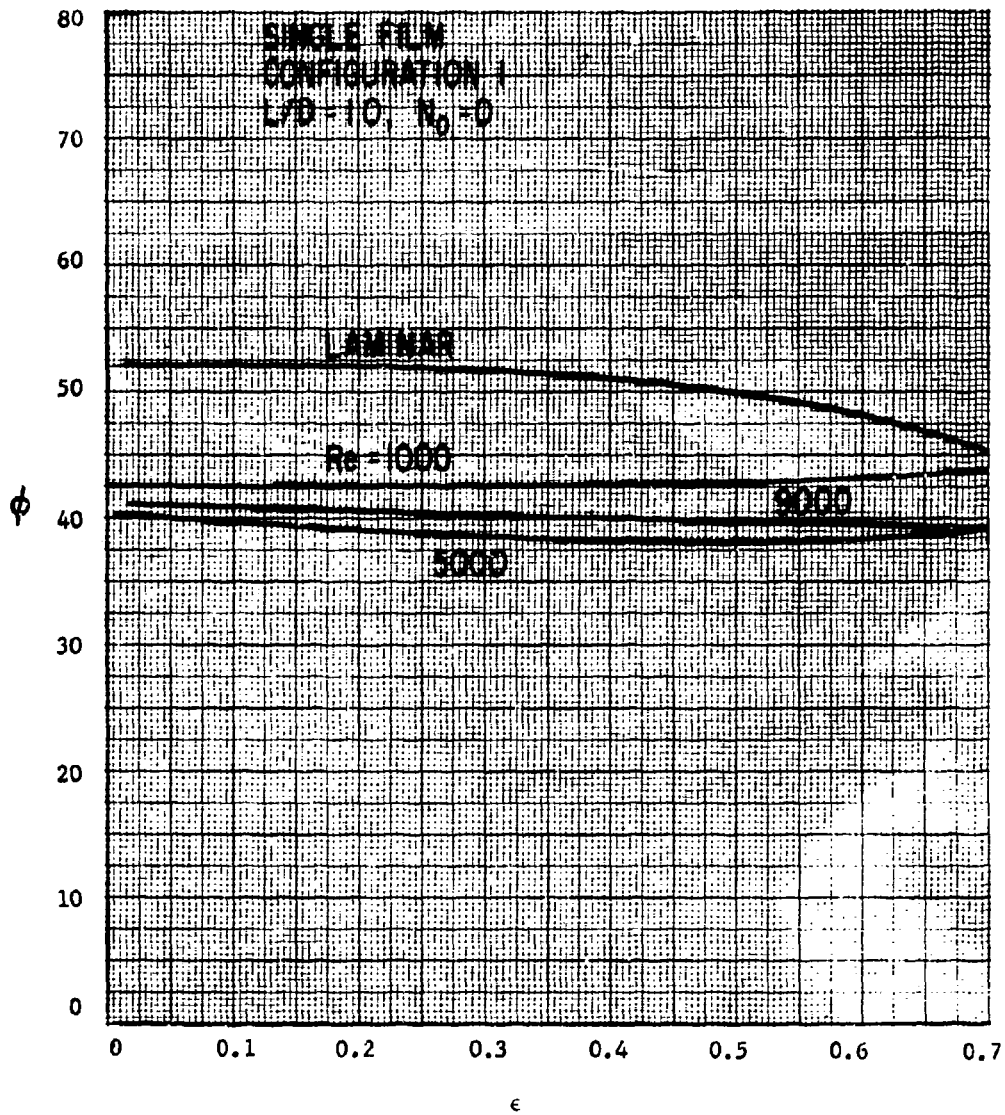


Figure 11. Attitude Angle vs. Eccentricity, Single Film Bearing

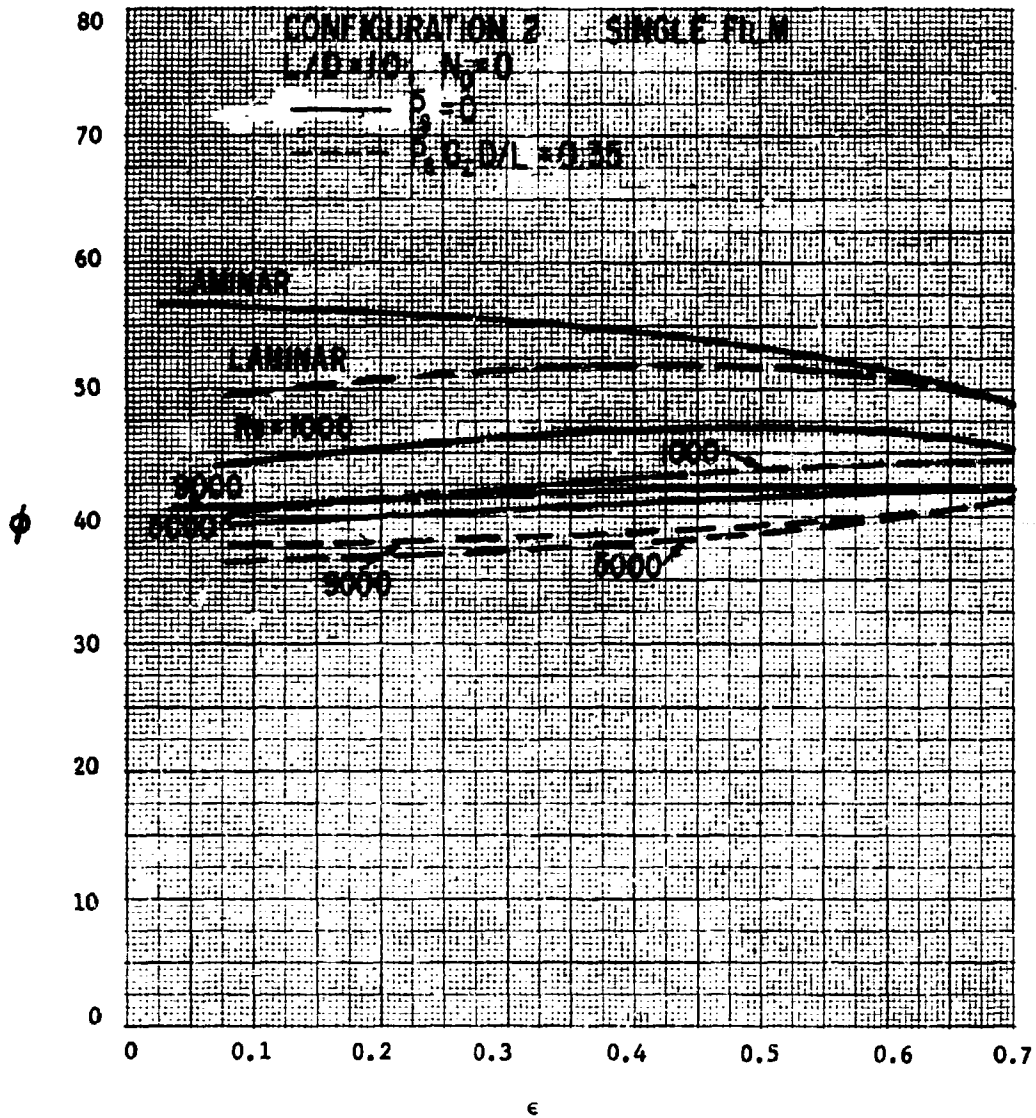


Figure 12. Attitude Angle vs. Eccentricity, Single Film Bearing

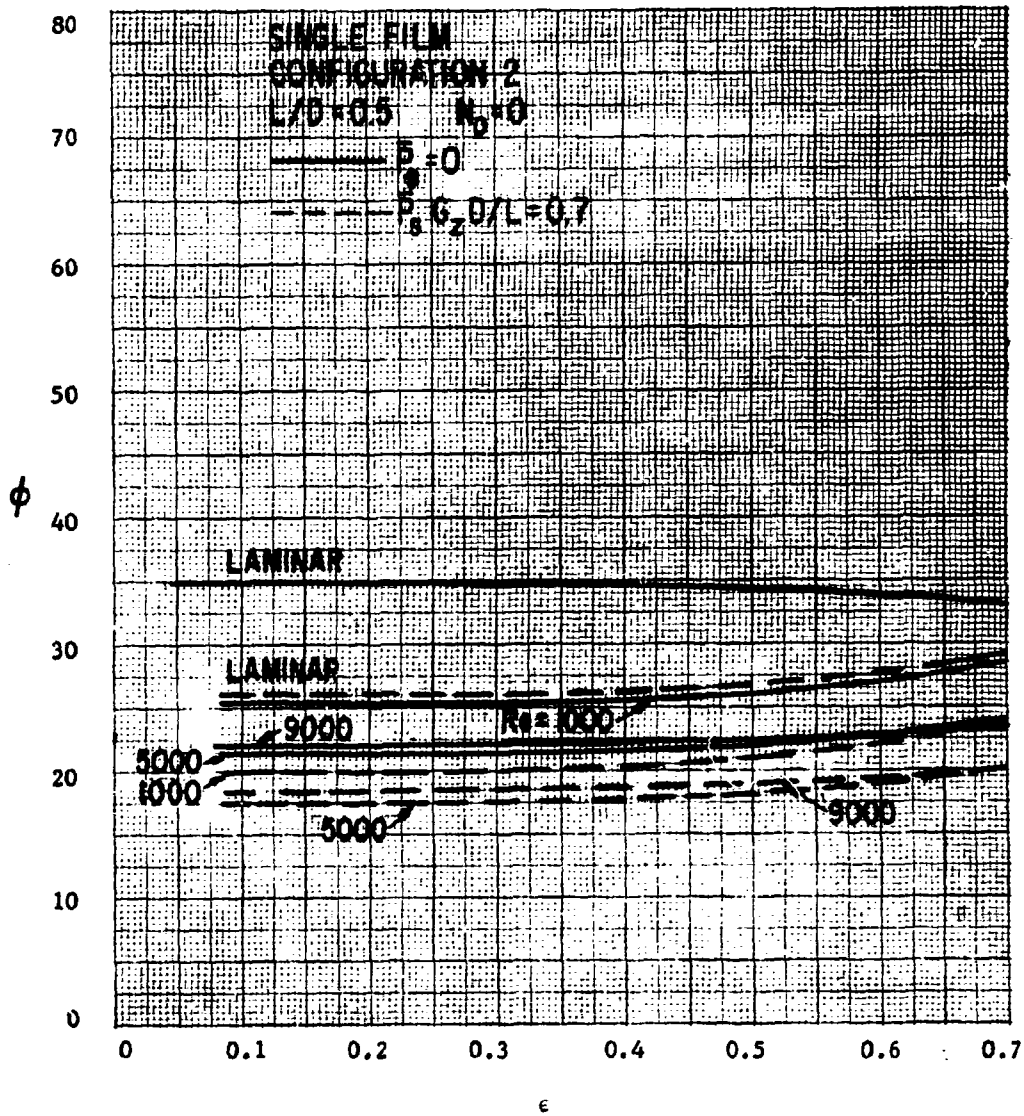


Figure 13. Attitude Angle vs. Eccentricity, Single Film Bearing

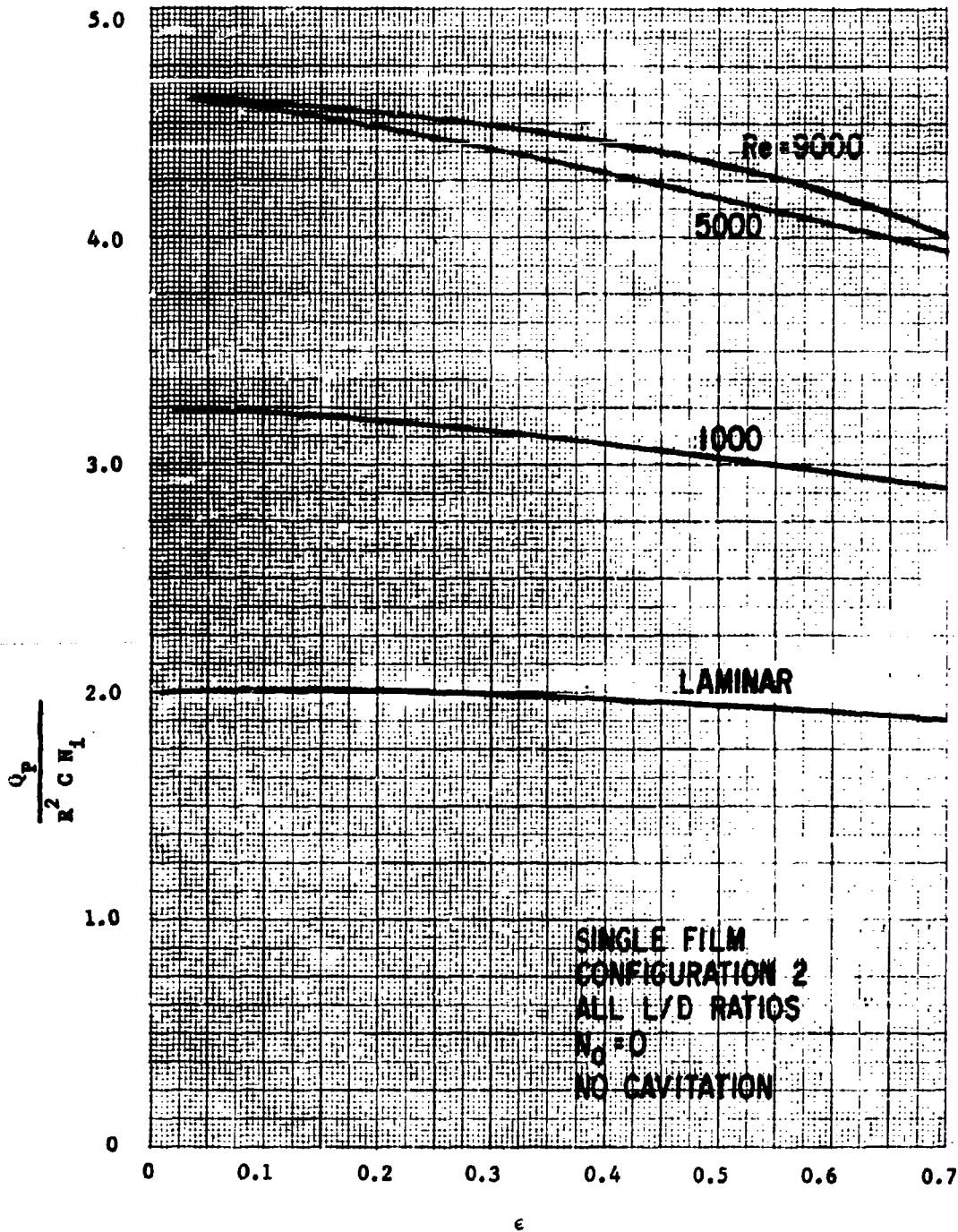


Figure 14. Single Film Bearing Flow Due to Self Pumping Effect of Spiral Grooves

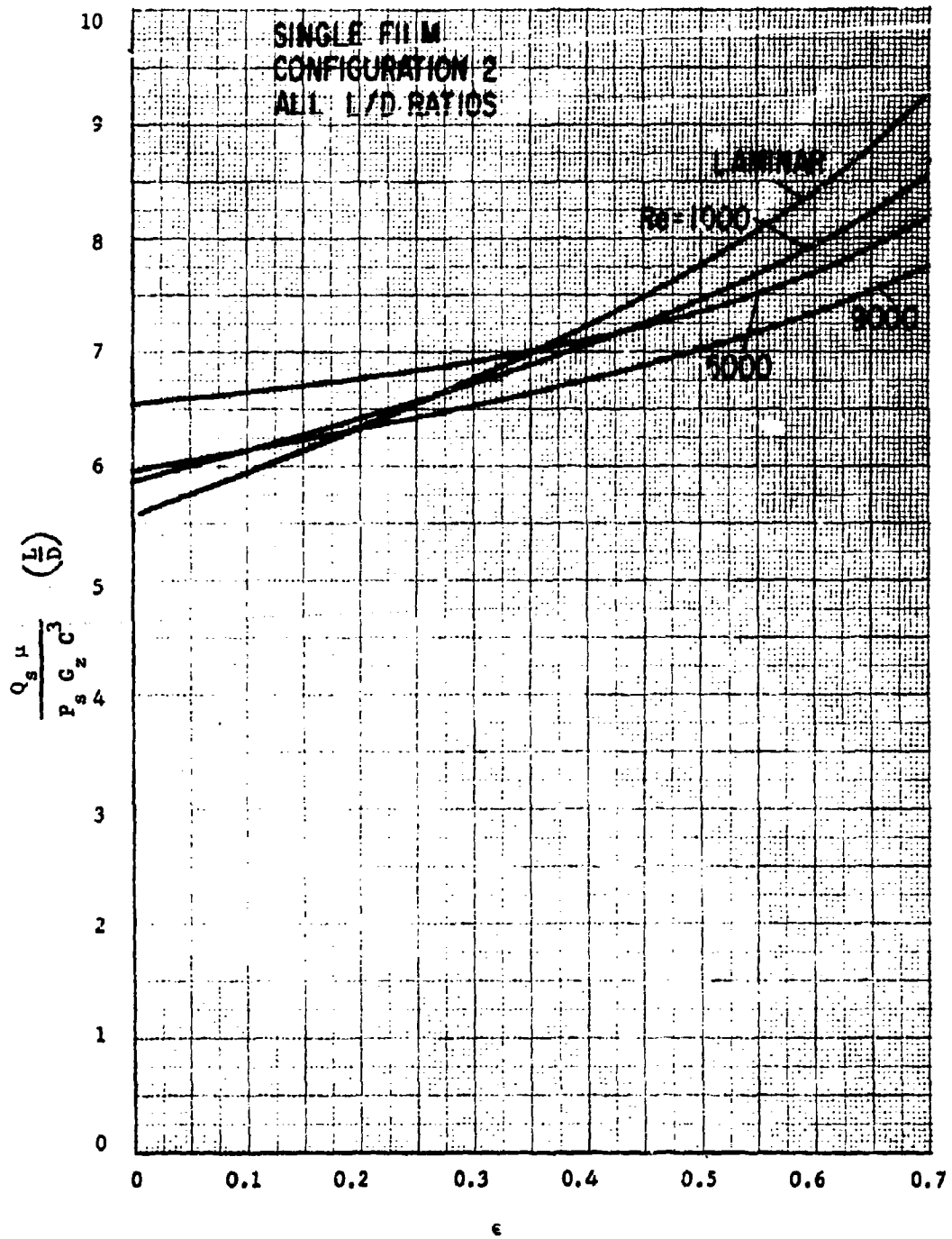


Figure 15. Single Film Bearing Flow Due to Pressurized Supply

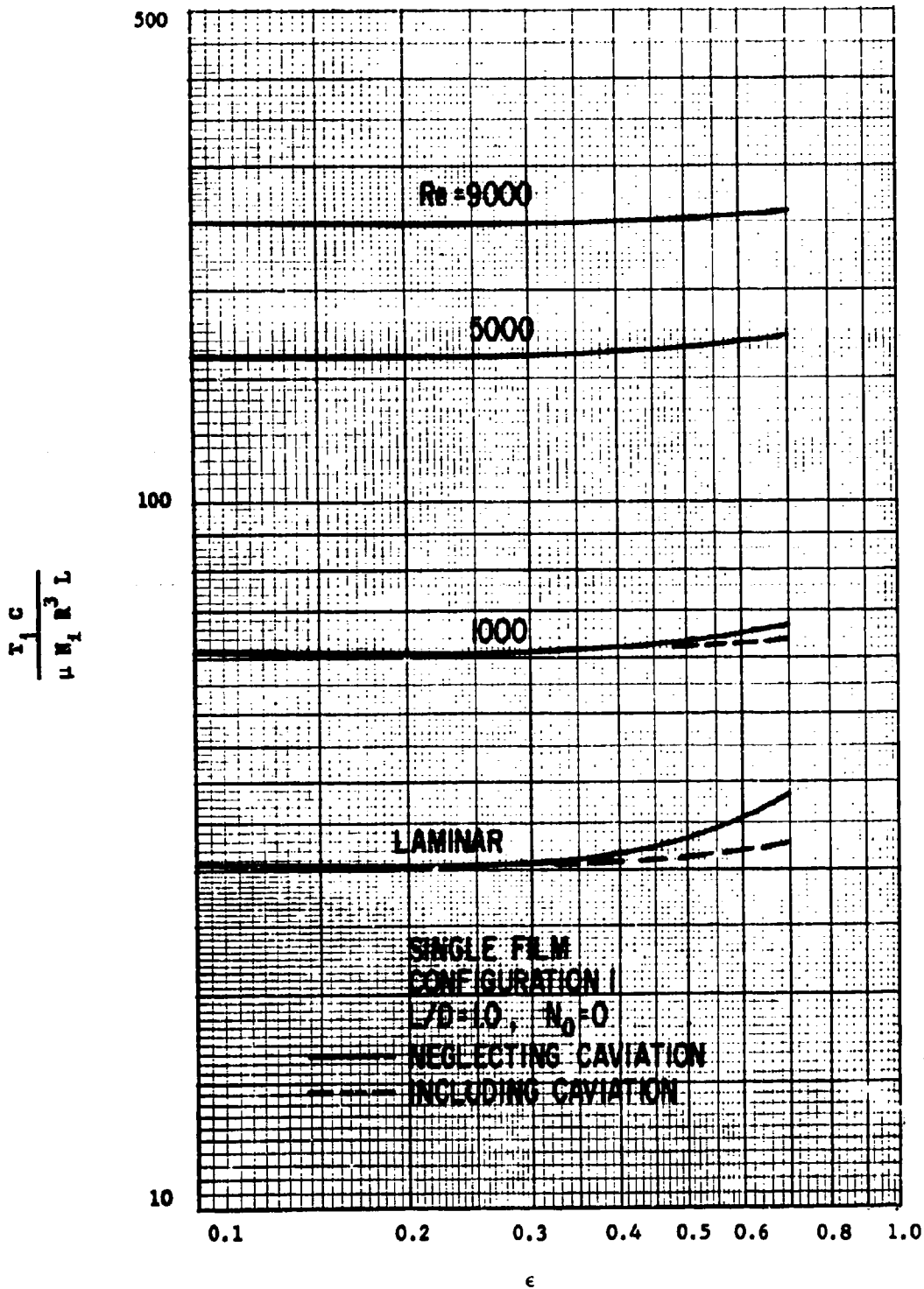


Figure 16. Torque vs. Eccentricity, Single Film Bearing

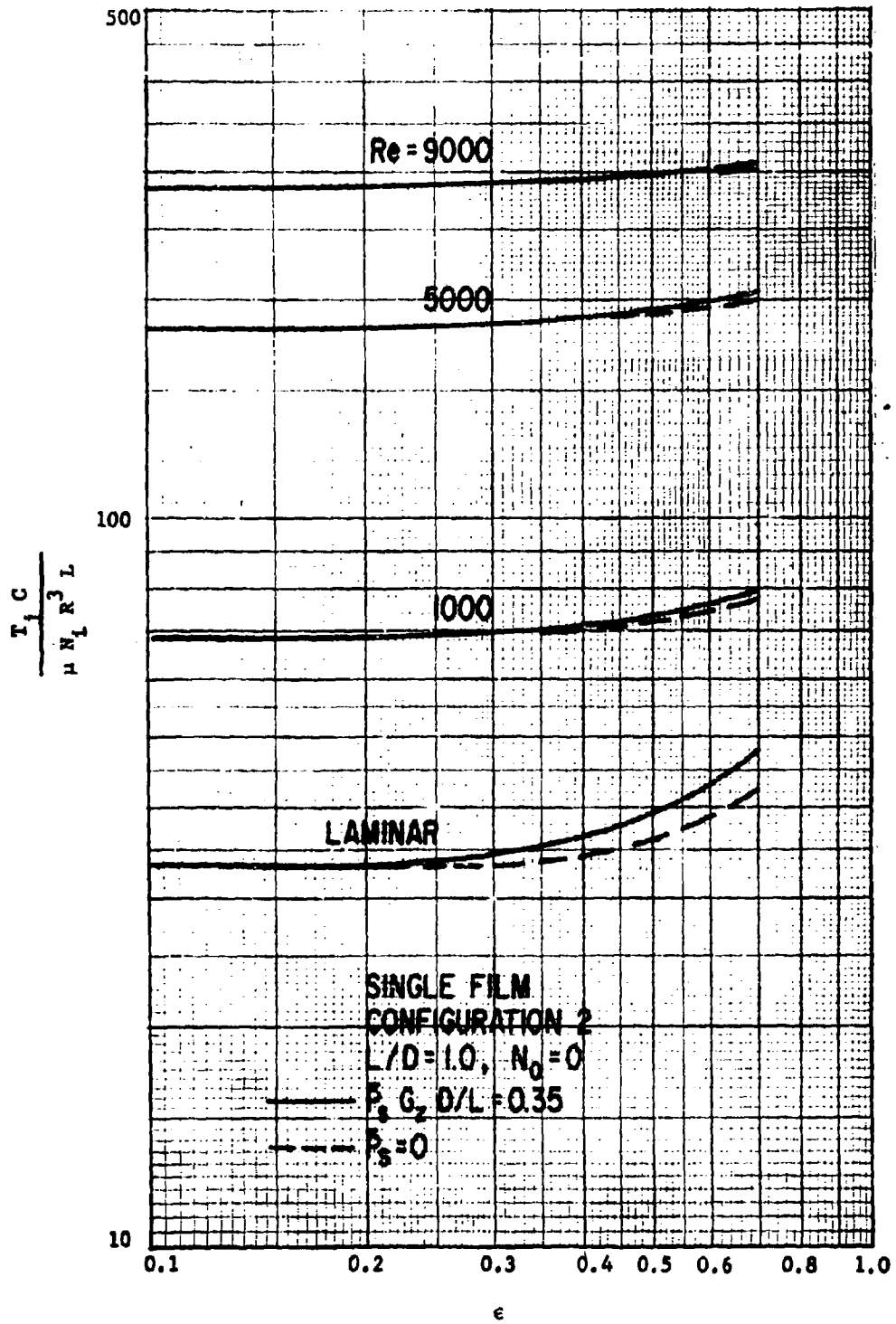


Figure 17. Torque vs. Eccentricity, Single Film Bearing

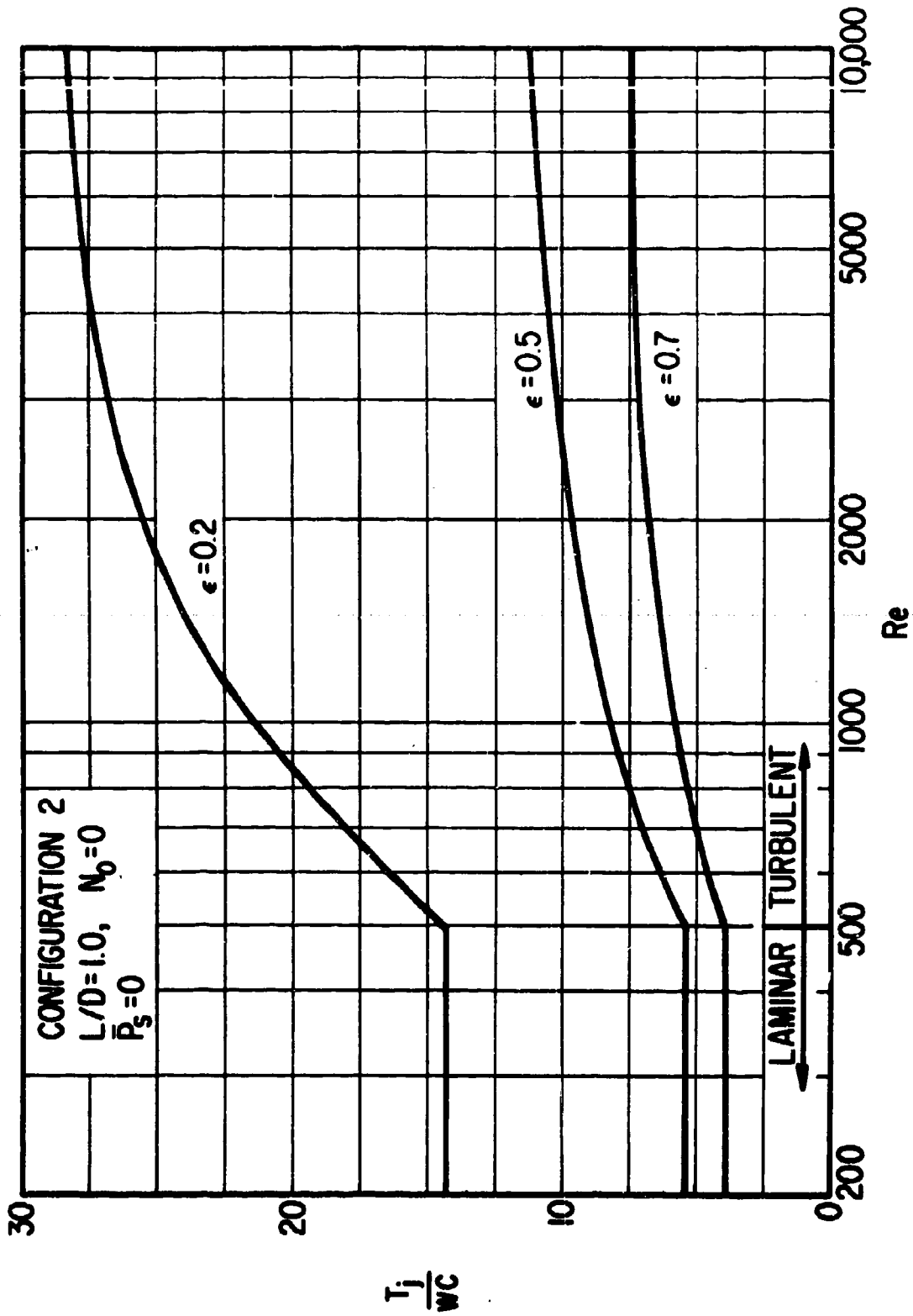


Figure 18. Torque to Load Ratio vs. Reynolds Number, Single Film Bearing

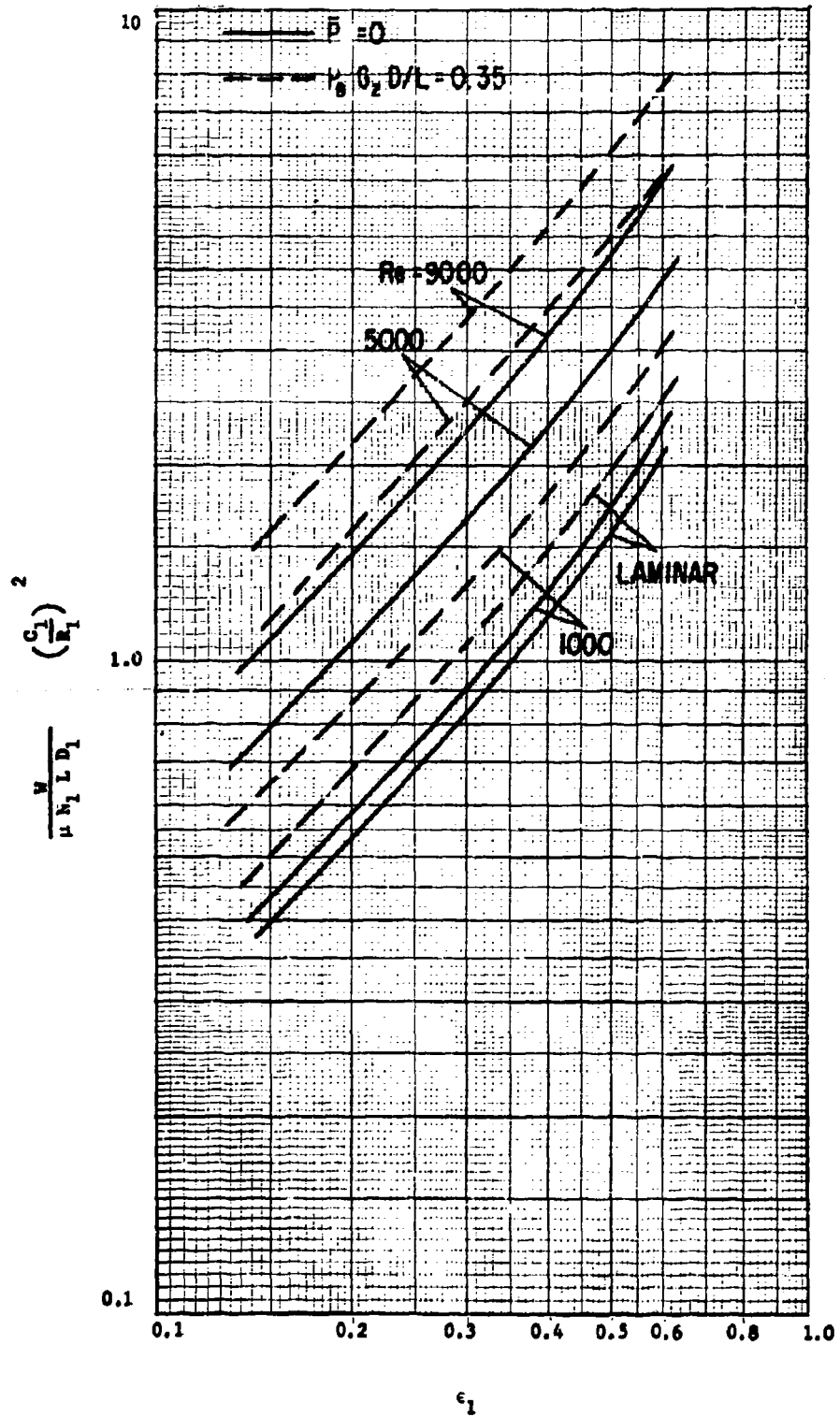


Figure 19. Load vs. Inner Film Eccentricity Ratio, Floating Ring Bearing

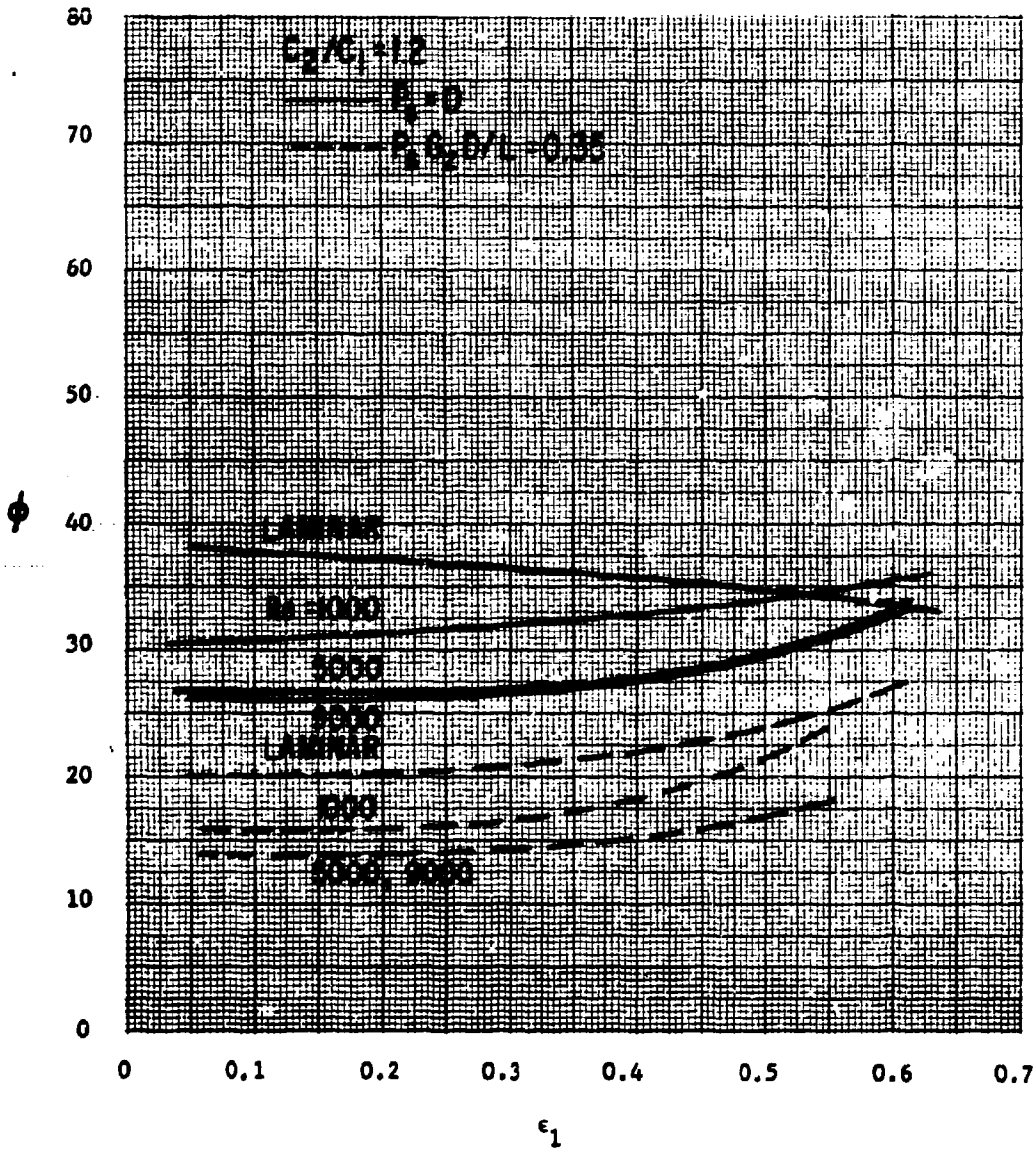


Figure 20. Attitude Angle vs. Inner Film Eccentricity Ratio, Floating Ring Bearing

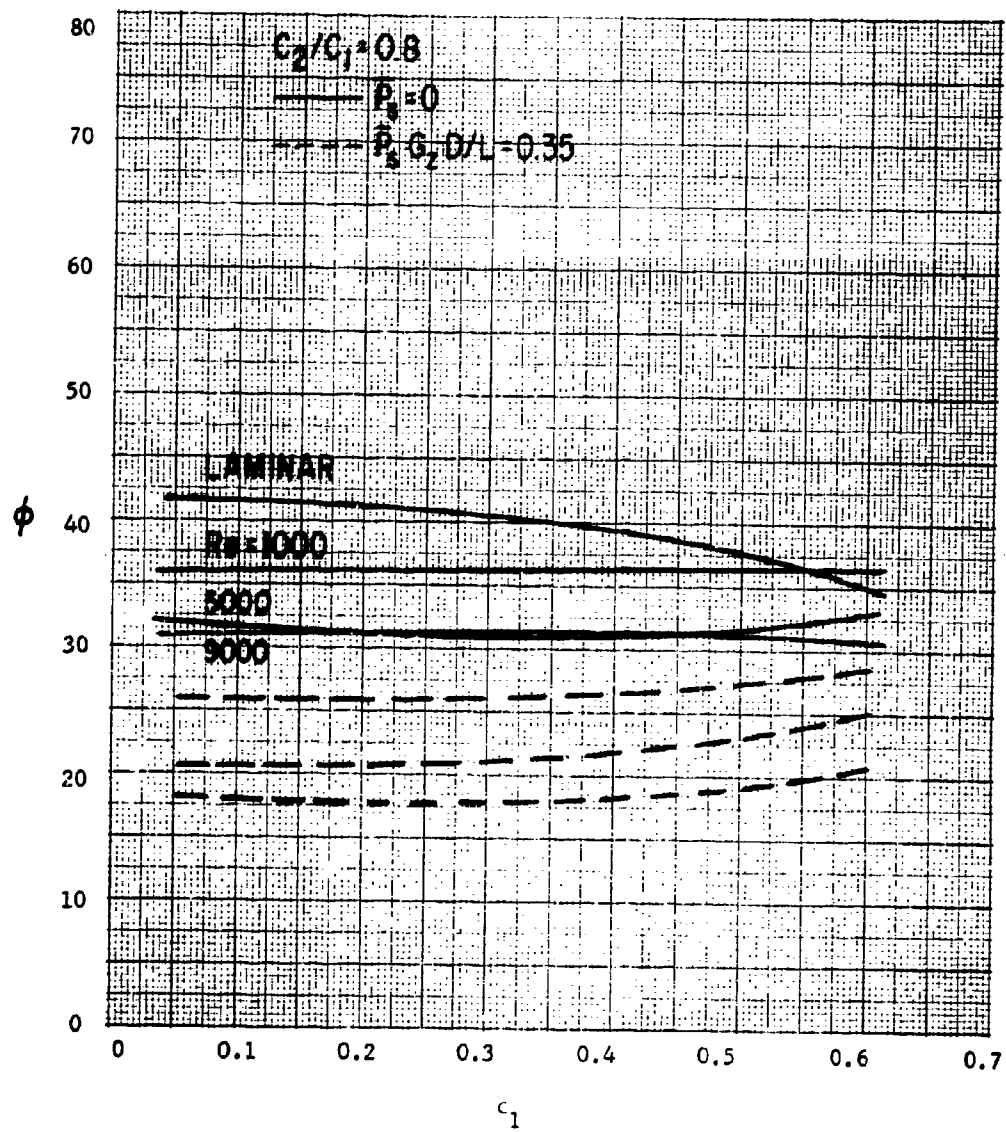


Figure 21. Attitude Angle vs. Inner Film Eccentricity Ratio, Floating Ring Bearing

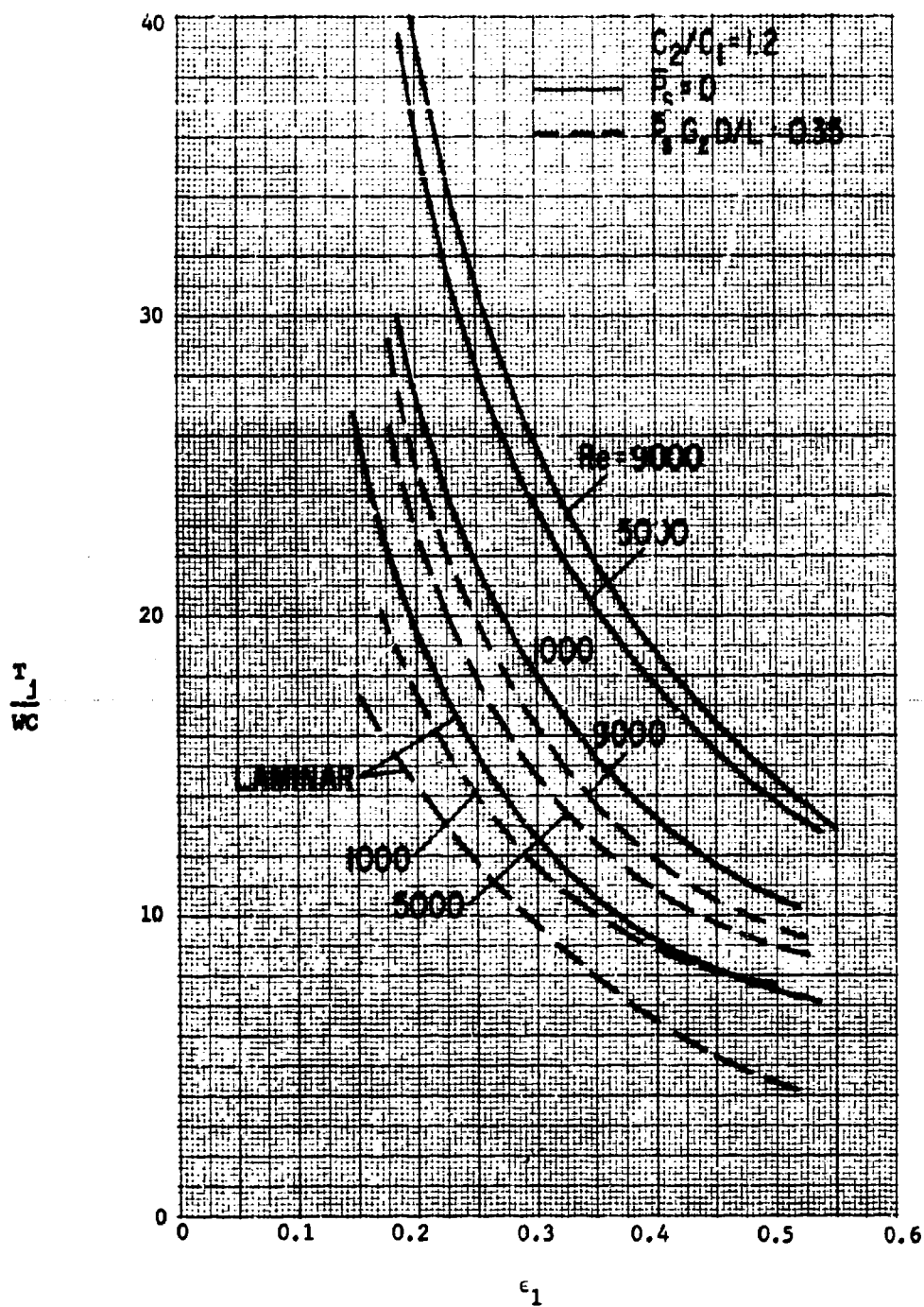


Figure 22. Torque to Load Ratio vs. Inner Film Eccentricity, Floating Ring Bearing

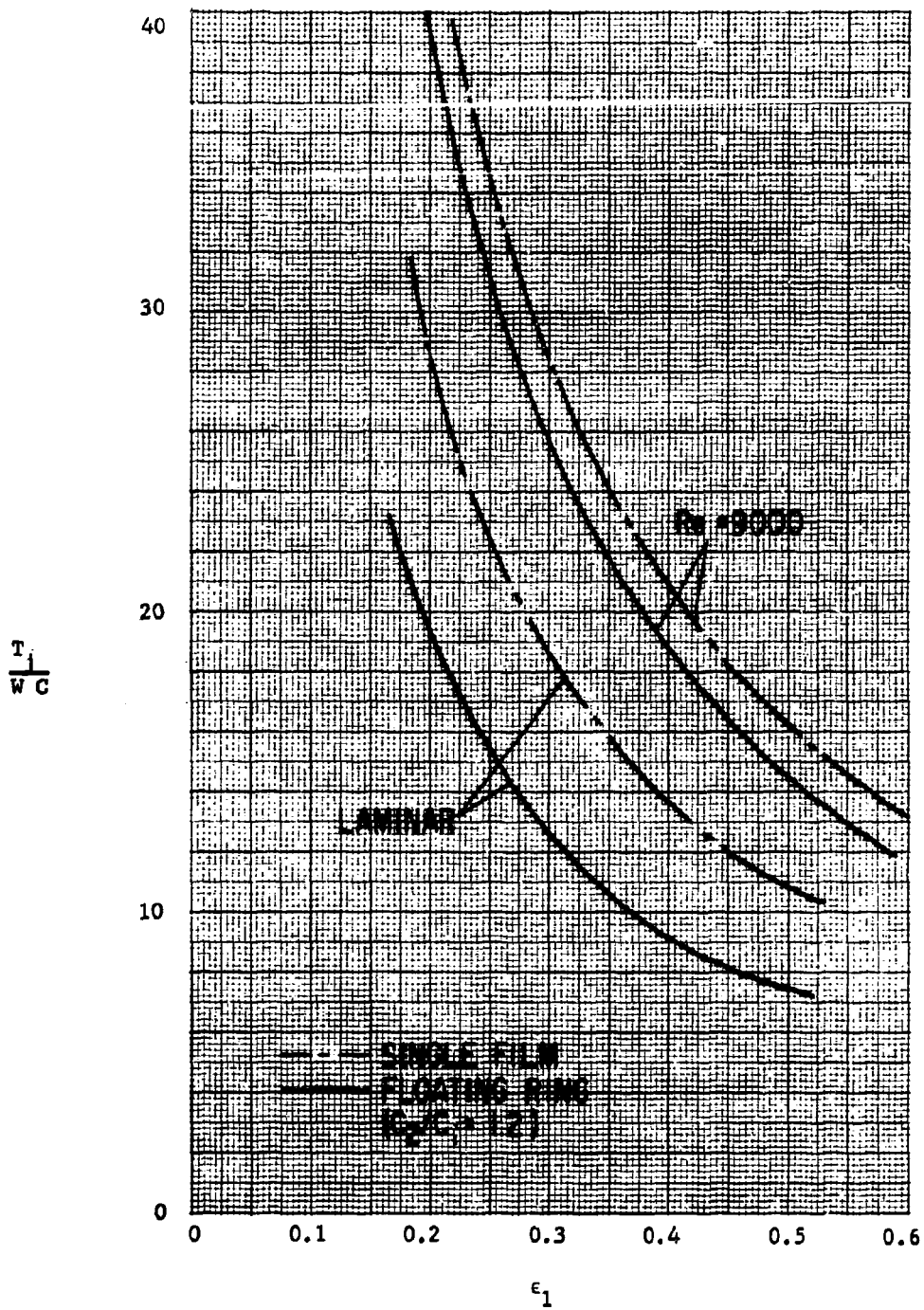


Figure 23. Torque to Load Ratio, Comparison between Single Film and Floating Ring Bearing

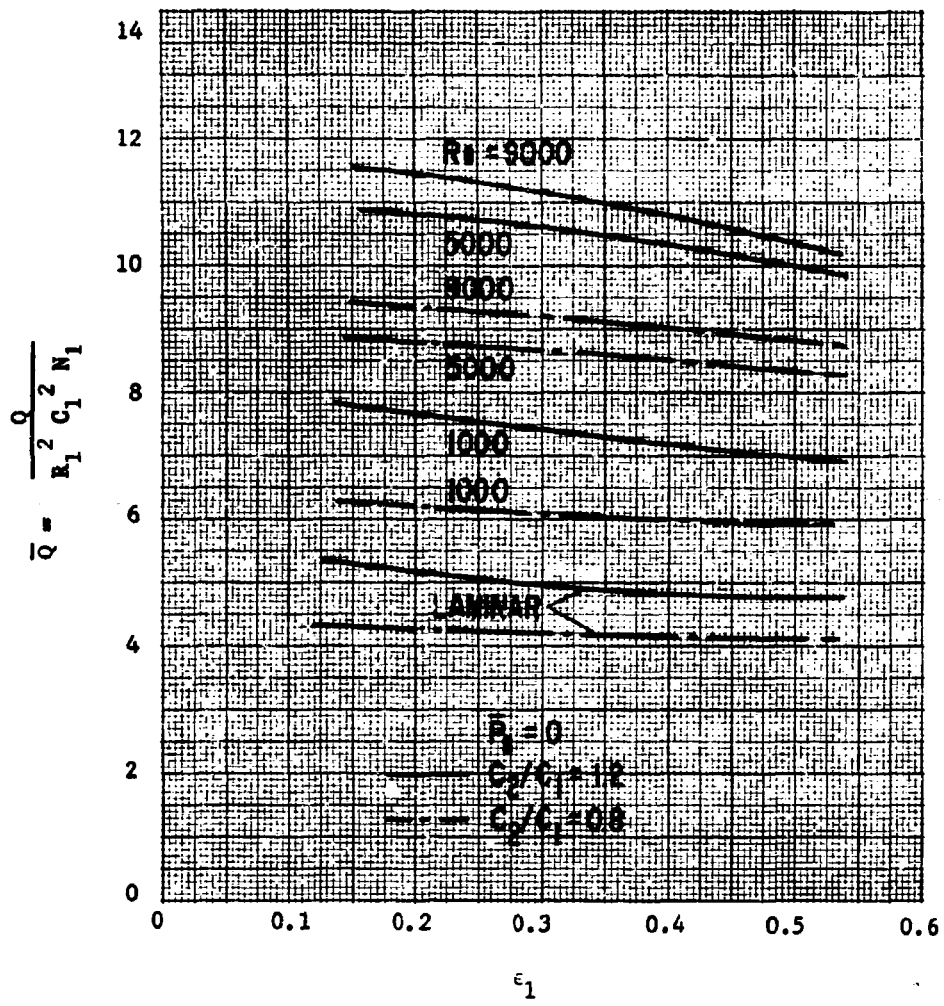


Figure 24. Floating Ring Bearing Flow due to Self-Pumping Effect of Spiral Grooves

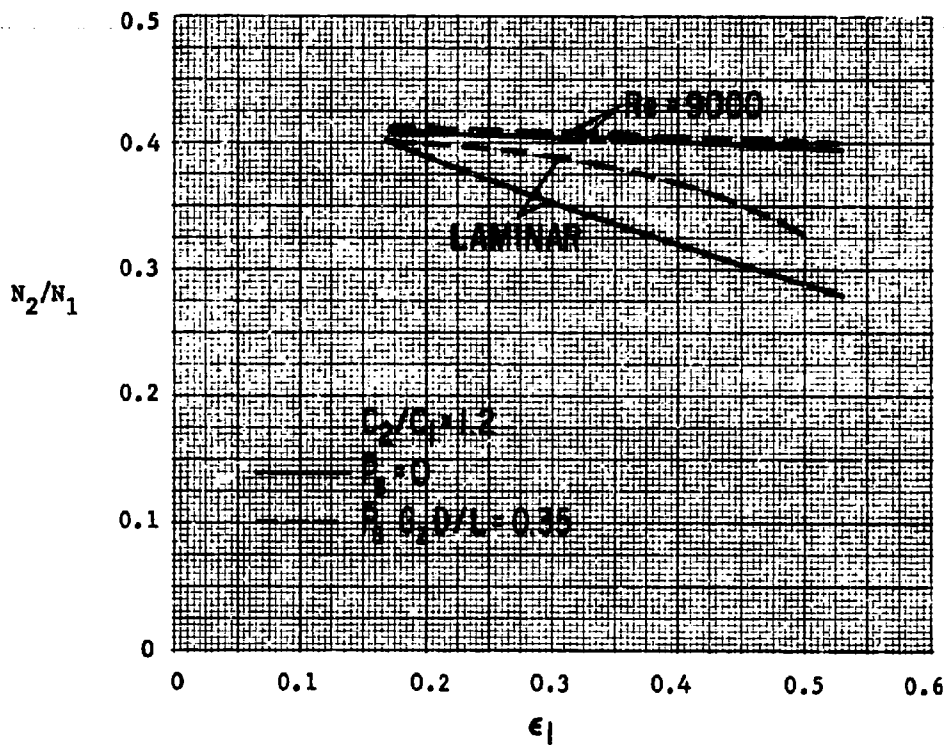
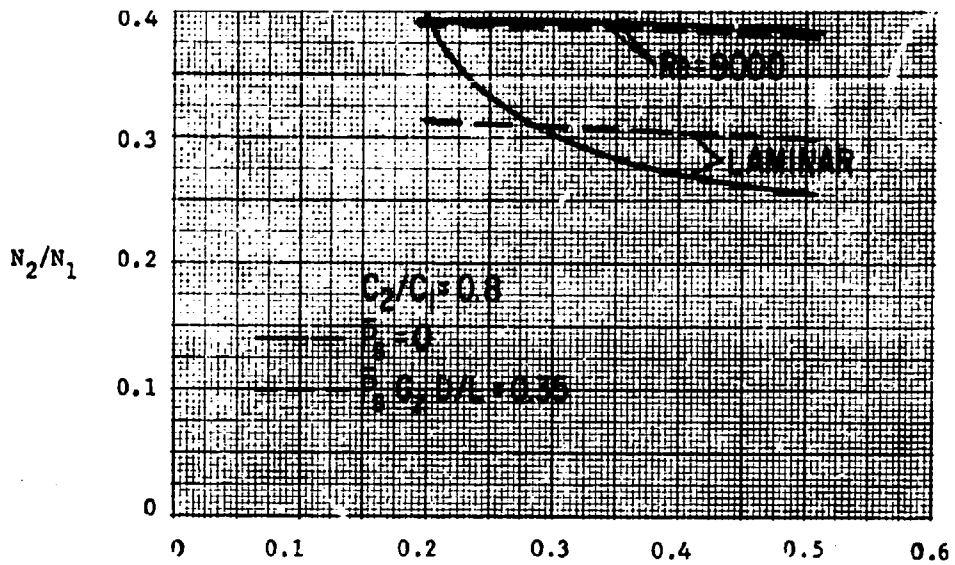


Figure 25. Ring Speed Ratio vs. Inner Film Eccentricity Ratio, Floating Ring Bearing

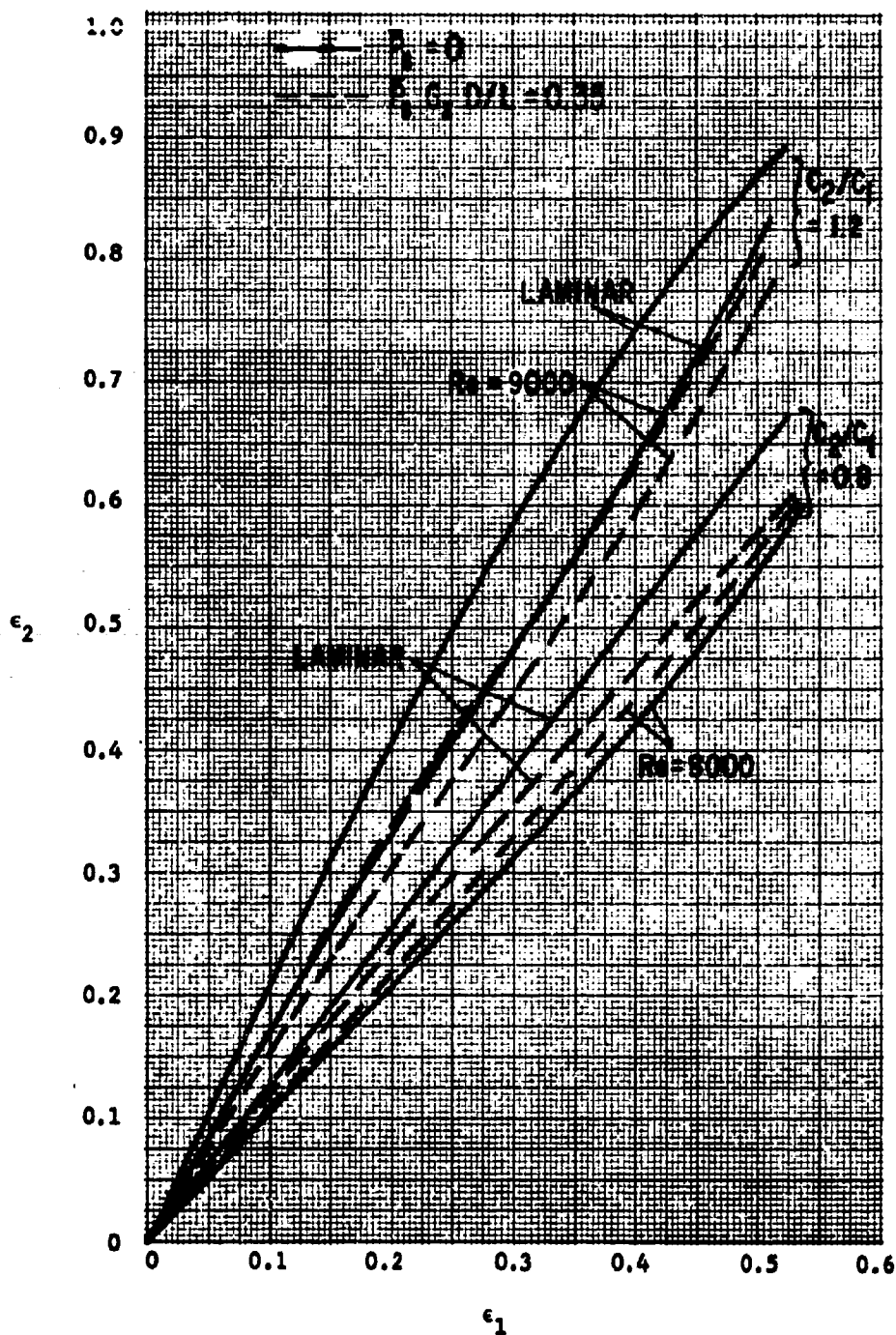


Figure 26. Outer Film Eccentricity Ratio vs. Inner Film Eccentricity Ratio, Floating Ring Bearing

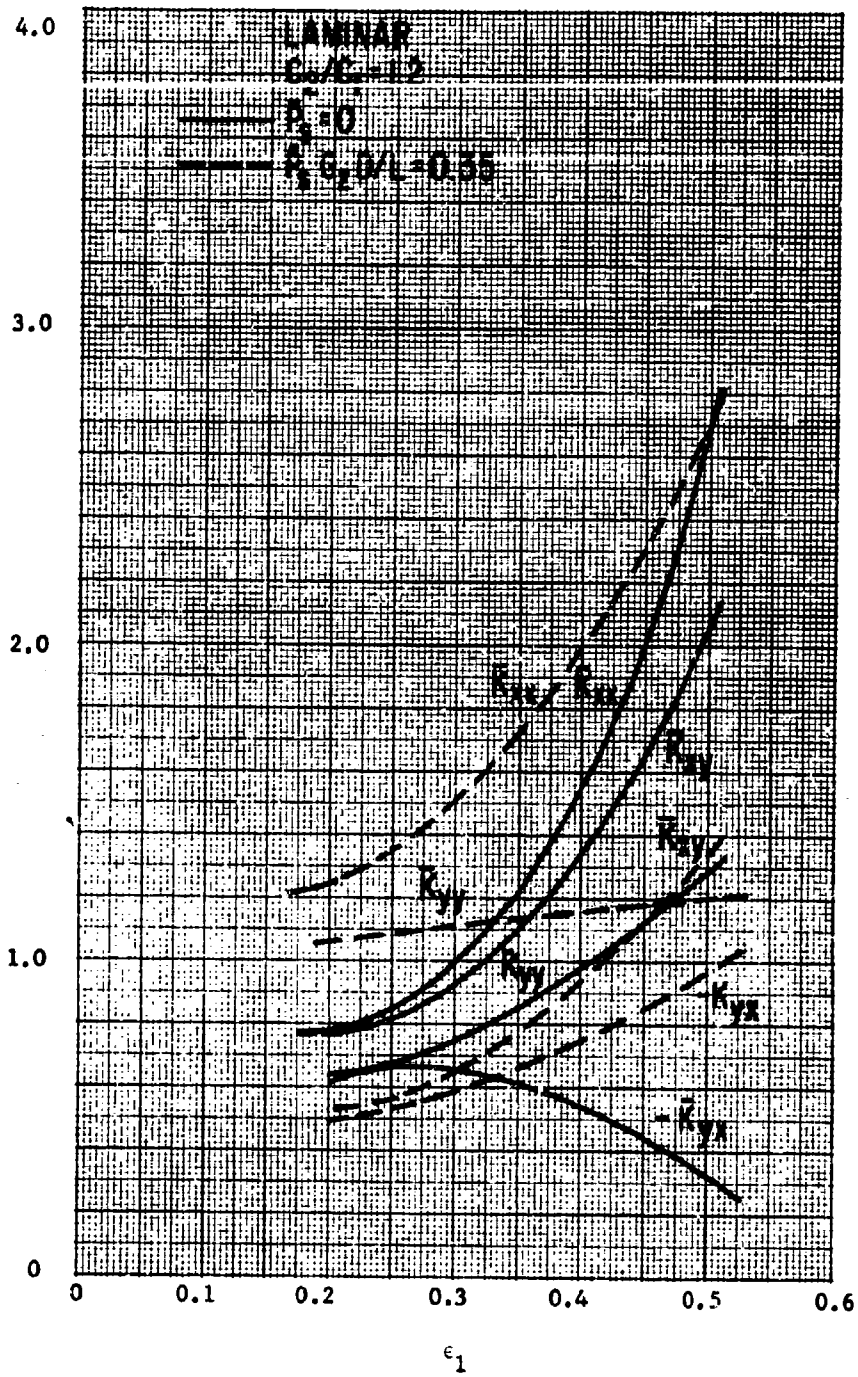


Figure 27. Stiffness Coefficients, Floating Ring Bearing

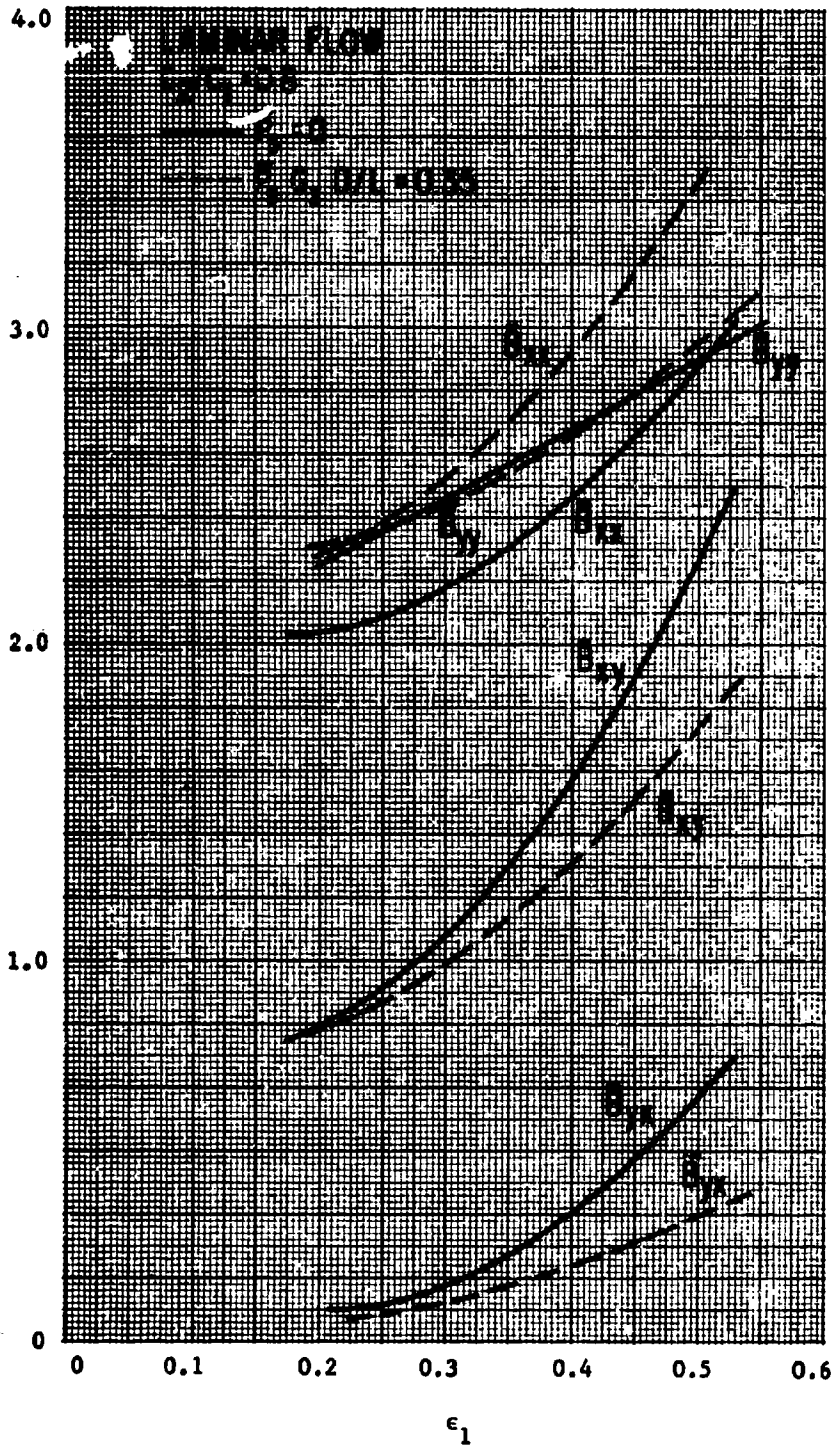


Figure 28. Damping Coefficients, Floating Ring Bearing

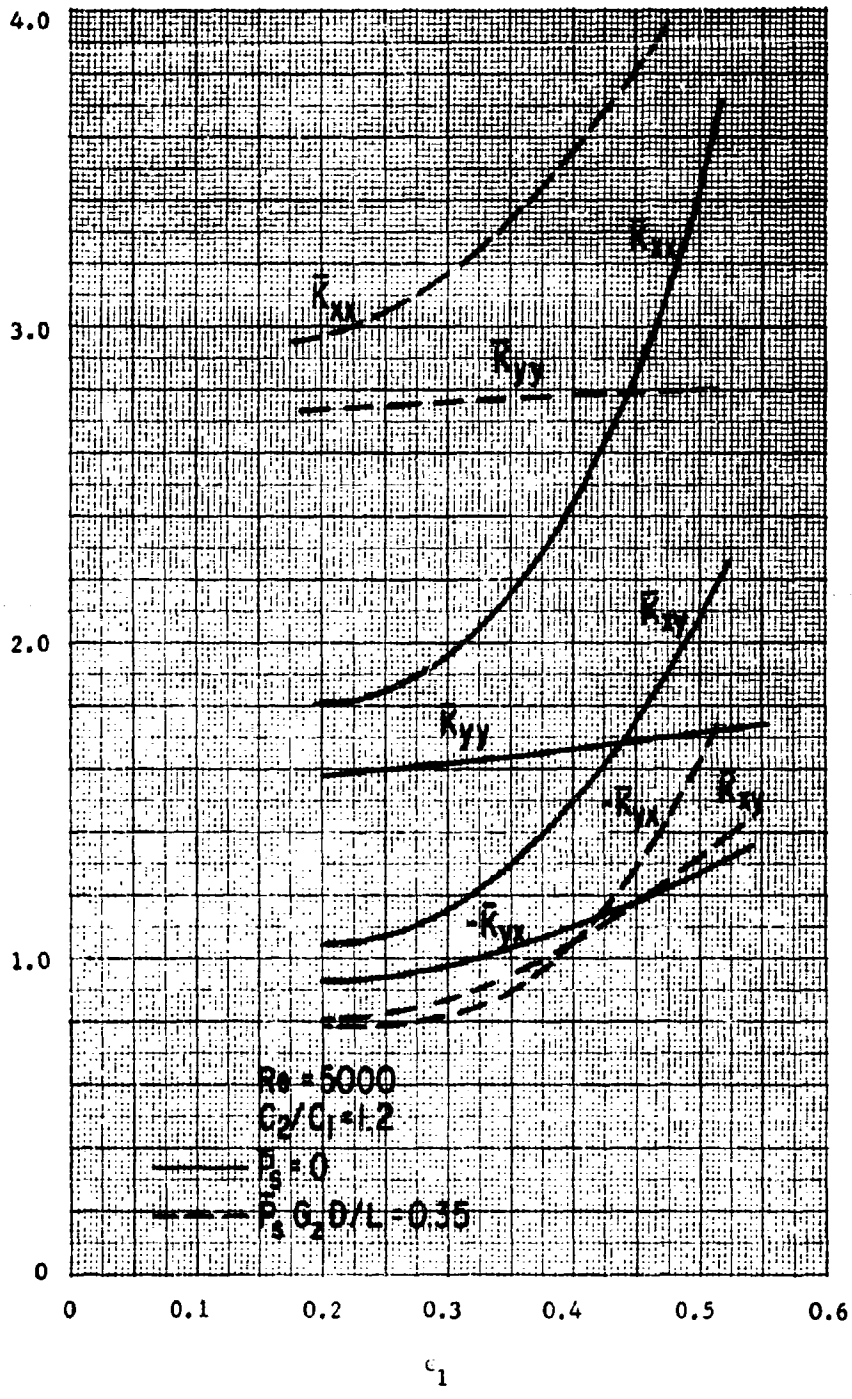


Figure 29. Stiffness Coefficients, Floating Ring Bearing

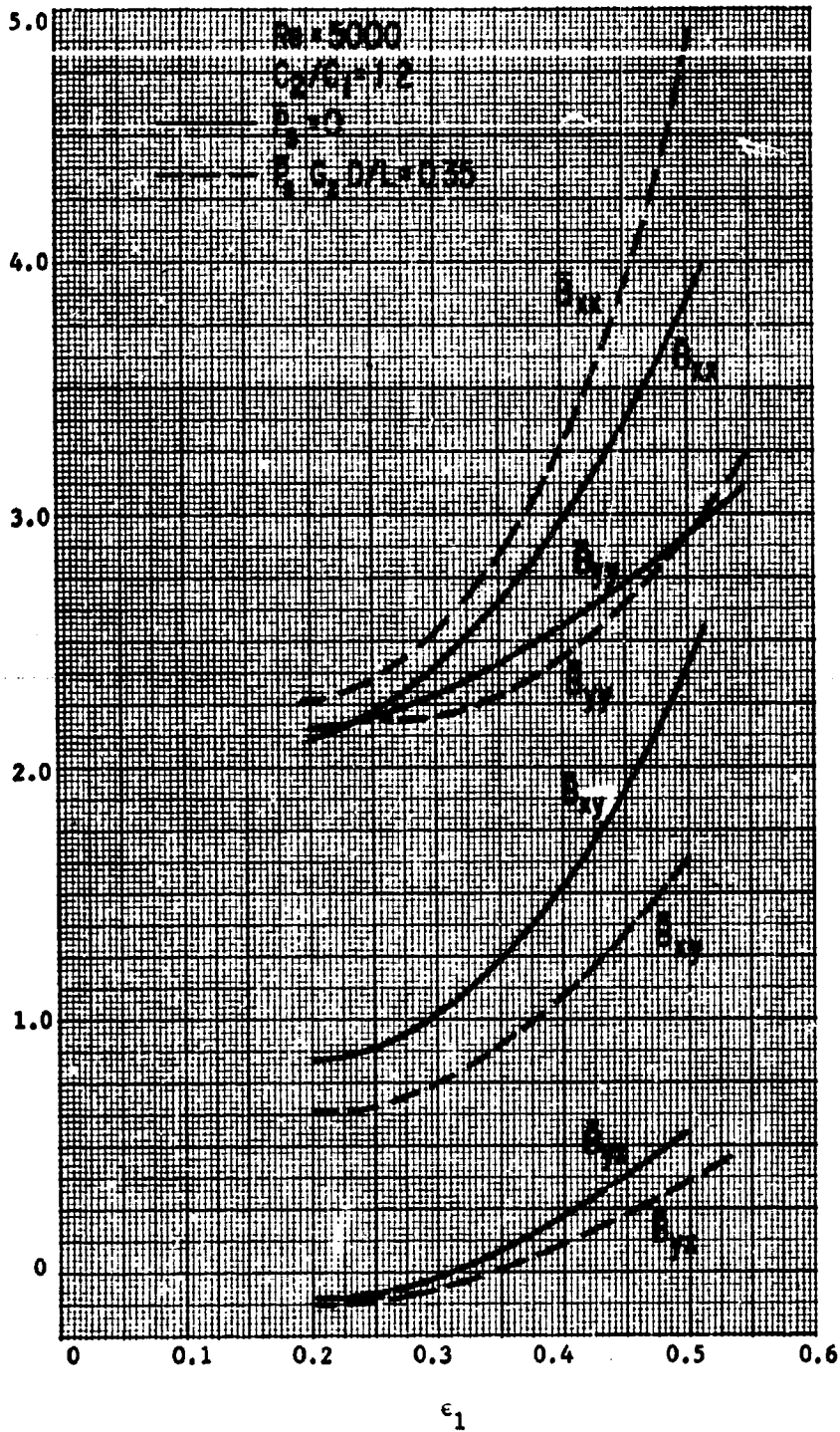


Figure 30. Damping Coefficients, Floating Ring Bearing

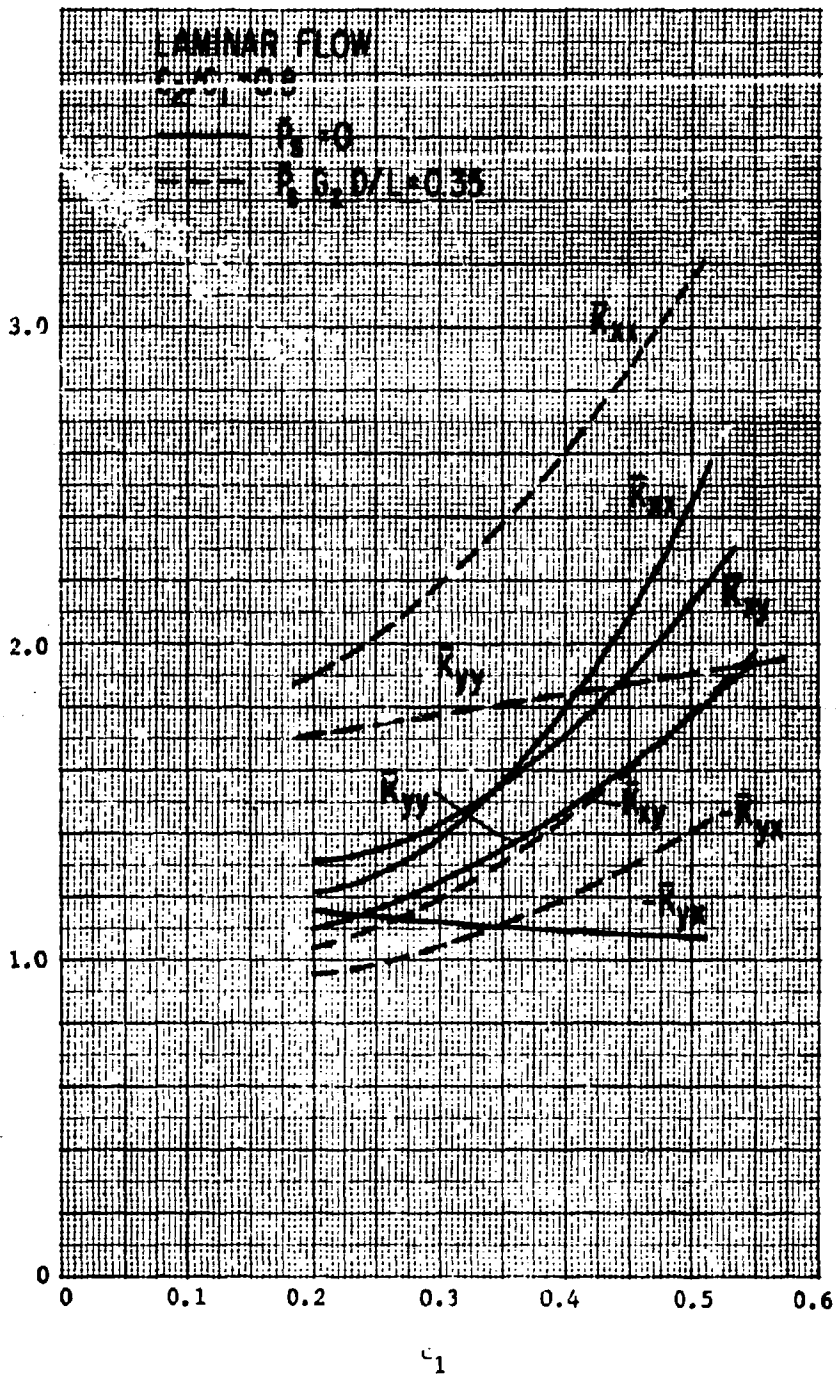


Figure 31. Stiffness Coefficients, Floating Ring Bearing

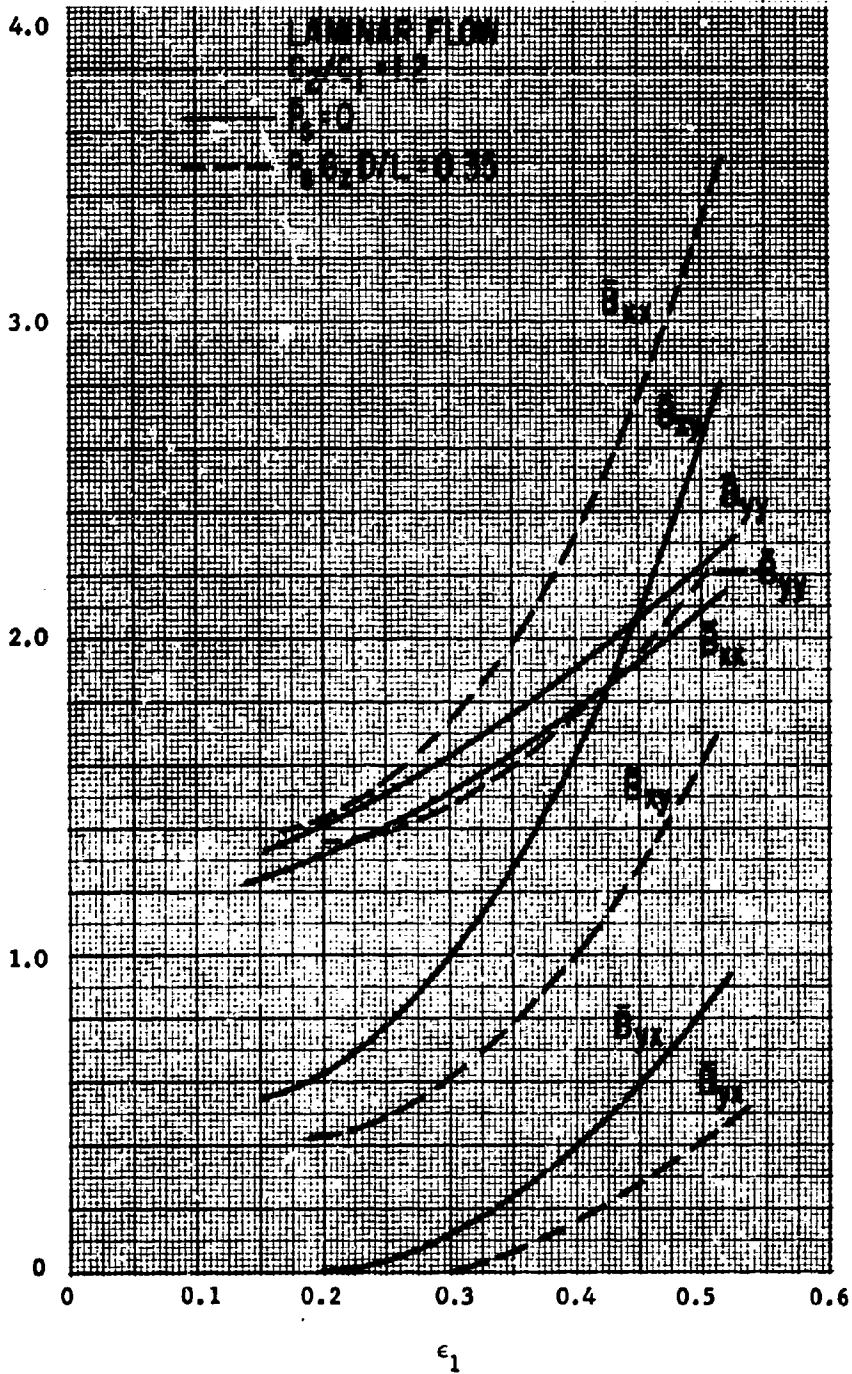


Figure 32. Damping Coefficients, Floating Ring Bearing

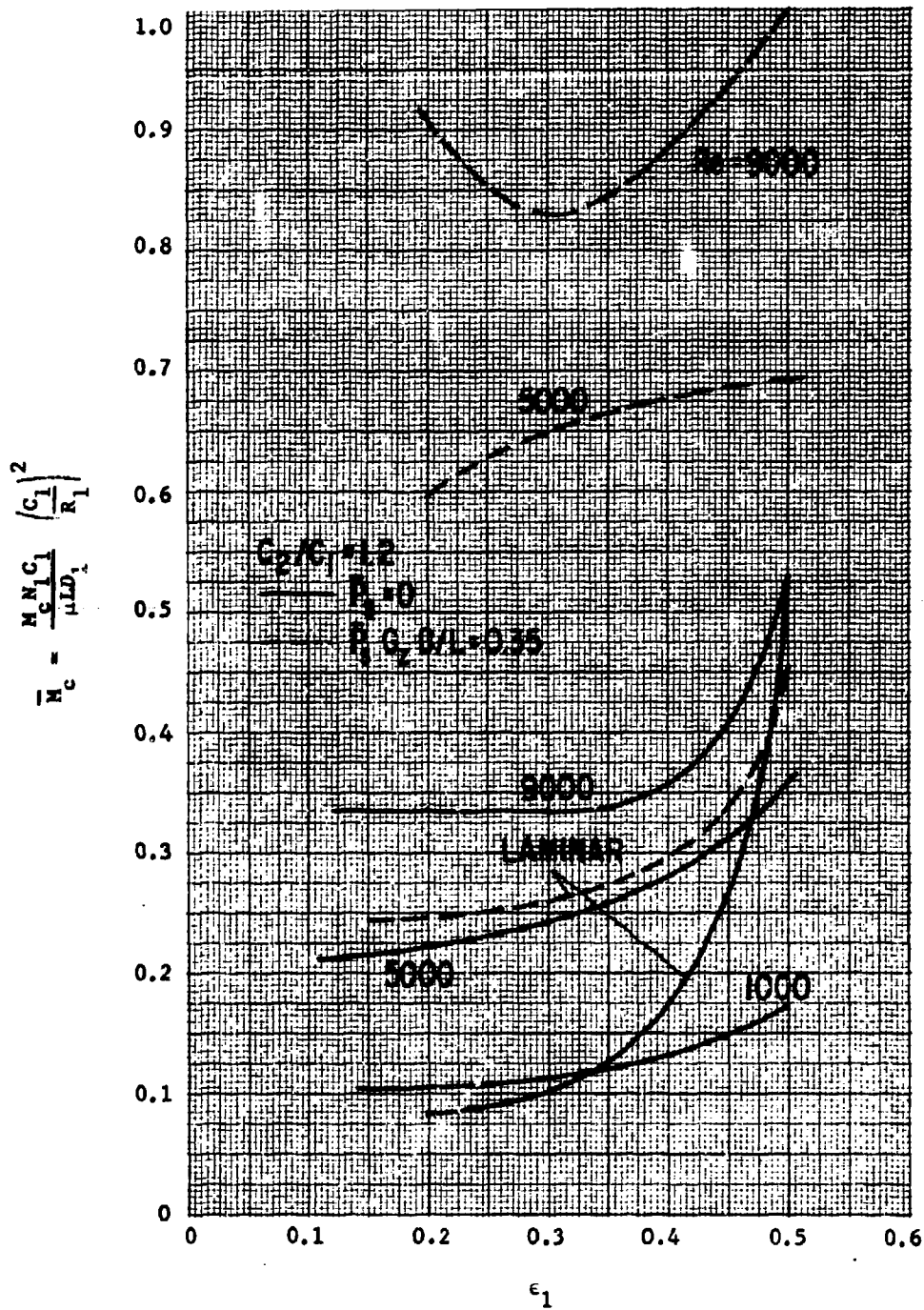


Figure 33. Critical Journal Mass, Floating Ring Bearing

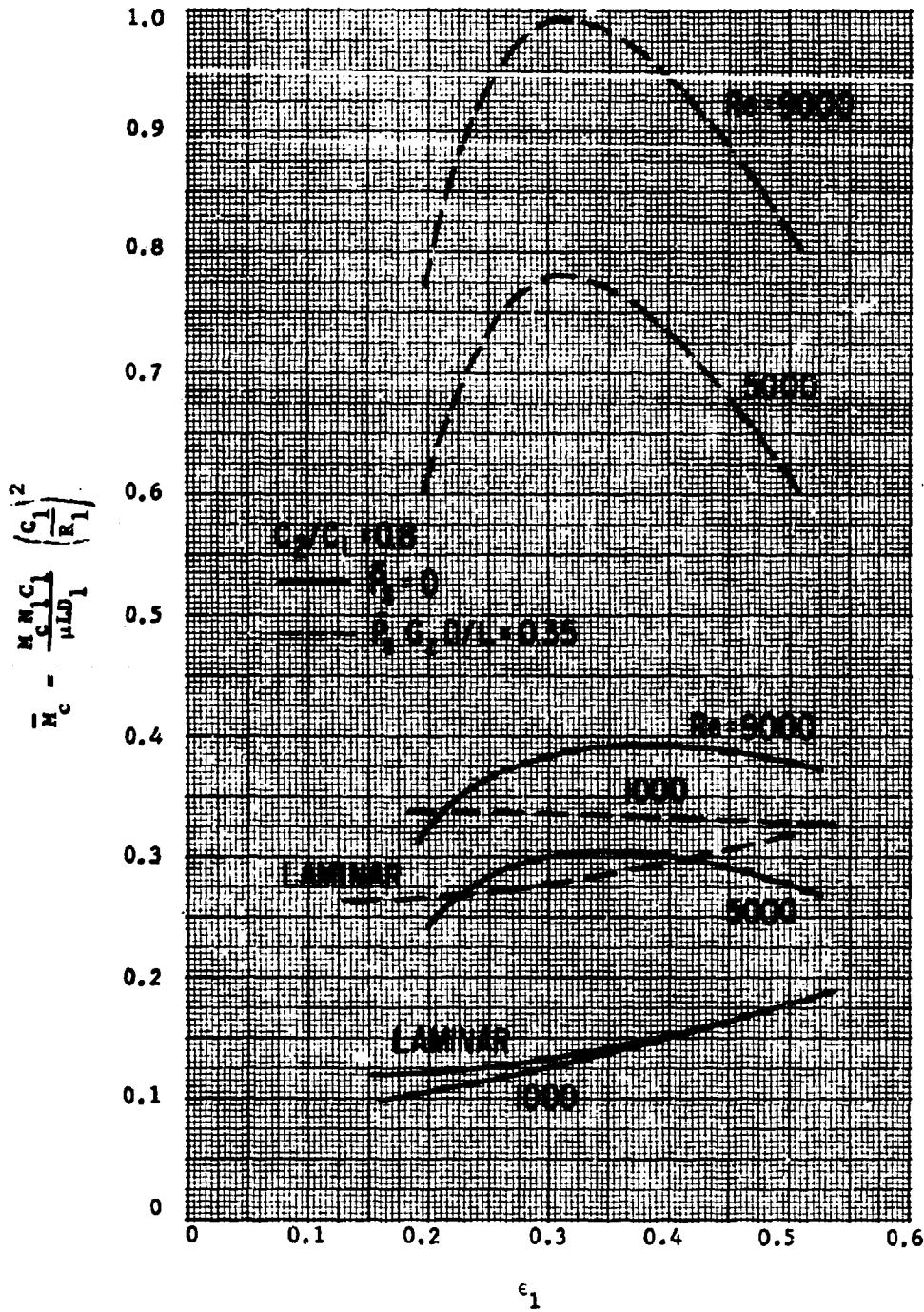


Figure 34. Critical Journal Mass, Floating Ring Bearing

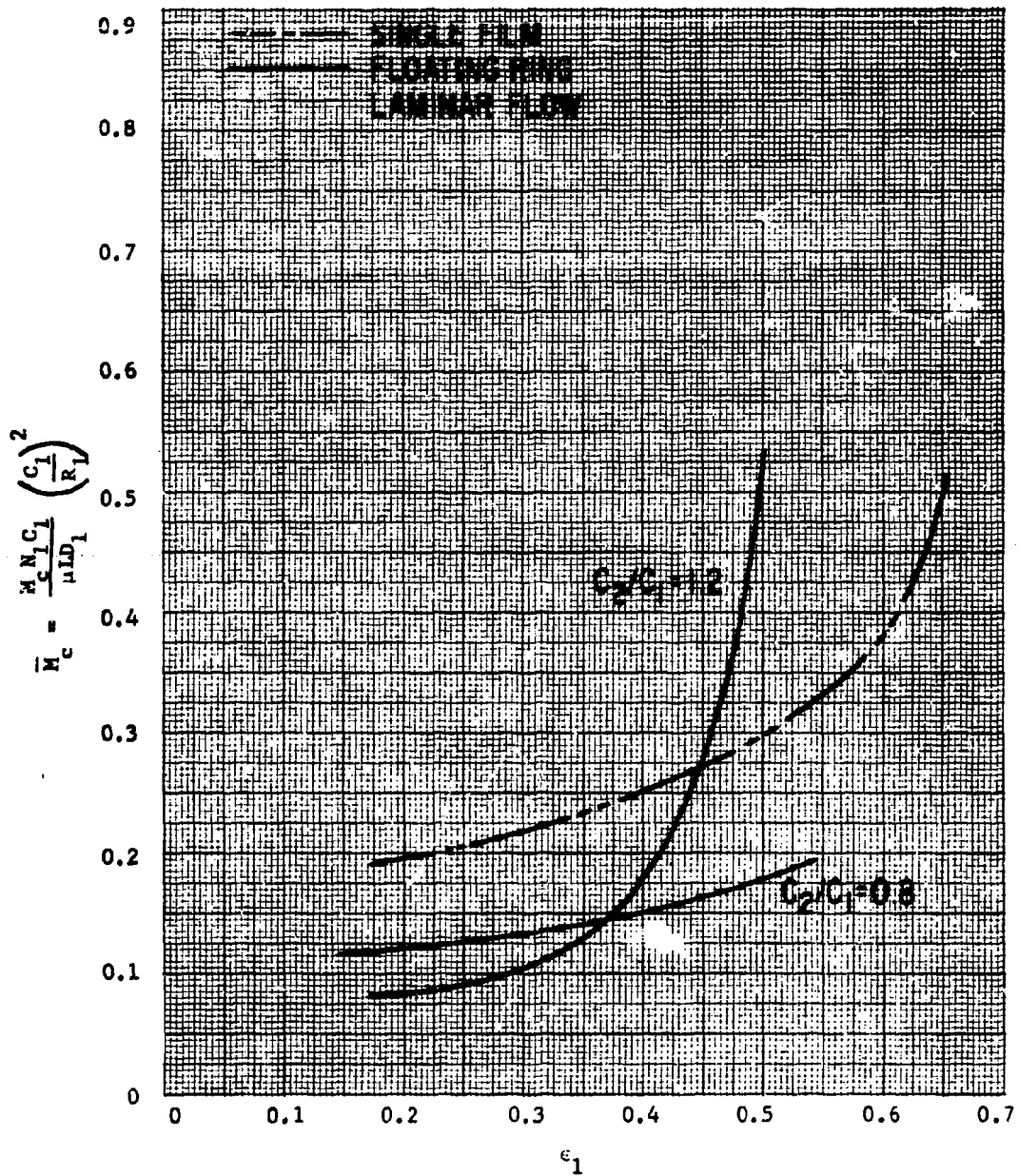


Figure 35. Critical Journal Mass, Comparison between Plain and Spiral-Grooved Floating Ring Bearings

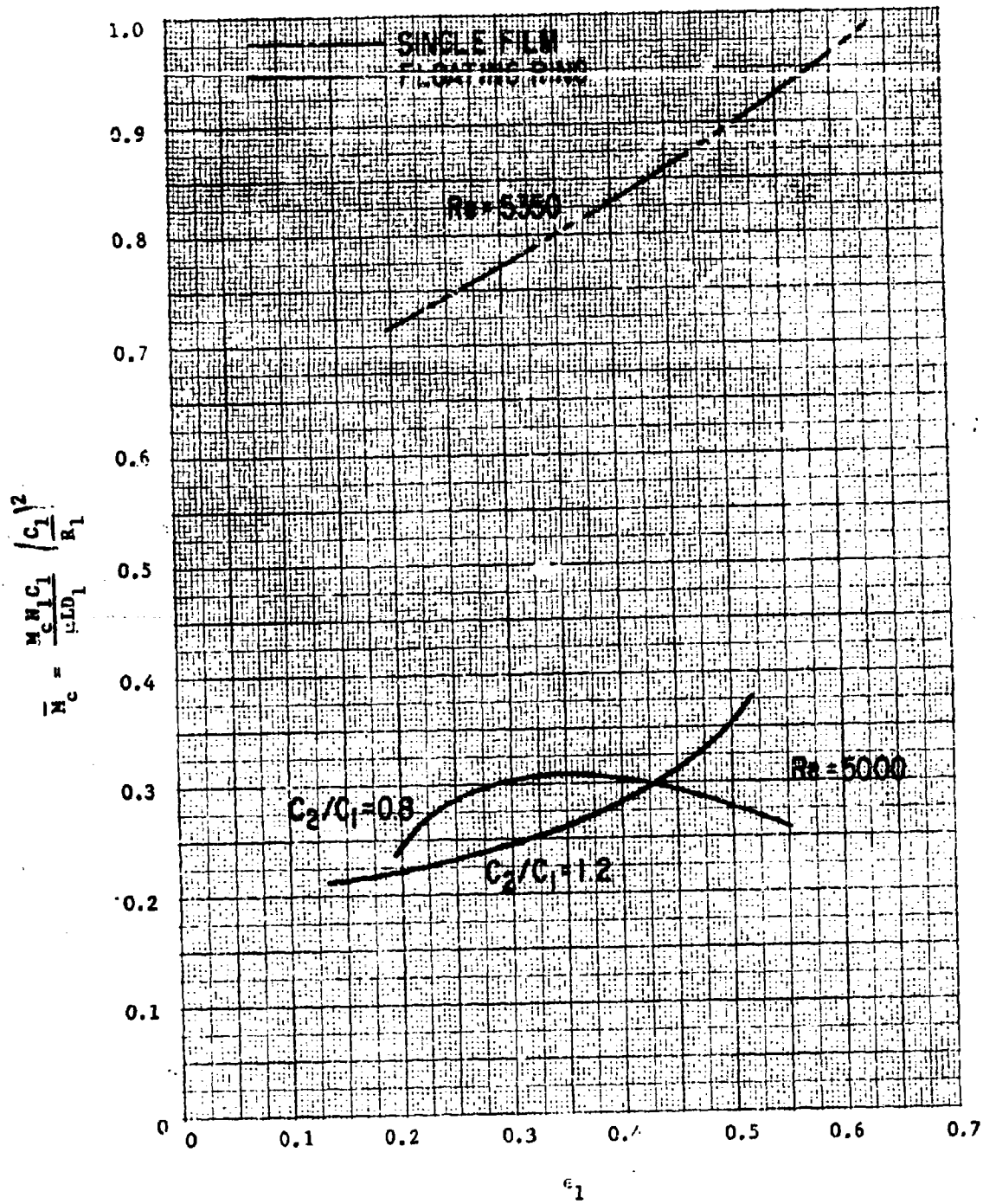


Figure 36. Critical Journal Mass, Comparison between Plain and Spiral-Grooved Floating Ring Bearings

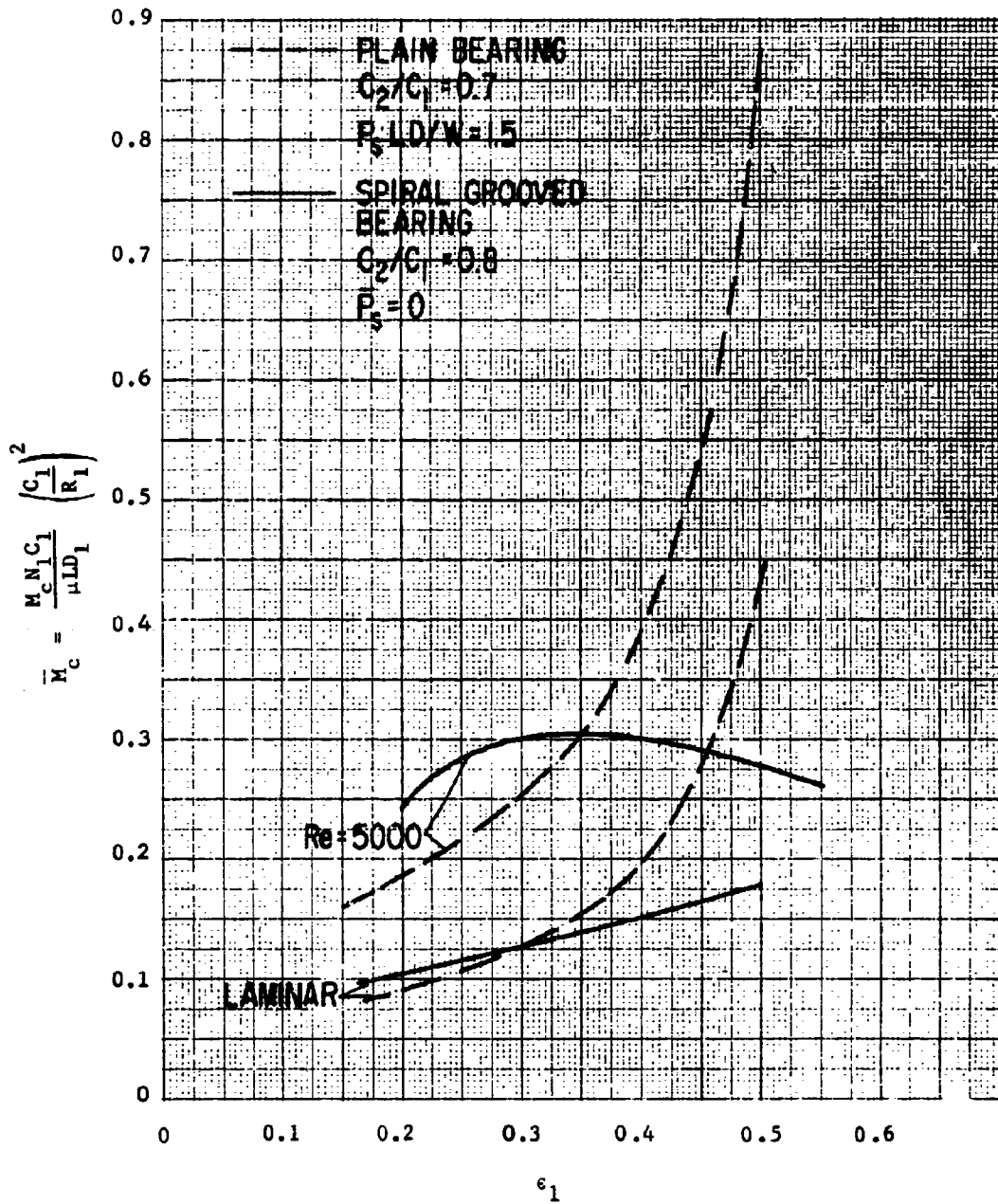


Figure 37. Critical Journal Mass, Comparison between Single Film and Floating Ring Spiral-Grooved Bearings

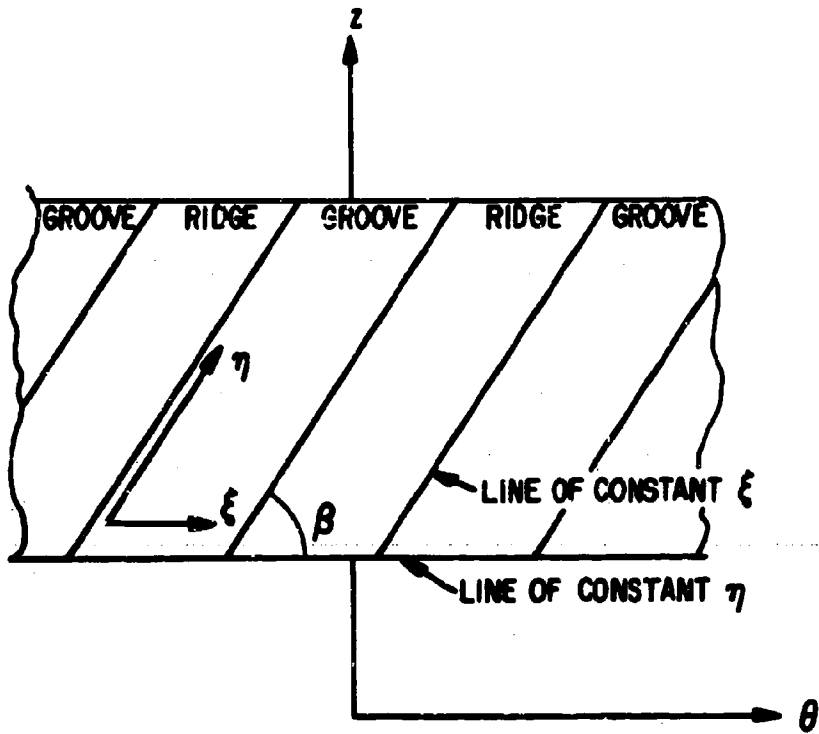


Figure 38. η and ξ Coordinates for Grooved Surface

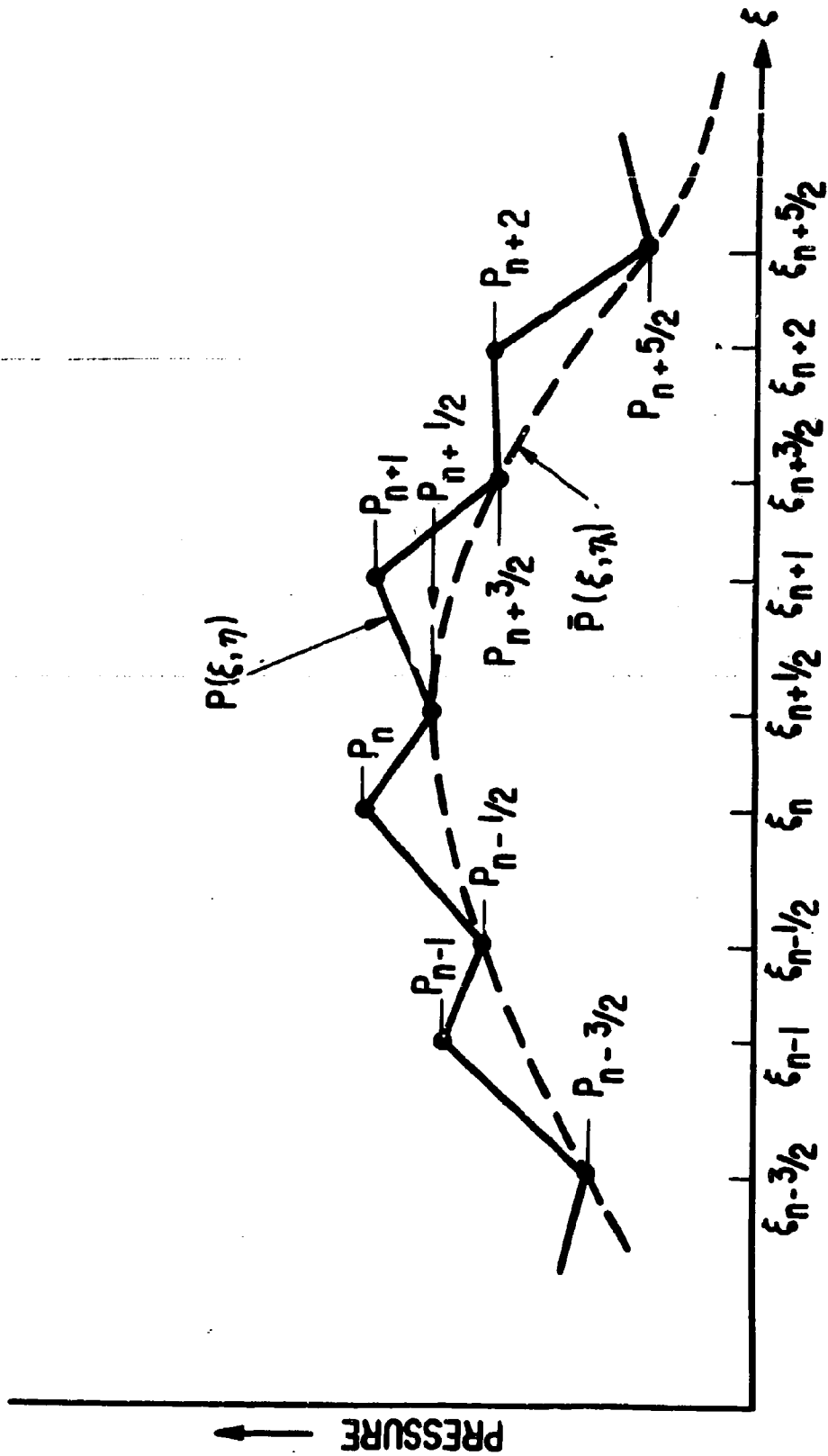


Figure 39. Pressure Distribution around Spiral-Grooved Journal Bearing

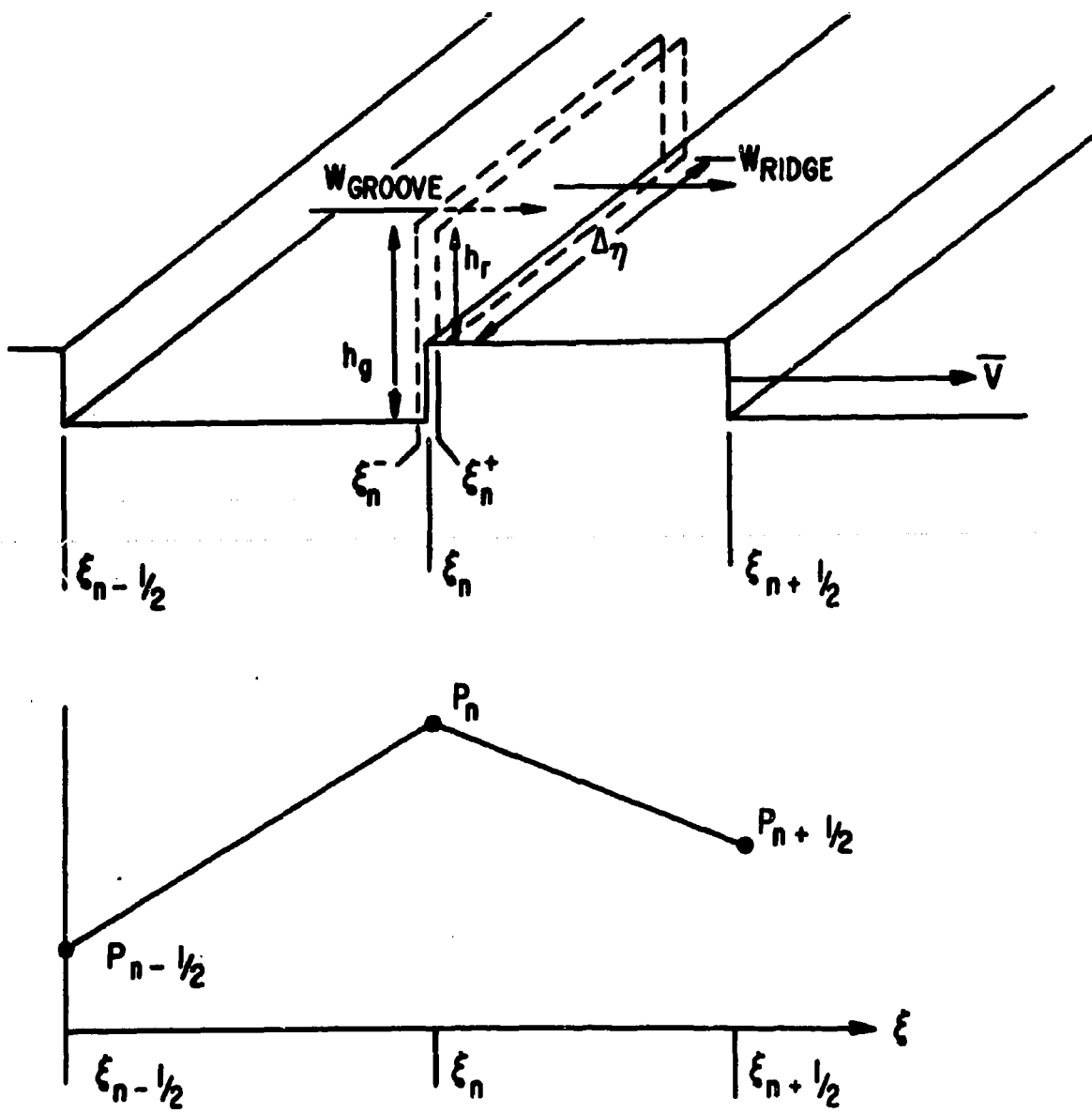


Figure 40. Continuity of Mass Flow across Groove-Ridge Interface and Pressure Variation across Groove-Ridge Pair

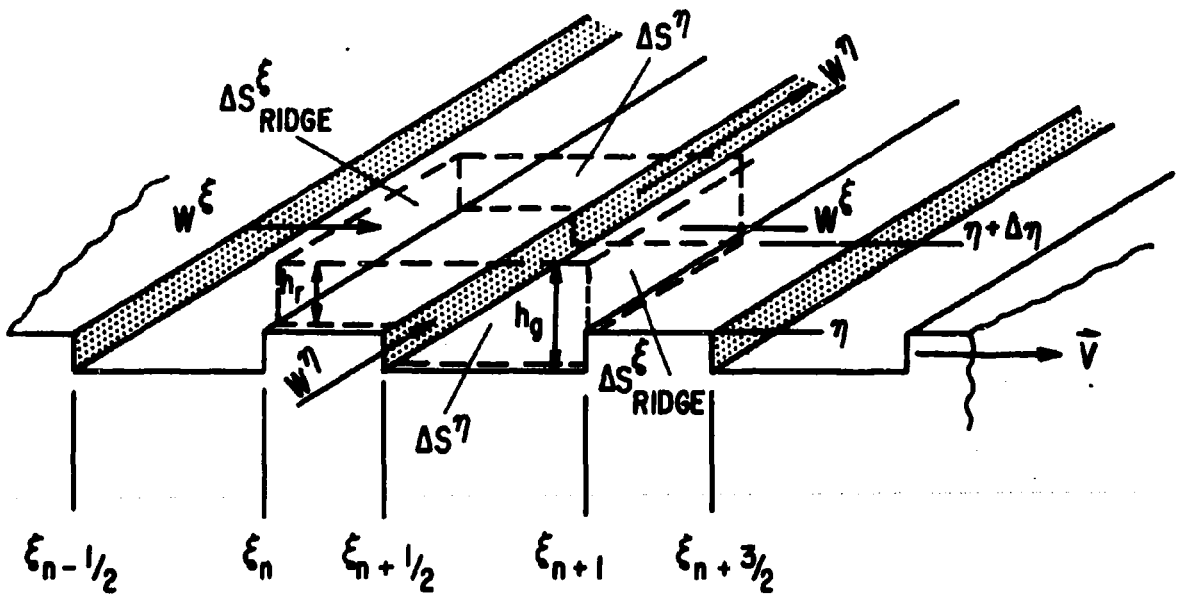


Figure 41. Control Volume for Mass Flow Continuity Analysis

BLANK PAGE

APPENDIX I
DERIVATION AND SOLUTION OF EQUATION FOR
TURBULENT SPIRAL-GROOVED JOURNAL BEARING

The differential equation for the pressure distribution around a spiral-grooved journal bearing has been derived previously by the present authors for the case of laminar flow (Ref. 1). In this appendix will be presented a re-derivation of this equation in which the effects of turbulence in the bearing film will be accounted for by means of the linearized turbulent lubrication theory developed by Ng and Pan (Ref. 4). The derivation will involve four major steps:

1. Express the local mass flows in the ridge and groove regions in terms of the local pressure gradients in those two regions.
2. Define an "overall" pressure profile around the bearing neglecting the zig-zag ripples in the profile which arise due to the discontinuous groove-ridge geometry.
3. Use the requirement that the flow normal to a groove-ridge interface be continuous across the interface in order to solve for local groove-ridge pressure gradients in terms of the "overall" pressure gradient.
4. Apply the principle of conservation of mass to obtain a differential equation for the overall pressure profile.

According to the linearized turbulent lubrication theory of Ng and Pan, the local turbulent mass flows in a bearing film can be expressed as

$$\bar{\rho}uh = -\frac{\rho h^3 G_x}{\mu} \frac{\partial P}{\partial x} + \rho \frac{(U+V)}{2} h \quad (51)$$

$$\bar{\rho}wh = -\frac{\rho h^3 G_z}{\mu} \frac{\partial P}{\partial z} \quad (52)$$

where x and z are the coordinates in the direction of rotation and the axial direction respectively and where U and V are the surface velocities of the bearing and journal respectively. The factors G_x and G_z can be considered, essentially, to be turbulent viscosity correction factors. In the linearized turbulent lubrication theory G_x and G_z are considered to be functions of the local Reynolds number, R_h , in the bearing film where $R_h = \rho(V-U)h/\mu$. A plot of G_x and G_z vs. R_h is shown in Fig. 5.

Next, we introduce the "skewed" ξ, η coordinate system shown in Fig. 38 in which lines parallel to groove-ridge interfaces are lines of constant ξ while planes perpendicular to the axis of the bearing are planes of constant η . The relationships between ξ and η and the cylindrical coordinates θ and z are given below

$$\xi = \theta - \frac{z \cot \beta}{R} \quad (53)$$

$$\eta = z/\sin \beta \quad (54)$$

$$\theta = \xi + \frac{\eta \cos \beta}{R} \quad (55)$$

$$z = \eta \sin \beta \quad (56)$$

note also that

$$\frac{\partial P}{\partial \theta} = \frac{\partial P}{\partial \xi} \quad (57)$$

$$\frac{\partial P}{\partial z} = \frac{\partial P}{\partial \eta} \frac{1}{\sin \beta} - \frac{\partial P}{\partial \xi} \frac{\cot \beta}{R} \quad (58)$$

$$\frac{\partial P}{\partial \xi} = \frac{\partial P}{\partial \theta} \quad (59)$$

$$\frac{\partial P}{\partial \eta} = \frac{\partial P}{\partial \theta} \frac{\cos \beta}{R} + \frac{\partial P}{\partial z} \sin \beta \quad (60)$$

In the ξ, η coordinate system, the pressure gradient $\partial P/\partial \eta$ is continuous everywhere in the bearing film because the geometry has no discontinuities in the η direction. On the other hand, the gradient $\partial P/\partial \xi$ is discontinuous at groove-ridge interfaces due to the discontinuity in film height. Consequently the pressure profile in the ξ (circumferential) direction will have the "zig-zag" appearance as shown schematically by the solid line in Fig. 39. In this figure the symbols ξ_n, ξ_{n+1} , etc., denote the interfaces at the beginning of ridge region while $\xi_{n+1/2}, \xi_{n+3/2}$, etc. denote the interfaces at the beginning of groove regions. Now, by neglecting the saw-toothed ripples in the actual pressure distribution, one can conceive of an approximate, smoothed "overall" pressure distribution around the journal shown in Fig. 39 as the dashed line through the pressures $P_{n-3/2}, P_{n-1/2}$, etc., at $\xi_{n-3/2}, \xi_{n-1/2}$, etc. Since the local pressure gradients within each groove and ridge region are bounded in magnitude, the saw-toothed fluctuations in pressure due to alternating groove and ridge regions will reduce to a negligible magnitude as the width of the groove-ridge pair becomes very small, i.e., as the number of grooves becomes very large. In the limit, as the width of each groove-ridge pair becomes very small, the smooth "overall" pressure distribution through the discrete points $P_{n-3/2}, P_{n-1/2}$, etc., will approach a continuous distribution $\bar{P}(\xi, \eta)$ which should provide a very good approximation to the actual "saw-toothed" pressure distribution around the journal. Formally, one can define the slope of $\bar{P}(\xi, \eta)$ in the ξ direction at the point ξ_n , as

$$\left. \frac{\partial \bar{P}(\xi, \eta)}{\partial \xi} \right|_{\xi_n} = \lim_{\Delta \xi \rightarrow 0} \frac{P_{n+1/2} - P_{n-1/2}}{\Delta \xi} = \lim_{\Delta \xi \rightarrow 0} \left[\alpha \frac{\partial P}{\partial \xi} \Big|_g + (1-\alpha) \frac{\partial P}{\partial \xi} \Big|_r \right] \quad (61)$$

where $\Delta \xi = \xi_{n+1/2} - \xi_{n-1/2}$ and where $\partial P/\partial \xi|_g$ and $\partial P/\partial \xi|_r$ refer to the local pressure gradients within the groove and ridge region respectively.

Having defined the overall gradient $\partial \bar{P}/\partial \xi$, we next consider writing an expression for the mass flux W^{ξ} normal to a moving groove-ridge interface (see Fig. 39). In terms of the mass fluxes $\rho u h$ and $\rho w h$, W^{ξ} is expressed as

$$W^E = \rho \left[(u-V) \sin \beta - w \cos \beta \right] h \quad (62)$$

Substituting for u and w in Eq. (62) by means of Eqs. (51) and (52) and noting that $\partial P / \partial x = \partial P / R \partial \theta$ we obtain

$$W_{\text{groove region}}^E = -\rho \left\{ \left[\frac{h^3 G_{xR}}{\mu} \frac{\partial P_R}{R \partial \theta} - \frac{(U-V)}{2} h_g \right] \sin \beta - \frac{h^3 G_{RR}}{\mu} \frac{\partial P_R}{\partial x} \cos \beta \right\} \quad (63)$$

$$W_{\text{ridge region}}^E = -\rho \left\{ \left[\frac{h^3 G_{xR}}{\mu} \frac{\partial P_R}{R \partial \theta} - \frac{(U-V)}{2} h_r \right] \sin \beta - \frac{h^3 G_{RR}}{\mu} \frac{\partial P_R}{\partial x} \cos \beta \right\} \quad (64)$$

Note that the factors G_x and G_z are subscripted x and g because they have different values in the ridge and groove regions.

Next we make the following useful definitions

$$G_1 = 12(G_x + G_z \cot^2 \beta) / R^2 \quad (65)$$

$$G_2 = - \frac{12 G_x \cos \beta}{R \sin^2 \beta} \quad (66)$$

$$G_3 = - \frac{12 G_z}{\sin^2 \beta} \quad (67)$$

If, in Eqs. (63) and (64), we transform the derivatives of P with respect to θ and z into derivatives with respect to ξ and η (see Eqs. (57) and (58)) and collect terms, we obtain

$$W_{\text{groove region}}^{\xi} = R \sin \beta \left\{ - \frac{\rho}{12\mu} h_g^3 \left[G_{1g} \frac{\partial P}{\partial \xi} + G_{2g} \frac{\partial P}{\partial \eta} \right] + \rho h_g \frac{(U-V)}{2R} \right\} \quad (68)$$

$$W_{\text{ridge region}}^{\xi} = R \sin \beta \left\{ - \frac{\rho}{12\mu} h_r^3 \left[G_{1r} \frac{\partial P}{\partial \xi} + G_{2r} \frac{\partial P}{\partial \eta} \right] + \rho h_r \frac{(U-V)}{2R} \right\} \quad (69)$$

Note that the derivative $\partial P / \partial \eta$ does not have to be identified by a subscript g or r since it is continuous everywhere within the bearing film.

Next we note that by continuity of mass flow

$$W_{\text{groove region}}^{\xi} = W_{\text{ridge region}}^{\xi} \quad (70)$$

Eqs. (61) and (70) constitute two linear equations in the "unknowns" $\partial P / \partial \xi$ and $\partial P_r / \partial \xi$. Eqs. (61) and (70) may therefore be solved to yield

$$\frac{\partial P}{\partial \xi} = (1-\alpha) \bar{B}_1 \frac{\partial P}{\partial \eta} + (1-\alpha) \bar{B}_2 - \bar{A}_1 \frac{\partial P}{\partial \xi} \quad (71)$$

$$\frac{\partial \bar{P}}{\partial \xi} = -\alpha \bar{B}_1 \frac{\partial \bar{P}}{\partial \eta} - \alpha \bar{B}_2 + \bar{A}_2 \frac{\partial \bar{P}}{\partial \xi} \quad (72)$$

where

$$\left. \begin{aligned} A_1 &= G_{1r} h_r^3 \\ A_2 &= -G_{1g} h_g^3 \\ A_3 &= A_2 - \alpha(A_2 + A_1) \\ B_1 &= G_{2g} h_g^3 - G_{2r} h_r^3 \\ B_2 &= \frac{6\mu(h_r - h_g)}{R} (U-V) \\ \bar{A}_1 &= A_1/A_3 \\ \bar{A}_2 &= A_2/A_3 \\ \bar{B}_1 &= B_1/A_3 \\ \bar{B}_2 &= B_2/A_3 \end{aligned} \right\} \quad (73)$$

Eqs. (71) and (72) may be substituted in either Eq. (66) or (67) to yield an expression for the mass flux W^E in terms of the overall pressure gradients $\partial \bar{P} / \partial \xi$ and $\partial \bar{P} / \partial \eta$ (note that $\partial \bar{P} / \partial \eta$ may be written as $\partial \bar{P} / \partial \eta$ because of the continuous nature of this derivative). The expression obtained is

$$W^{\xi} = R \sin \beta \left\{ - \frac{\rho}{12\mu} h_r^3 \left[G_{1r} (\bar{A}_2 \frac{\partial \bar{P}}{\partial \xi} - \alpha \bar{B}_1 \frac{\partial \bar{P}}{\partial \eta} - \alpha \bar{B}_2) \right. \right. \\ \left. \left. + G_{2r} \frac{\partial \bar{P}}{\partial \eta} \right] + \rho h_r \frac{(U-V)}{2R} \right\} \quad (74)$$

Next, consider the control volume ΔV , for one ridge-groove pair shown in Fig. 41. We take the control volume to move with the grooved surface at velocity \bar{V} and we consider that, at the instant shown in Fig. 41, the various ridge-groove interfaces are located at $\xi_n, \xi_{n+1/2}, \xi_{n+1}$ etc., as depicted. The mass flows entering and leaving the moving control volume through the surfaces ΔS_{ridge}^{ξ} we denote as $W_{ridge}^{\xi} \Delta \eta$ whereas the mass flows entering and leaving the control volume through the surfaces ΔS^{η} we denote as $W^{\eta} (\xi_{n+1} - \xi_n)$. The total time rate of change of the mass, ΔM contained in ΔV is given by

$$\frac{\partial}{\partial t} (\Delta M) + \bar{V} \cdot \nabla (\Delta M) \quad (75)$$

By the conservation of mass we obtain that

$$\left[W_{ridge}^{\xi} \Big|_{\xi_{n+1}} - W_{ridge}^{\xi} \Big|_{\xi_n} \right] \Delta \eta + \left[W^{\eta} \Big|_{\eta+\Delta \eta} - W^{\eta} \Big|_{\eta} \right] (\xi_{n+1} - \xi_n) \\ + \frac{\partial}{\partial t} (\Delta M) + \bar{V} \cdot \bar{\nabla} (\Delta M) = 0 \quad (76)$$

Dividing Eq. (76) through by $\Delta \xi \Delta \eta$ where $\Delta \xi = \xi_{n+1} - \xi_n$, and taking the limit as $\Delta \xi$ and $\Delta \eta$ go to zero we have

$$\frac{\partial W^{\xi}}{\partial \xi} + \frac{\partial W^{\eta}}{\partial \eta} + \frac{\partial}{\partial t} \frac{(\Delta M)}{\Delta \xi \Delta \eta} + \bar{V} \cdot \bar{\nabla} \frac{(\Delta M)}{\Delta \xi \Delta \eta} = 0 \quad (77)$$

where $\frac{\partial W^{\xi}}{\partial \xi}$ is defined to be

$$\frac{\partial W^{\xi}}{\partial \xi} = \lim_{\Delta \xi \rightarrow 0} \frac{W^{\xi}|_{\xi_{i+1}} - W^{\xi}|_{\xi_i}}{\Delta \xi} \quad (78)$$

The subscript ridge has been dropped from W^{ξ} because of the equality condition expressed by Eq. (70). The expression for W^{ξ} is given by equation (74).

The expression for the mass flux W^{η} is

$$W^{\eta} = -\rho \left[\frac{(1-\alpha)h_r^3}{\mu} \frac{\partial P_r}{\partial z} G_{zr} + \frac{ch_g^3}{\mu} \frac{\partial P_g}{\partial z} G_{zg} \right] \quad (79)$$

If we transform $\frac{\partial P_r}{\partial z}$ and $\frac{\partial P_g}{\partial z}$ into $\xi - \eta$ coordinates by means of Eq. (58) we will obtain an expression for W^{η} in terms of $\frac{\partial P}{\partial \eta}$, $\frac{\partial P_r}{\partial \xi}$ and $\frac{\partial P_g}{\partial \xi}$. We then can substitute for $\frac{\partial P_r}{\partial \xi}$ and $\frac{\partial P_g}{\partial \xi}$ by means of Eqs. (71) and (72) to obtain, finally

$$W^{\eta} = R \sin \beta \frac{\rho}{12\mu} \left\{ \alpha h_g^3 \left[G_{3g} \frac{\partial \bar{P}}{\partial \eta} - G_{2g} (-\bar{A}_1 \frac{\partial \bar{P}}{\partial \xi} + (1-\alpha) \bar{B}_1 \frac{\partial \bar{P}}{\partial \eta} + (1-\alpha) \bar{B}_2) \right] \right. \\ \left. + (1-\alpha) h_r^3 \left[G_{3r} \frac{\partial \bar{P}}{\partial \eta} - G_{2r} (\bar{A}_2 \frac{\partial \bar{P}}{\partial \xi} - \alpha \bar{B}_1 \frac{\partial \bar{P}}{\partial \eta} - \alpha \bar{B}_2) \right] \right\} \quad (80)$$

where \bar{A}_2 , \bar{B}_1 and \bar{B}_2 were defined previously by Eqs. (73)

The quantity $\frac{\Delta M}{\Delta \xi \Delta \eta}$ in Eq. (77) is

$$\frac{\Delta M}{\Delta \xi \Delta \eta} = \rho R \sin \beta \left[(1-\alpha) h_r + \alpha h_g \right] \quad (81)$$

while

$$\bar{v} \cdot \bar{v} = \frac{V}{R} \frac{\partial}{\partial \xi} \quad (82)$$

Substitution of Eqs. (74), (80), (81) and (82) into Eq. (77) yields a second-order differential equation in $\bar{P}(\xi, \eta)$ the overall pressure distribution around the spiral-grooved journal. To solve this equation, we must first transform it back into the orthogonal θ - z coordinate system. This is done by means of Eqs. (59) and (60). The result is

$$\frac{\partial^2 W^{\xi}}{\partial \theta^2} + \frac{\cos \beta}{R} \frac{\partial^2 W^{\eta}}{\partial \theta^2} + \sin \beta \frac{\partial^2 W^{\eta}}{\partial z^2} + \left(\frac{\partial}{\partial t} + \frac{V}{R} \frac{\partial}{\partial \theta} \right) \left\{ R \rho \sin \beta \left[\alpha h_g + (1-\alpha)h_r \right] \right\} = 0 \quad (83)$$

Expressions for W^{ξ} and W^{η} in the θ - z coordinate system may be obtained by substituting Eqs. (59) and (60) into Eqs. (74) and (80).

The Numerical Solution

Eq. (83) is solved for any combination of groove and seal arrangement with or without feed or vent in the middle of the journal (Fig. 2). Thus, it can provide the solution for a seal-groove, groove-seal, fully grooved or herringbone journal containing up to three distinct sections. The basic technique is first to divide the bearing into a numerical grid with dimensions $m \times n$. Then write the differential equation into a finite difference form of three columns. Thus, each point in concern is related to the five neighboring points. At the boundaries, the pressures are given. Therefore $m \times n$ equations are established for $m \times n$ unknowns. By means of the columnwise matrix inversion solution routine developed by Castelli, Pirvics and Shapiro, the pressure field is obtained.

This technique is fully discussed in References 6 and 7.

Once the pressure field is obtained, loads, moments, torques, etc. are obtained by numerically evaluating the following expressions.

Radial component of force (cosine component)

$$F_r = - \int_0^L \int_0^{2\pi} (\bar{P} - P_a) R \cos \theta \, d\theta \, dz \quad (84)$$

Tangential component of force (sine component)

$$F_t = \int_0^L \int_0^{2\pi} (\bar{P} - P_a) R \sin \theta \, d\theta \, dz \quad (85)$$

Radial component of moment (cosine component)

$$M_r = - \int_0^L \int_0^{2\pi} (\bar{P} - P_a) R z \cos \theta \, d\theta \, dz \quad (86)$$

Tangential component of moment (sine component)

$$M_t = \int_0^L \int_0^{2\pi} (\bar{P} - P_a) R z \sin \theta \, d\theta \, dz \quad (87)$$

Attitude angles

$$\phi = \tan^{-1} \frac{F_r}{F_t}, \quad \phi' = \tan^{-1} \frac{M_r}{M_t} \quad (88)$$

Bearing torque

$$T_B = \frac{R\omega(U-V)^2}{8} \int_0^z \int_0^{2\pi} C_f R d\theta \, dz + \frac{R}{2} \int_0^z \int_0^{2\pi} h \frac{\partial P}{\partial \theta} \, d\theta \, dz \quad (89)$$

where C_f is the Couette friction factor which is plotted in Fig. 6 against R_{h_0} . $\partial P / \partial \theta$ is the local pressure gradient. By Eqs. (71), (72), (59) and (60) the second term of Equation (89), the Poiseuille torque, can be written in terms of the overall pressure gradients.

$$\begin{aligned} \frac{R}{2} \int_0^z \int_0^{2\pi} h \frac{\partial P}{\partial \theta} \, d\theta \, dz &= \frac{R}{2} \int_0^z \left\{ \alpha h_0 \left[(1-\alpha) \bar{B}_1 \left(\frac{\partial \bar{P}}{\partial s} + \frac{\cot \beta}{R} \frac{\partial \bar{P}}{\partial \theta} \right) \sin \beta \right. \right. \\ &+ (1-\alpha) \bar{B}_2 - \bar{A}_1 \left. \frac{\partial \bar{P}}{\partial \theta} \right] + (1-\alpha) h_r \left[\bar{A}_2 \frac{\partial \bar{P}}{\partial \theta} - \alpha \bar{B}_1 \left(\frac{\partial \bar{P}}{\partial s} + \frac{\cot \beta}{R} \frac{\partial \bar{P}}{\partial \theta} \right) \sin \beta \right. \\ &\left. \left. - \alpha \bar{B}_2 \right] \right\} dz \quad (90) \end{aligned}$$

Journal torque

$$T_j = T_B + \epsilon C W \sin \phi \quad (91)$$

$$\text{Where } W = \text{load} = \sqrt{F_r^2 + F_t^2}$$

Flow

$$Q = R \int_0^{2\pi} W^\eta d\theta \quad (92)$$

where W^η is defined by Eq. (80).

APPENDIX II
DERIVATION OF RELATIONSHIPS FOR
CALCULATING STIFFNESS AND DAMPING COEFFICIENTS

Consider the reference axes shown in Fig. 3. The relationship between the forces F_x and F_y and the forces F_r and F_t can be written in matrix form as

$$\begin{Bmatrix} F_x \\ F_y \end{Bmatrix} = \begin{Bmatrix} -W \\ 0 \end{Bmatrix} = - \begin{Bmatrix} \cos \phi & \sin \phi \\ \sin \phi & -\cos \phi \end{Bmatrix} \cdot \begin{Bmatrix} F_r \\ F_t \end{Bmatrix} \quad (93)$$

For an infinitesimally small motion around the steady state position the dynamic forces become

$$\begin{Bmatrix} dF_x \\ dF_y \end{Bmatrix} = - \begin{Bmatrix} \cos \phi & \sin \phi \\ \sin \phi & -\cos \phi \end{Bmatrix} \cdot \begin{Bmatrix} dF_r + F_t d\phi \\ dF_t - F_r d\phi \end{Bmatrix} \quad (94)$$

The infinitesimal dynamic motion of the journal center is described by the coordinates (x,y) :

$$x = d(e \cos \phi) \quad y = d(e \sin \phi)$$

or

$$\begin{Bmatrix} dx \\ dy \end{Bmatrix} = \begin{Bmatrix} -\sin \phi & \cos \phi \\ \cos \phi & \sin \phi \end{Bmatrix} \cdot \begin{Bmatrix} x \\ y \end{Bmatrix} \quad (95)$$

The velocities transform similarly:

$$\begin{Bmatrix} \dot{d} \\ e\dot{\theta} \end{Bmatrix} = \begin{Bmatrix} \cos \phi & \sin \phi \\ -\sin \phi & \cos \phi \end{Bmatrix} \cdot \begin{Bmatrix} \dot{x} \\ \dot{y} \end{Bmatrix} \quad (96)$$

If, in the differential equation for pressure P obtained in Appendix I, we introduce the following dimensionless variables

$$\left. \begin{aligned} \omega &= (U+V)/R \\ z' &= z/L \\ h' &= h/C \\ \bar{P} &= \frac{2\pi P}{\mu \omega} \left(\frac{C}{R}\right)^2 \\ \epsilon &= e/C \\ \frac{\dot{\epsilon}}{\omega} &= \frac{1}{\omega} \frac{\partial \epsilon}{\partial t} \\ \dot{\theta} &= \frac{1}{\omega} \frac{\partial \theta}{\partial t} \end{aligned} \right\} \quad (97)$$

we obtain the result that the dimensionless pressure \bar{P} in a spiral-grooved bearing of fixed geometry is a function only of the dimensionless variables ϵ , ϵ/ω and $\dot{\theta}/\omega$ i.e.

$$\bar{P} = \bar{P} \left(\epsilon, \frac{\dot{\epsilon}}{\omega}, \frac{\dot{\theta}}{\omega} \right) \quad (98)$$

The resulting fluid film forces in radial and tangential directions are:

$$\begin{aligned}
 F_r &= -\lambda\omega \iint \bar{P} \cos \theta \, dx' \, dz' \\
 &= \lambda\omega \bar{F}_r \left(\epsilon, \frac{\dot{\epsilon}}{\omega}, \frac{\dot{\phi}}{\omega} \right)
 \end{aligned}
 \tag{99}$$

$$\begin{aligned}
 F_t &= \lambda\omega \iint \bar{P} \sin \theta \, dx' \, dz' \\
 &= \lambda\omega \bar{F}_t \left(\epsilon, \frac{\dot{\epsilon}}{\omega}, \frac{\dot{\phi}}{\omega} \right)
 \end{aligned}
 \tag{100}$$

where:

$$\begin{aligned}
 \lambda &= \frac{\mu RL}{\pi} \left(\frac{R}{C} \right)^2 \\
 \bar{F}_r &= \frac{F_r}{\mu NDL} \left(\frac{C}{R} \right)^2 \\
 \bar{F}_t &= \frac{F_t}{\mu NDL} \left(\frac{C}{R} \right)^2
 \end{aligned}
 \tag{101}$$

Differentiating Eqs. (99) and (100) we obtain

$$dF_r = \frac{\lambda\omega}{C} \left[\frac{\partial \bar{F}_r}{\partial \epsilon} d\epsilon + \frac{1}{\omega} \frac{\partial \bar{F}_r}{\partial \left(\frac{\dot{\epsilon}}{\omega} \right)} d\dot{\epsilon} + \frac{1}{\epsilon\omega} \frac{\partial \bar{F}_r}{\partial \left(\frac{\dot{\phi}}{\omega} \right)} \epsilon d\dot{\phi} \right]
 \tag{102}$$

$$dF_t = \frac{\lambda \omega}{c} \left[\frac{\partial \bar{F}_t}{\partial \epsilon} de + \frac{1}{\omega} \frac{\partial \bar{F}_t}{\partial \left(\frac{\dot{\epsilon}}{\omega}\right)} d\dot{\epsilon} + \frac{1}{\epsilon \omega} \frac{\partial \bar{F}_t}{\partial \left(\frac{\dot{\phi}}{\omega}\right)} \epsilon d\dot{\phi} \right] \quad (103)$$

By substitution of Eqs. (102 and (103) into Eq. (94)

$$\begin{Bmatrix} dF_x \\ dF_y \end{Bmatrix} = -\frac{1}{c} \lambda \omega \begin{Bmatrix} \cos \phi & \sin \phi \\ \sin \phi & -\cos \phi \end{Bmatrix} \cdot \left[\begin{Bmatrix} \frac{\partial \bar{F}_r}{\partial \epsilon} & \frac{\bar{F}_t}{\epsilon} \\ \frac{\partial \bar{F}_t}{\partial \epsilon} & -\frac{\bar{F}_r}{\epsilon} \end{Bmatrix} \begin{Bmatrix} de \\ \epsilon d\dot{\phi} \end{Bmatrix} + \frac{1}{\omega} \begin{Bmatrix} \frac{\partial \bar{F}_r}{\partial \left(\frac{\dot{\epsilon}}{\omega}\right)} & \frac{\partial \bar{F}_r}{\epsilon \partial \left(\frac{\dot{\phi}}{\omega}\right)} \\ \frac{\partial \bar{F}_t}{\partial \left(\frac{\dot{\epsilon}}{\omega}\right)} & \frac{\partial \bar{F}_t}{\epsilon \partial \left(\frac{\dot{\phi}}{\omega}\right)} \end{Bmatrix} \begin{Bmatrix} d\dot{\epsilon} \\ \epsilon d\dot{\phi} \end{Bmatrix} \right]$$

The stiffness and damping coefficients are defined by:

$$\begin{aligned} dF_x &= -K_{xx}x - B_{xx}\dot{x} - K_{xy}y - B_{xy}\dot{y} \\ dF_y &= -K_{yx}x - B_{yx}\dot{x} - K_{yy}y - B_{yy}\dot{y} \end{aligned} \quad (105)$$

To determine the 8 coefficients, substitute Eq. (95) and (96) into Eq. (104) and collect the terms in accordance with Eq. (105) to get:

$$K_{xx} = \frac{1}{c} \lambda \omega \left[\frac{\partial \bar{F}_r}{\partial \epsilon} \cos^2 \phi + \frac{\partial \bar{F}_t}{\partial \epsilon} \cos \phi \sin \phi - \frac{\bar{F}_t}{\epsilon} \sin \phi \right] \quad (106)$$

$$\begin{aligned} B_{xx} &= \frac{1}{c} \lambda \omega \left[\frac{\partial \bar{F}_r}{\partial \left(\frac{\dot{\epsilon}}{\omega}\right)} \cos^2 \phi + \frac{\partial \bar{F}_t}{\partial \left(\frac{\dot{\epsilon}}{\omega}\right)} \cos \phi \sin \phi \right. \\ &\quad \left. - \frac{\sin \phi}{\epsilon} \left(\frac{\partial \bar{F}_r}{\partial \left(\frac{\dot{\phi}}{\omega}\right)} \cos \phi + \frac{\partial \bar{F}_t}{\partial \left(\frac{\dot{\phi}}{\omega}\right)} \sin \phi \right) \right] \end{aligned} \quad (107)$$

$$K_{xy} = \frac{1}{C} \lambda \omega \left[\frac{\partial \bar{F}_r}{\partial \epsilon} \sin^2 \phi + \frac{\partial \bar{F}_r}{\partial \epsilon} \cos \phi \sin \phi + \frac{\bar{F}_r}{\epsilon} \cos \phi \right] \quad (108)$$

$$\omega_B_{xy} = \frac{1}{C} \lambda \omega \left[\frac{\partial \bar{F}_r}{\partial \left(\frac{\epsilon}{B}\right)} \sin^2 \phi + \frac{\partial \bar{F}_r}{\partial \left(\frac{\epsilon}{B}\right)} \cos \phi \sin \phi \right. \\ \left. + \frac{\cos \phi}{\epsilon} \left(\frac{\partial \bar{F}_r}{\partial \left(\frac{\epsilon}{B}\right)} \cos \phi + \frac{\partial \bar{F}_r}{\partial \left(\frac{\epsilon}{B}\right)} \sin \phi \right) \right] \quad (109)$$

$$K_{yx} = \frac{1}{C} \lambda \omega \left[- \frac{\partial \bar{F}_r}{\partial \epsilon} \cos^2 \phi + \frac{\partial \bar{F}_r}{\partial \epsilon} \cos \phi \sin \phi + \frac{\bar{F}_r}{\epsilon} \sin \phi \right] \quad (110)$$

$$\omega_B_{yx} = \frac{1}{C} \lambda \omega \left[- \frac{\partial \bar{F}_r}{\partial \left(\frac{\epsilon}{B}\right)} \cos^2 \phi + \frac{\partial \bar{F}_r}{\partial \left(\frac{\epsilon}{B}\right)} \cos \phi \sin \phi \right. \\ \left. - \frac{\sin \phi}{\epsilon} \left(\frac{\partial \bar{F}_r}{\partial \left(\frac{\epsilon}{B}\right)} \sin \phi - \frac{\partial \bar{F}_r}{\partial \left(\frac{\epsilon}{B}\right)} \cos \phi \right) \right] \quad (111)$$

$$K_{yy} = \frac{1}{C} \lambda \omega \left[\frac{\partial \bar{F}_r}{\partial \epsilon} \sin^2 \phi - \frac{\partial \bar{F}_r}{\partial \epsilon} \cos \phi \sin \phi - \frac{\bar{F}_r}{\epsilon} \cos \phi \right] \quad (112)$$

$$\omega_B_{yy} = \frac{1}{C} \lambda \omega \left[\frac{\partial \bar{F}_r}{\partial \left(\frac{\epsilon}{B}\right)} \sin^2 \phi - \frac{\partial \bar{F}_r}{\partial \left(\frac{\epsilon}{B}\right)} \cos \phi \sin \phi \right. \\ \left. + \frac{\cos \phi}{\epsilon} \left(\frac{\partial \bar{F}_r}{\partial \left(\frac{\epsilon}{B}\right)} \sin \phi - \frac{\partial \bar{F}_r}{\partial \left(\frac{\epsilon}{B}\right)} \cos \phi \right) \right] \quad (113)$$

where, in the coordinate system selected,

$$\bar{F}_x = \frac{-W}{\mu NLD} \left(\frac{R}{C}\right)^2 \quad (114)$$

$$\bar{F}_y = 0 \quad (115)$$

and all forces and derivatives are calculated for the given steady state position, defined by (ϵ_0, ϕ_0) .

APPENDIX III - COMPUTER PROGRAM PN 412
PERFORMANCE OF A HERRINGBONE JOURNAL BEARING
OPERATED IN THE TURBULENT REGIME

Input

All input data appears in the form of name list. A full description of name list can be found in Ref. 10. The input are contained in the namelist "INPUT".

The input data are:

1. REN = Reynolds number
= $2 \pi \frac{N_i - N_o}{\nu} RC$

where N_i and N_o are the rotational velocities of the journal and bearing in cycles/sec., respectively.

R = Radius of journal, in.

C = Nominal radial clearance, in.

ν = Kinematic viscosity, in²/sec.

2. ALOVD = Length-diameter ratio
= L/D

where L = Length of journal, in.

D = Diameter of journal, in.

3. COR = Film clearance ratio
= C/R

4. PFIX = Dimensionless gage pressures at the ends and the middle of the bearing.

= $\frac{P \text{ (Pressure, PSIC)}}{\mu \left(\frac{R}{C}\right)^2 (N_i + N_o)}$

where μ = dynamic viscosity, lb-sec/in².

The pressure at the initial end appears first, then at the middle and finally at the final end.

5. I1 = Number of axial grid points in the first region of the bearing counted from the initial end of journal (see Fig. 2). An odd number is required and also it must be at least 2 less than I2. The minimum permissible value for I1 is 3.

6. I2 = Number of axial grid points counted from the initial end of the journal to the end of the second region. For a vented bearing, I2 represents the grid points of one half of a bearing. For a three region, non-vented bearing, I2 represents the grid points for the initial end up to the interface of the second and third region (see Fig. 2). The minimum permissible value for I2 is 5 and the maximum is 17. Again, I2 must be an odd number.
7. MORE = Indicator to specify whether or not there is another set of input cards to follow the present set.
 MORE = F, last set of input
 MORE = T, another set of input to follow
8. SIGN = $\frac{N_o - N_i}{N_o + N_i}$
9. N = Number of grid points in the circumferential direction. The maximum permissible value for N is 19.
10. EDOT = $\dot{e}/2\pi (N_i + N_o)$
 where \dot{e} = time rate change of eccentricity ratio of the journal.
11. PHDOT = Dimensionless whirl velocity ratio
 = $\dot{\phi}/2\pi (N_i + N_o)$
 where $\dot{\phi}$ = journal whirl velocity, rad/sec.
12. GAMDOT = $\dot{\gamma}/2\pi (N_i + N_o)$
 where $\dot{\gamma}$ = time rate change of angular misalignment.
13. EPS = Eccentricity ratio
 = e/c
 where e = eccentricity of journal, in.
14. GAM = Misalignment of journal, degrees.
15. VENT = Indicator to specify whether or not the middle of bearing is vented. Set VENT = T only for a bearing vented at the middle. For non-vented bearings, set VENT = F.

16. BETA = Groove angle in degrees. Beta must be specified for the first region of the bearing (first value) and the second region of the bearing (second value). If VENT = F, the value of BETA in the third region must be specified. For a pump-in design, with grooving in the first region, and a smooth seal in the second region, BETA should be read in as an obtuse angle, the same value for BETA being read in for the second region as the first region. For a pump-out design, with grooving in the second region of the bearing and a seal in the first region, BETA should be read in as acute angle with the same value of BETA being read in for the first region as for the second region. If VENT = F, the value of BETA in the third region should be given. The third value of BETA should be a conjugate of the first value of BETA, i.e. $BETA(3) = 180^\circ - BETA(1)$. Never set BETA = 0.

17. DEP = Groove recess ratios in two or three regions of the journal with the first value referring to the first region, etc.
 = δ/c
 where δ = groove recess, in.
 To impose the condition of a smooth bearing (no grooving) in either region, set DEP = 0 for that region.

18. ALPHA = Fractional groove width in two or three regions of the journal with the first value referring to the first region, etc.

$$= \frac{a_g}{a_g + a_r}$$

where a_g and a_r are the widths in inches in the groove and ridge portion respectively. To impose the conditions of a smooth portion in either region, set ALPHA = 0 for that region.

19. PPOUT = Indicator to specify whether the pressure distribution in the bearing is required as a part of output.
 PPOUT = T, pressure distribution is printed out; no pressure is printed out when PPOUT = F.

Output

1. Under the heading of INPUT, the complete set of input in the namelist "INPUT" is printed out. Each quantity is identified by the same symbol as used in the namelist "INPUT".
2. In the case of PPOUT = T, a heading of "Final Pressure Distribution" is printed out. Below the heading, if VENT = T, there are a total of I2 number of lines of pressures with the first line referring to the initial end of the bearing. If N is less or equal to 10, each line contains N number of pressures starting at $\phi = 0$ (see Fig. 1). For the case of $N > 10$, the number of lines are double. If VENT = F, there are a total of (I2 + I1-1) lines when $N \leq 10$; The number of lines will be double for the case of $N > 10$.

3. Regular Output:

There are a total of nine quantities in one line under the heading of REN NO., ECC., TORQUE J., TORQUE B., RADIAL LOAD, TANG. LOAD, FLOW, COS. MOMENT, SIN MOMENT, which are defined below.

a. REN NO. = Same as the input.

b. EPS = Same as the input.

c. TORQUE J. = Dimensionless torque on bearing

$$= \frac{T_j}{WC}$$

where T_j = torque on journal, in-lb.

W = total load, lb.

d. TORQUE B. = Dimensionless torque on bearing

$$= \frac{T_b}{WC}$$

where T_b = torque on bearing, in-lb.

e. RADIAL LOAD = Dimensionless radial component of load

$$= \frac{F_r}{\mu (N_i + N_o) \left(\frac{R}{C}\right)^2 R^2}$$

where F_r = radial component of load, lb.

f. TANG. LOAD = Dimensionless tangential component of load

$$= \frac{F_t}{\mu (N_1 + N_0) \left(\frac{R}{C}\right)^2 p^2}$$

where F_t = tangential component of load, lb.

g. FLOW = Dimensionless flow

$$= \frac{Q}{R^2 C (N_1 + N_0)}$$

where Q = flow, cu. in/sec.

h. COS. MOMENT = Dimensionless radial (cosine) component of moment,
about the initial end of journal.

$$= \frac{M_r}{\mu (N_1 + N_0) \left(\frac{R}{C}\right)^2 R^3}$$

where M_r = radial component of moment, lb-in.

i. SIN MOMENT = Dimensionless tangential (sin) component of moment,
about the initial end of journal.

$$= \frac{M_t}{\mu (N_1 + N_0) \left(\frac{R}{C}\right)^2 R^3}$$

where M_t = tangential component of moment, lb-in.

A Fortran listing of Program PN 406 is provided in the next few pages.
Typical listings of input and output are also given.

```

C          MERRINGBONE JOURNAL
C          WITH LARGE ECCENTRICITY AND MISALIGNMENT
C          IN TURBULENCE REGIME
COMMON MDIAG,DELX,DELZ,DELZ5,M,MS,MG1,MG2,N,NP(17,19),A1(2,5,1
19),B1(2,19),CC(2,19),AF1(17,19),AF2(17,19),AF3(17,19),AF4(17,19),A
2F6(17,19),AF7(17,19),AF5(17,19),PHI(17,19)
DIMENSION BETA(3),DEP(3),ALPHA(3),PFI(3),          QQQ(19),H9(17
1,19),QQQQ(19),PP(17),PPP(17),PPX(17),PPPX(17),AX1(17,19),AX2(17,19
2),AX3(17,19),AX6(17,19),AX7(17,19),AX8(17,19),AX9(17,19),WS11(17,1
39),WS12(17,19),WS13(17,19),WS14(17,19),XX(17),AXL(2,19),CZ(2,19)
DIMENSION KUPT(17,19)
LOGICAL PPOUT,VENT,TORQ,MORE
NAMELIST/INPUT/REN,ALOVD,COR,PFI,I1,I2,
IMORE,SIGN,          N, EDOT,PHDOT,GAMDOT,EPS,GAM,VENT,BETA,DEP,ALPHA,
IPPOUT
2 FORMAT(7E14.7)
4 FORMAT(/10(I1,F11.7))
9 FORMAT(29HOFINAL PRESSURE DISTRIBUTION. //)
11 FORMAT(6H1INPUT)
10 READ(5,INPUT)
WRITE(6,11)
WRITE(6,INPUT)
MDIAG=0
MD=0
RATLD=2.*ALVD
MG1=I1-1
AMG=MG1
MS=I2-I1
IF(VENT) GO TO 102
M=I2+I1-1
BMM1=M-1
MG2=MG1
GO TO 101
102 M=I2
RATLD=2.*RATLD
BMM1= M-1
BMM1=BMM1*2.
MG2=0
101 DO 30 I=1,M
DO 30 J=1,N
30 NP(I,J)=0
DO 20 J=1,N
NP(I,J)=1
20 NP(M,J)=1
35 KK=1
100 AN=N
PI=3.14159265358979
DTHETA=2.*PI/AN
DTHE2=0.5/DTHETA
TPS=2.*PI*SIGN
CON1=6.*TPS
RADIAN=.017453292519943
GAL=GAM*RADIAN
EDT=0.0
CON2=CON1/REN
TORQ=.FALSE.
TPS1=TPS/8.0
TRQ=TPS1*REN
DELX=DTHETA
DELZ=RATLD/BMM1
TPS1=(2.*PI)**2*8.

```

AMS=MS	81
DELZS=DELZ	81
ANG=0.0	90
PHIMC=PHDOT-(1.-SIGN)*0.5	90
IND=1	90
ERO2=1.	90
L1=1	90
L2=11	90
38 DO 40 J=1,N	90
CC(L1,J)=0.0	90
AXL(L1,J)=0.	90
CZ(L1,J)=0.	90
A1(L1,2,J)=0.0	100
A1(L1,3,J)=0.0	100
40 AF7(L2,J)=0.0	100
IF(IND.EQ.2)GO TO 48	100
IF(VENT) GO TO 48	100
L1=2	100
L2=12	100
IND=2	100
GO TO 38	100
48 NR=1	100
MN=MG1	110
MM=11	110
ISS=1	110
DEL=DELZ	110
DZ=0.5/DELZ	110
IS=1	110
Z=0.0	110
200 BET=BETA(NR)*RADIAN	110
DEPH=DEP(NR)	110
ALPHA=ALPH(NR)	110
ALM1=1.-ALPH	120
ALTAL1=ALPH*ALM1	120
SINB=SIN(BET)	120
COSB=COS(BET)	120
SINB2=SINB*SINB	120
COSB2=COSB*COSB	120
COT2=COSB2/SINB2	120
DLZ=DEL*UTHEA	120
IF(TORG) GO TO 1001	120
DO 2000 I=IS,MM	120
XX(I)=Z	130
ZCOR=Z/COR	130
EPZGH=EPS+GA1*ZCOR	130
EDZR=EDOT+GAMDOT*ZCOR	130
EPZG=EPZGH*PHIMC	130
DO 2001 J=1,N	130
SI=SIN(ANG)	130
CO=COS(ANG)	130
H=1.+CO*EPZGH	130
H9(I,J)=H	130
H3=H**H	140
HG=H*DEPH	140
HGHR=HG/H	140
AX9(I,J)=(EDZR*CO+EPZG*SI)*SINB*PI*24.0	140
HG3=HG**3	140
HGHR3=HG3/H3	140
S1=1./SINB2	140
S2=-COSB/SINB2	140
REN=REN*H	140

RENG=REN*HG	149
GXR=GTCF(REN R)*12.	150
GXG=GTCF(RENG)*12.	151
GZR=GZCF(REN R)*12.	152
GZG=GZCF(RENG)*12.	153
S5=(GXR+GZR*COT2)	154
S6=(GXG+GZG*COT2)	155
S7=GZG*S2	156
S8=GZR*S2	157
S9=GZG*S1	158
S10=GZR*S1	159
S11=-S5/S6/HGHR3	160
S12=1.-S11*ALPH-ALPH	161
S13=(S7-S8/HGHR3)/S6/S12	162
S14=REN R/HG3/S12*(1.-HGHR)/S6	163
ALH3=ALPH*HG3	164
A1S=SINB*(ALH3*S6*S11-ALM1*S5*H3)/S12	165
A2=-ALM1*(ALPH*S5*S13+S8)*H3	166
A2=(A2+ALH3*(ALM1*S6*S13-S7))*SINB	167
A3=ALTAL1*S14*(S6*HG3-S5*H3)/REN	168
A3=CON1*(A3+H*ALM1+HG*ALPH)*SINB	169
DMY=H3*ALM1	170
S7H=HGHR3*S7	171
B1S=-H3/S12*(S8*ALM1-S7H*ALPH*S11)*SINB	172
B2=ALH3*(S9-S7*S13*ALM1)+DMY*(S10+ALPH*S8*S13)	173
B3=CON1*ALTAL1*S14*(S8-S7H)	174
B2=-B2*SINB	175
AX1(I,J)=A1S+A2*COSB	176
B3=-B3*H3*SINB/REN	177
AX2(I,J)=A2*SINB	178
WS11(I,J)=S11/S12	179
WS12(I,J)=1./S12	180
WS13(I,J)=S13	181
WS14(I,J)=S14	182
AX3(I,J)=A3	183
AX6(I,J)=B1S+B2*COSB	184
AX7(I,J)=B2*SINB	185
AX8(I,J)=B3	186
IF(MD.NE.2) GO TO 2001	187
IF(I.EQ.1S. AND.J.EQ.1)	188
1 WRITE(6,2) AX1(I,J),AX2(I,J),AX3(I,J),AX6(I,J),AX7(I,J),AX8(I,J),AX9(I,J)	189
2001 ANG=ANG+DTHETA	191
Z=Z+DEL	192
2000 CONTINUE	193
IF(NR.EQ.1) GO TO 2010	194
IF(NR.EQ.3) GO TO 2014	195
IF(VENT) GO TO 2014	196
GO TO 2020	197
2010 IK=1	198
GO TO 3800	199
2014 IK=MM	200
GO TO 3800	201
COMPUTE THE DIFFERENCES IN XS AND COEFFICIENT	202
3800 I=IK	203
DO 4010 J=1,N	204
AF1(I,J)=0.0	205
AF2(I,J)=0.0	206
AF3(I,J)=0.0	207
AF4(I,J)=0.0	208
AF5(I,J)=0.0	209

	AF6(I,J)=1.0	210
	AF7(I,J)=-PFIX(NR)	211
4010	CONTINUE	212
2020	IST=IS+1	213
	MM1=MM-1	214
	DO 4000 I=IST,MM1	215
	IO=I-1	216
	I7=I+1	217
	DO 4000 J=1,N	218
	DTH=DTHE2	219
	IF(J.EQ.1.OR.J.EQ.N) GO TO 4004	220
	J0=J-1	221
	J1=J+1	222
	GO TO 4008	223
4004	IF(J.EQ.1) GO TO 4006	224
	J0=N-1	225
	J1=1	226
	GO TO 4008	227
4006	J0=N	228
	J1=2	229
4008	AF1(I,J)=SINB*AX7(I,J)	230
	AF2(I,J)=(AX2(I,J1)-AX2(I,J0)+COSB*(AX7(I,J1)-AX7(I,J0)))*DTH	231
1	+SINB*(AX7(I7,J)-AX7(I0,J))*DZ	232
	AF3(I,J)=AX2(I,J)+COSB*AX7(I,J)+SINB*AX6(I,J)	233
	AF4(I,J)=(AX1(I,J1)-AX1(I,J0)+COSB*(AX6(I,J1)-AX6(I,J0)))*DTH	234
1	+SINB*(AX6(I7,J)-AX6(I0,J))*DZ	235
	AF5(I,J)=AX1(I,J)+COSB*AX6(I,J)	236
	AF6(I,J)=0.0	237
	AF7(I,J)=(AX3(I,J1)-AX3(I,J0)+COSB*(AX8(I,J1)-AX8(I,J0)))*DTH	238
1	+SINB*(AX8(I7,J)-AX8(I0,J))*DZ+AX9(I,J)	239
	IF(MD.EQ.2 .AND. J. EQ. 1)	240
1	WRITE(6,2) AF1(I,J),AF2(I,J),AF3(I,J),AF4(I,J),AF5(I,J),AF7(I,J)	241
		242
4000	CONTINUE	243
	IF(NR.EQ.1) GO TO 4020	244
	IF(NR.EQ.2) GO TO 4040	245
	II=2	246
	IE=12	247
	GO TO 4090	248
4020	II=1	249
	IE=MM	250
	GO TO 4090	251
4040	II=1	252
	IE=IS	253
4090	DO 4100 J=1,N	254
	A1(II,1,J)=0.0	255
	A1(II,5,J)=0.0	256
	TRS=AX7(IE,J)	257
	TRSZ=TRS*DZ*2.0	258
	A1(II,4,J)=-TRSZ	259
	A1(II,2,J)=A1(II,2,J)-TRSZ*ERO2	260
	DDT=AX6(IE,J)*DTHE2	261
	CC(II,J)=CZ(II,J)-DDT	262
	CZ(II,J)=DDT	263
	B1(II,J)=-CC(II,J)	264
	A1(II,3,J)=A1(II,3,J)+TRSZ	265
	AF7(IE,J)=AXL(II,J)-AX8(IE,J)	266
	AXL(II,J)=AX8(IE,J)	267
	AF1(IE,J)=0.0	268
	AF2(IE,J)=0.0	269
	AF3(IE,J)=0.0	270

AF4(IE,J)=0.0	271
AF5(IE,J)=0.0	272
AF6(IE,J)=0.0	273
IF(MD.EQ.2.AND.J.EQ.N)	274
1 WRITE(6,2) A1(1,2,J):A1(1,4,J),A1(1,3,J),B1(1,J)	275
1),CC(1,J),AF7(IE,J)	276
4100 CONTINUE	277
IF(NR.EQ.1) GO TO 4102	278
GO TO 4150	279
4102 IS=11	280
NR=2	281
MM=12	282
ERO2=0.	283
DEL=DELZS	284
DZ=0.5/DELZS	285
GO TO 200	286
4160 IF(VENT) GO TO 4190	287
IF(KK.EQ.1) GO TO 4180	288
IS=12	289
MM=M	290
NR=3	291
ERO2=0.	292
DEL=DELZ	293
DZ=0.5/DELZ	294
GO TO 200	295
4180 IE=12	296
ERO2=1.	297
KK=2	298
II=2	299
GO TO 4090	300
4150 IF(NR.EQ.2) GO TO 4160	301
4190 MTSR=MD	302
MD =MTSR	303
CALL CIC1 (MD)	304
MD=0	305
IF(PPOUT) WRITE(6,9)	306
DO 575 I=1,M	307
IF(PPOUT) WRITE(6,4)(PHI(I,J),J=1,N)	308
DO 575 J=1,N	309
KUPT(I,J)=0	310
IF(PHI(I,J).GE.0.0) GO TO 575	311
PHI(I,J)=0.0	312
KUPT(I,J)=1	313
575 CONTINUE	314
C DIMENSIONLESS FLOW Q/C(N1+N2)R*R	315
IP=11-1	316
4204 AFLOW=0.0	317
DO 4200 J=1,N	318
IF(J.EQ.1.OR.J.EQ.N) GO TO 4220	319
YF1=(PHI(IP,J+1)-PHI(IP,J-1))*DTHE2	320
4210 AFLOW=(YF1*AX6(IP,J))+AX8(IP,J)+AX7(IP,J)*(PHI(IP+1,J)-PHI(IP-1,J))	321
1)*DZ+AFLOW	322
IF(MDIAG.EQ.2) WRITE(6,2)YF1,AFLOW	323
GO TO 4200	324
4220 IF(J.EQ.N) GO TO 4230	325
YF1=(PHI(IP,2)-PHI(IP,N))*DTHE2	326
GO TO 4210	327
4230 YF1=(PHI(IP,1)-PHI(IP,N-1))*DTHE2	328
GO TO 4210	329
CONTINUE	330
AFLOW=AFLOW*DTHE2/12.	331

C	TORQUE DIVIDED BY MUANARXXXXX/C	332
	NR=1	333
	TORQ=.TRUE.	334
	TQ=0.0	335
	IT1=1	336
	IT2=11	337
	TC1=0.0	338
	GO TO 200	339
1001	DO 1000 I=IT1,IT2	340
	DO 1000 J=1,N	341
	IF(KUPT(I,J).EQ.1) GO TO 1000	342
	IF(I.EQ.IT1.OR.I.EQ.IT2) GO TO 1800	343
	DPDZ=(PHI(I+1,J)-PHI(I-1,J))/DZ	344
	AFTR=1.0	345
1200	IF(J.EQ.1.OR.J.EQ.N) GO TO 1600	346
	DPDT=(PHI(I,J+1)-PHI(I,J-1))*DTHE2	347
1240	H=H9(I,J)	348
	BQ=H*ALTAL1*DEPH	349
	AQ=(-BQ*COSB*WS13(I,J)-H*ALM1*WS12(I,J)-ALPH*WS11(I,J))*(H+DEPH)*	350
	DPDT	351
	AQ=AQ+BQ*(-CON2*WS14(I,J)-WS13(I,J)*DPDZ*SINB)	352
	TQ=TQ+AQ*DLZ*0.5*AFTR	353
	GO TO 1010	354
1600	IF(J.EQ.N) GO TO 1610	355
	DPDT=(PHI(I,2)-PHI(I,N))*DTHE2	356
	GO TO 1240	357
1610	DPDT=(PHI(I,1)-PHI(I,N-1))*DTHE2	358
	GO TO 1240	359
1800	AFTR=.5	360
	IF(I.EQ.IT2) GO TO 1810	361
	DPDZ=(PHI(IT1+1,J)-PHI(IT1,J))/DELZ	362
	GO TO 1200	363
1810	DPDZ=(PHI(IT2,J)-PHI(IT2-1,J))/DELZ	364
	GO TO 1200	365
1010	RE=REN*H	366
	TC2=TCC(RE)*ALM1	367
	RE=REN*(H+DEPH)	368
	TC1=TC1+(TC2+TCC(RE)*ALPH)*TRQ*DLZ*AFTR	369
	IF(J.NE.1) GO TO 1000	370
	IF(MD.EQ.2.AND.I.EQ.IT1)	371
	WRITE(6,2)AQ,TQ,RE,TC1,TC2	372
1000	CONTINUE	373
	IF(MD.EQ.2)WRITE(6,2)WS11(I,J),WS12(I,J),WS13(I,J),WS14(I,J)	374
	IF(NR.EQ.1) GO TO 1400	375
	IF(NR.EQ.2) GO TO 1410	376
	GO TO 578	377
1400	NR=2	378
	IT1=11	379
	IT2=12	380
	GO TO 200	381
1410	IF(VENT) GO TO 578	382
	NR=3	383
	IT1=12	384
	IT2=M	385
	GO TO 200	386
578	TQO= TQ+TC1	387
	IF (SIGN.LT.0.) TQO=-TQO	388
	THE=0.0	389
	DO 580 J=1,N	390
	QQQ(J)=SIN(THE)	391
	QQQ(J)=COS(THE)	392

580	THE=DTHETA+THE	393
	DO 590 I=1,M	394
	PP(I)=0.0	395
	PPP(I)=0.0	396
	DO 600 J=1,N	397
	DUM=PHI(I,J)	398
	PP(I)=PP(I)+QQQ(J)*DUM	399
600	PPP(I)=PPP(I)+QQQQ(J)*DUM	400
	PP(I)=PP(I)*DTHETA	401
	PPP(I)=PPP(I)*DTHETA	402
	PPX(I)=PP(I)*XX(I)	403
590	PPPX(I)=PPP(I)*XX(I)	404
	FSIN=SUM(PP,M,DELZ)	405
	FCOS=SUM(PPP,M,DELZ)	406
	FMSIN=SUM(PPX,M,DELZ)	407
	FMCOS=SUM(PPPX,M,DELZ)	408
	FMCOS=-FMCOS	409
	FCOS=-FCOS	410
	WLOAD=FCOS**2+FSIN**2	411
	WLOAD=SQRT(WLOAD)	412
	TQO=TQO/WLOAD	413
	TQI=TQO+EPS*FSIN/WLOAD	414
	WRITE (6,6)	415
	WRITE (6,7) REN, EPS, TQI, TQO, FCOS, FSIN, AFLOW, FMCOS, FMSIN	416
6	FORMAT (112H REN NO. EPS. TORQUE J. TORQUE B. RADIAL LOA	417
	1D TANG. LOAD FLOW COS. MOMENT SIN. MOMENT)	418
7	FORMAT (F9.2,1X,F6.3,7(1XE13.6))	
599	IF(MORE) GO TO 10	420
	STOP	
	END	422

SUBROUTINE CIC1(M)	2
COMMON MDIAG,DELX,DELZ,DELZS,M,MS,MG1,MG2,N,NP(17,19),A1(2,5,1	3
19),B1(2,19),CC(2,19),AF1(17,19),AF2(17,19),AF3(17,19),AF4(17,19),A	4
2F6(17,19),AF7(17,19),AF5(17,19),PHI(17,19)	5
DIMENSION A(17,17),B(17,17),C(17,17),D(17,17),F(20,17),AK(17,17),G	6
1N(17,17),S(20,17),AFJI(17),HD(17,17),BF(17),DD(17,17),DS(17),GI(17,	7
217),GI(17,17),E(17,17)	8
AN=1.0/DELX	9
NC=0	10
M=MS+MG1+MG2+1	11
MN1=MG1+1	12
MN2=MN1+MS	13
DX1=AN*0.5	14
DX2=AN**2	15
203 DO 205 I=1,M	16
DO 204 II=1,M	17
E(I,II)=0.	18
204 D(I,II)=0.	19
F(I,I)=0.	20
205 D(I,I)=1.	21
DO 300 J=1,N	22
WRITE(7)((E(I,II),D(I,II),I=1,M),II=1,M)	23
IF(MD.NE.2) GO TO 240	24
WRITE(6,103) AF1(1,J),AF2(1,J),AF3(1,J),AF4(1,J),AF5(1,J),AF6(1,J)	25
1),AF7(1,J)	26
WRITE(6,103)	27
1 A1(1,1,J),A1(1,2,J),A1(1,3,J),A1(1,4,J),A1(1,5,J),B1(MN1,	28
1J),CC(MN1,J)	29
WRITE(6,103)	30
1 A1(2,1,J),A1(2,2,J),A1(2,3,J),A1(2,4,J),A1(2,5,J),	31
1B1(MN2,J),CC(MN2,J)	32
240 DZ1=0.5/(DELZ)	33
DZ2=1./(DELZ)**2	34
241 DO242 I=1,M	35
DO 242 II=1,M	36
B(I,II)=0.	37
A(I,II)=0.	38
242 C(I,II)=0.	39
DO 250 I=1,M	40
206 IF(I-MG1-1) 212,210,212	41
209 AFJI(I)=-AF7(I,J)	42
A(I,I)=1.	43
GO TO 250	44
210 IF(MS) 211,212,211	45
211 DZ1=0.5/DELZS	46
DZ2=1./(DELZS)**2	47
IF(NP(I,J))209,232,209	48
232 IF(MG1) 233,212,233	49
233 IF(NC.EQ.2) GO TO 600	50
A(I,I-2)=A1(1,1,J)	51
A(I,I-1)=A1(1,2,J)	52
A(I,I)=A1(1,3,J)	53
A(I,I+1)=A1(1,4,J)	54
A(I,I+2)=A1(1,5,J)	55
B(I,I)=B1(1,J)	56
C(I,I)=CC(1,J)	57
600 AFJI(I)=-AF7(I,J)	58
GO TO 250	59
212 IF(NP(I,J))209,234,209	60
234 IF(I-MG1-MS-1) 215,213,215	61
213 IF(MS) 214,215,214	62

214	DZ1=.5/DELZ	63
	DZ2=(1./DELZ)**2	64
	IF(NC.EQ.2) GO TO 601	65
	A(I,I-2)=A1(2,1,J)	66
	A(I,I-1)=A1(2,2,J)	67
	A(I,I)=A1(2,3,J)	68
	A(I,I+1)=A1(2,4,J)	69
	A(I,I+2)=A1(2,5,J)	70
	B(I,I)=B1(2,J)	71
	C(I,I)=CC(2,J)	72
601	AFJI(I)=-AF7(I,J)	73
	GO TO 250	74
215	IF(NC.EQ.2) GO TO 602	75
	B(I,I-1)=AF3(I,J)*DX1*DZ1	76
	B(I,I)=AF5(I,J)*DX1-AF4(I,J)*DX1	77
	B(I,I+1)=-AF3(I,J)*DX1*DZ1	78
	A(I,I-1)=AF1(I,J)*DZ2-AF2(I,J)*DZ1	79
	A(I,I)=AF6(I,J)-2.0*(AF1(I,J)*DZ2 +AF5(I,J)*DX2)	80
	A(I,I+1)=AF1(I,J)*DZ2+AF2(I,J)*DZ1	81
	C(I,I-1)=-AF3(I,J)*DX1*DZ1	82
	C(I,I)=AF4(I,J)*DX1+AF5(I,J)*DX2	83
	C(I,I+1)=AF3(I,J)*DX1*DZ1	84
602	AFJI(I)=-AF7(I,J)	85
250	CONTINUE	86
	IF(NC.EQ.2) GO TO 603	87
	DO 260 I=1,M	88
	DO 260 II=1,M	89
	AK(I,II)=A(I,II)	90
	DO 260 III=1,M	91
260	AK(I,II)=AK(I,II)+B(I,III)*E(III,II)	92
	IF(MDIAG.LT.2) GO TO 262	93
	WRITE(6,101)J	94
	DO 261 I=1,M	95
261	WRITE(6,100) (AK(I,II),II=1,M)	96
262	CALL MATINV(AK,M,DUM,0,DUM1)	97
603	CONTINUE	98
	DO 404 I=1,M	99
	BF(I)=AFJI(I)	100
	F(J+1,I)=0.	101
	DO 404 II=1,M	102
	E(I,II)=0.	103
	BD(I,II)=0.	104
	DO 403 III=1,M	105
	E(I,II)=E(I,II)-AK(I,III)*C(III,II)	106
403	BD(I,II)=BD(I,II)+B(I,III)*D(III,II)	107
404	BF(I)=BF(I)-B(I,II)*F(J,II)	108
	DO 406 I=1,M	109
	DO 406 II=1,M	110
	D(I,II)=0.	111
	DO 405 III=1,M	112
405	D(I,II)=D(I,II)-AK(I,III)*BD(III,II)	113
406	F(J+1,II)=F(J+1,II)+AK(II,III)*BF(III)	114
300	CONTINUE	115
	DO 505 I=1,M	116
	DO 504 II=1,M	117
504	DD(I,III)=D(I,II)	118
505	DD(I,II)=1.+DD(I,II)	119
	IF(MDIAG.LT.2) GO TO 264	120
	WRITE(6,101)	121
	DO 263 I=1,M	122
263	WRITE(6,100) (DD(I,II),II=1,M)	123

266	CALL MATINV(DUM,M,DUM,0,DUM)	124
	DO 507 I=1,M	125
	S(N,I)=0.	126
	DO 507 II=1,M	127
	GN(I,II)=0.	128
	DO 506 III=1,M	129
	GN(I,II)=GN(I,II)+DD(I,III)*E(III,II)	130
506	G(I,II)=GN(I,II)	131
507	S(N,I)=S(N,I)+DD(I,II)*F(N+1,II)	132
	J=N+1	133
	DO 512 K=2,N	134
	WRITE(8) ((G(I,II),I=1,M),II=1,M)	135
	BACKSPACE 7	136
	READ(7) ((L(I,II),D(I,II),I=1,M),II=1,M)	137
	BACKSPACE 7	138
	IF(MDIAG.EQ.2) WRITE(6,100) ((L(I,II),D(I,II),I=1,M),II=1,M)	139
	J=J-1	140
	DO 509 I=1,M	141
	S(J-1,I)=F(J,I)	142
	DO 509 II=1,M	143
	GI(I,II)=0.	144
	DO 508 III=1,M	145
	GI(I,II)=GI(I,II)+D(I,III)*GN(III,II)+L(I,III)*G(III,II)	146
	IF(MDIAG.NE.2) GO TO 508	147
508	CONTINUE	148
509	S(J-1,I)=S(J-1,I)+E(I,II)*S(J,II)+D(I,II)*S(N,II)	149
	DO 512 I=1,M	150
	DO 512 II=1,M	151
512	G(I,II)=GI(I,II)	152
280	DO 511 I=1,M	153
	DO 510 II=1,M	154
510	DD(I,II)=-G(I,II)	155
511	DD(I,II)=1.+DD(I,II)	156
	IF(MDIAG.LT.2) GO TO 266	157
	WRITE (6,101)	158
	DO 269 I=1,M	159
269	WRITE (6,102) (D(I,II),II=1,M)	160
266	CALL MATINV(DUM,M,DUM,0,DUM)	161
	IF(MDIAG.LT.2) GO TO 270	162
	1=0	163
	WRITE (6,101)	164
	DO 273 I=1,M	165
273	WRITE (6,100) (DD(I,II),II=1,M)	166
270	DO 515 I=1,M	167
	PHI(I,1)=0	168
	DO 515 II=1,M	169
515	PHI(I,1)=DD(I,II)*S(1,II)+PHI(I,1)	170
	DO 516 J=2,N	171
	BACK SPACE 8	172
	READ(8) ((G(I,II),I=1,M),II=1,M)	173
	BACKSPACE 8	174
	DO 516 I=1,M	175
	PHI(I,J)=S(J,I)	176
	DO 516 II=1,M	177
516	PHI(I,J)=PHI(I,J)+G(I,II)*PHI(II,1)	178
	REWIND 7	179
	REWIND 8	180
	IF (MD.EQ.2) GO TO 110	181
	IF(MDIAG.LT.2) GO TO 268	182
110	WRITE (6,102)	183
	DO 267 I=1,M	184

267 WRITE (6,100) (PHI(I,J),J=1,N)	185
268 RETURN	186
100 FORMAT(1X,1P10E11.4)	187
101 FORMAT(5NOC1C1-15)	188
102 FORMAT(1H0.30X10HFINAL PHI /1H0)	189
103 FORMAT (1X,1P7E11.4)	190
END	191

	SUBROUTINE MATINV(A,N,B,M,DETER)	4
C	MATRIX INVERSION WITH ACCOMPANYING SOLUTION OF LINEAR EQUATIONS	5
	DIMENSION IPIVO(17),A(17,17),B(17,1),INDEX(17,2),PIVOT(17)	6
	EQUIVALENCE (IROW,JROW), (ICOLU ,JCOLU), (AMAX, T, SWAP)	7
C	INITIALIZATION	8
C		9
	10 DETER =1.0	10
	15 DO 20 J=1,N	11
	20 IPIVO (J)=0	12
	30 DO 550 I=1,N	13
C		14
C	SEARCH FOR PIVOT ELEMENT	15
C		16
	40 AMAX=0.0	17
	45 DO 105 J=1,N	18
	50 IF (IPIVO (J)-1) 60, 105, 60	19
	60 DO 100 K=1,N	20
	70 IF (IPIVO (K)-1) 80, 100, 740	21
	80 IF (ABS (AMAX)-ABS (A(J,K))) 85, 100, 100	22
	85 IROW=J	23
	90 ICOLU =K	24
	95 AMAX=A(J,K)	25
	100 CONTINUE	26
	105 CONTINUE	27
	110 IPIVO (ICOLU)=IPIVO (ICOLU)+1	28
C		29
C	INTERCHANGE ROWS TO PUT PIVOT ELEMENT ON DIAGONAL	30
C		31
	130 IF (IROW-ICOLU) 140, 260, 140	32
	140 DETER =-DETER	33
	150 DO 200 L=1,N	34
	160 SWAP=A(IROW,L)	35
	170 A(IROW,L)=A(ICOLU ,L)	36
	200 A(ICOLU ,L)=SWAP	37
	205 IF(M) 260, 260, 210	38
	210 DO 250 L=1, M	39
	220 SWAP=B(IROW,L)	40
	230 B(IROW,L)=B(ICOLU ,L)	41
	250 B(ICOLU ,L)=SWAP	42
	260 INDEX(I,1)=IROW	43
	270 INDEX(I,2)=ICOLU	44
	310 PIVOT(I)=A(ICOLU ,ICOLU)	45
	320 DETER =DETER *PIVOT(I)	46
C		47
C	DIVIDE PIVOT ROW BY PIVOT ELEMENT	48
C		49
	330 A(ICOLU ,ICOLU)=1.0	50
	340 DO 350 L=1,N	51
	350 A(ICOLU ,L)=A(ICOLU ,L)/PIVOT(I)	52
	355 IF(M) 380, 380, 360	53
	360 DO 370 L=1,M	54
	370 B(ICOLU ,L)=B(ICOLU ,L)/PIVOT(I)	55
C		56
C	REDUCE NON-PIVOT ROWS	57
C		58
	380 DO 550 LI=1,N	59
	390 IF(LI-ICOLU) 400, 550, 400	60
	400 T=A(LI,ICOLU)	61
	420 A(LI,ICOLU)=0.0	62
	430 DO 450 L=1,N	63
	450 A(LI,L)=A(LI,L)-A(ICOLU ,L)*T	64

455 IF(M) 550, 550, 460	63
460 DO 500 L=L,M	64
500 B(L,L)=B(L,L)-B(JCOLU ,L)*T	65
550 CONTINUE	66
C	67
C INTERCHANGE COLUMNS	68
C	69
600 DO 710 I=1,N	70
610 L=N+1-I	71
620 IF (INDEX(L,1)-INDEX(L,2)) 630, 710, 630	72
630 JROW=INDEX(L,1)	73
640 JCOLU =INDEX(L,2)	74
650 DO 705 K=1,N	75
660 SWAP=A(K,JROW)	76
670 A(K,JROW)=A(K,JCOLU)	77
700 A(K,JCOLU)=SWAP	78
705 CONTINUE	79
710 CONTINUE	80
740 RETURN	81
END	82

```

FUNCTION TCC(RE)
IF(RE.GT.100.0) GO TO 10
TCC=8./RE
GO TO 100
10 IF(RE.GT.400.0) GO TO 20
TCC=4.175/(RE)**.86
GO TO 100
20 IF(RE.GT.1000.0) GO TO 30
TCC=.547/(RE)**.521
GO TO 100
30 IF(RE.GT.4000.0) GO TO 40
TCC=.342/(RE)**.453
GO TO 100
40 TCC=.064/(RE)**.25
100 RETURN
END

```

```

-----
4
4
6
7
8
9
10
11
12
13
14
15
16
17

```

FUNCTION SUM(P,M,DX)	2
DIMENSION P(17)	3
K=2	4
KK=M-1	5
KKK=2	6
SUM=0.0	7
10 DO 20 I=K,KK,KKK	8
20 SUM=SUM+P(I)	9
GO TO (30,40,50),K	10
30 SUM=SUM*DX/3.0	11
RETURN	12
40 K=3	13
45 SUM=SUM*2.0	14
GO TO 10	15
50 K=1	16
KK=M	17
KKK=M-1	18
GO TO 45	19
END	20

FUNCTION GZCF(REYN)	
RE=REYN	
IF(RE.LE.70.0)GO TO 20	
IF((RE.GT.70.0).AND.(RE.LE.4000.0))GO TO 30	
10 IF((RE.GT.4000.0).AND.(RE.LE.7.0E+03)) GO TO 40	
IF((RE.GT.7000.0).AND.(RE.LE.2.0E+04)) GO TO 50	
GZCF=25.6/(RE)**.756	
RETURN	
20 GZCF=1.0/12.0	10
RETURN	11
30 GZCF=1.858 E-09*(RE)**2-1.878E-05*RE+.0846	12
RETURN	13
40 GZCF=9.62/(RE)**.652	14
RETURN	15
50 GZCF=11.3/(RE)**.674	16
RETURN	17
END	18

FUNCTION GTCF(REYN)	2
RE=REYN	3
IF (RE.LE.70.0) GO TO 20	4
IF ((RE.GT.70.0).AND.(RE.LE.2000.0)) GO TO 30	5
10 IF ((RE.GT.2000.0).AND.(RE.LE.5.5E+03)) GO TO 40	6
IF ((RE.GT.5500.0).AND.(RE.LE.2.0E+04)) GO TO 50	7
GTCF=20.5/(RE)**0.784	8
RETURN	9
20 GTCF=1.0/12.0	10
RETURN	11
30 GTCF=.619E-08*(RE)**2-3.465E-05*RE+.08569	12
RETURN	13
40 GTCF=4.90/(RE)**.628	14
RETURN	15
50 GTCF=10.35/(RE)**.716	16
RETURN	17
END	18

```

INPUT
NAMELIST INPUT
RPN 0.10000000E 02 ALBUN 0.00000000E 00 COP 0.00000000E 00
PP1X (1)
1 0. 3 12 0. 7
II NONE Y
SIGN -0.10000000E 01
N 12
EDDY 0. PADDY 0.90000000E 00 SANDDY 0. EPS 0.30000000E 01
BAH 0.
VBT Y
DATA (1)
1 0.14000000E 03 0.31000000E 02 0.31000000E 02
DEP (1)
1 0. 0.24000000E 01 0.
ALPHA (1)
1 0. 0.55000000E 00 0.55000000E 00
PPOUT Y
VORR 0.
END NAMELIST INPUT

```

FJNAL PRESSURE DISTRIBUTION.

0.	0.	0.	0.	0.	0.	0.	0.	0.	0.
0.6789010	0.6927785	0.7180269	0.7485089	0.7761385	0.7924057	0.7923074	0.7760784	0.7489701	0.7188989
0.6937008	-0.6792456								
1.3543577	1.3634561	1.4337994	1.4953438	1.5513639	1.5891544	1.5862498	1.5546936	1.5008398	1.4390732
1.3883323	1.3872372								
1.0180076	1.0221377	1.0647648	1.1083063	1.1513494	1.1814016	1.1892059	1.1724800	1.1367066	1.0926132
1.0521661	1.0292619								
0.6799845	0.6894406	0.7037073	0.7306586	0.7594643	0.7819976	0.7914106	0.7848128	0.7644212	0.7364897
0.7088211	0.6884140								
0.3410142	0.3418344	0.3492073	0.3615078	0.3757176	0.3879441	0.3945387	0.3934595	0.3851026	0.3726764
0.3581250	0.3468832								
0.	0.	0.	0.	0.	0.	0.	0.	0.	0.
0.	0.								
WER NO.	EPS	TORQUE J.	TORQUE S.	RADIAL LOAD	TANG. LOAD	FLOW	COP.	MOMENT	SIQ. MOMENT
10.00	0.050	0.177719E 03	0.177713E 03	0.177580E 00	0.208569E-01	-0.230333E 01	0.181375E 00	0.370138E-02	

BLANK PAGE

APPENDIX IV

COMPUTER PROGRAM PN 406

STATIC PERFORMANCE OF A SPIRAL-GROOVED, FLOATING-RING JOURNAL BEARING OPERATED IN THE TURBULENT REGIME

Input

All input data appear in the form of name list except when the characteristics of inner and outer film are known and need not be computed within the program. In that case, two sets of data, each containing 9 cards in a specified form as explained in detail below, are required to provide the information on the film characteristics.

For the readers who would like to be familiar with the format of namelist, it is recommended that he read pages 14 and 19 of Ref. (10).

The choice of whether to provide or to compute the film characteristics is indicated by the first word of the namelist "NGPUT". The preparation of input for each case is shown below:

Case I: The film data generated within the program -

the namelist contains two listings; these are "NGPUT" and "INPUT".

A. "NGPUT" includes the following input:

1. INPRD, INPRD \neq 1: The film characteristics will be generated within the program and the information in the namelist "INPUT" must be provided.
2. NEPS = Number of (inner film) eccentricities ratios to be examined (maximum 10).
3. NCASE, NCASE = 0: Last set of input.
NCASE \neq 0: More input follows, starting from the namelisting "NGPUT".
4. NN = Number of iterations to be allowed to achieve an equilibrium condition in the floating-ring system (recommend 10).
5. R2R1 = Radius ratio of ring and journal.
= R_2/R_1 , R_1 = radius of journal, in.; R_2 = radius of ring, in.
6. ANTT = Initial guess, on the speed ratio; ω_2/ω_1 ,
 ω_2 = speed of ring, rad/sec.; ω_1 = speed of journal, rad/sec.

7. DN = Incremental value of the ring speed ratio during the iteration (recommend .15).
8. REY = Overall Reynolds number under which the bearing is to be operated.

$$= \frac{\omega_1 R_1 C_1}{\nu}$$
 C_1 = inner film thickness, in.,
 ν = kinematic viscosity in²/sec.
9. EPIS = Eccentricity ratios of inner film to be examined. There are NEPS number of eccentricity ratios to be provided (maximum 10).
10. COR1 = Inner film clearance ratio

$$= C_1/R_1$$
11. COR2 = Outer film clearance ratio

$$= C_2/R_2$$
12. PRES = Overall dimensionless gauge pressure measures at the end and the middle of the bearing.

$$= 2 \times P \text{ (pressure, psig)} / \mu \omega_1 \left(\frac{R_1}{C_1} \right)^2$$
where μ is the dynamic viscosity, $\frac{\text{lb-sec}}{\text{in}^2}$

The pressure at the end appears first.

B. "INPUT" includes the following input:

1. RINSP = The starting value of ring-speed ratio under which the film data will be generated. It is noted that $0 \leq \text{RINSP} \leq 1$. Since the film data of each film covers three different speeds, a small number for RINSP, say .25, is recommended.
2. DELSP = The incremental ring-speed ratio, DELSP, should be sufficiently small such that $\text{RINSP} + 2 \times \text{DELSP} \leq 1$. The recommended value for DELSP is 0.15.
3. BLOVD = Length diameter ratio, $L/2R_1$, where L is the length of journal.
4. I1 = Number of axial grid points in the first region of the bearing counted from the initial end of journal (see Fig. 2). An odd number is required and also it must be at least 2 less than I2. The minimum permissible value for I1 is 3.

- B. 5. I2 = Number of axial grid points counted from the initial end of the journal to the middle of the journal. The minimum permissible value for I2 is 5 and the maximum is 17. Again, I2 must be an odd number. The number of grid points in the second region is I2-I1+1 which gives (I2-I1) intervals.
6. N9 = Number of grid points in the circumferential direction, maximum permissible value for N9 is 19.
7. EPS1 = An array of three values of ϵ_1 for which inner bearing film data are to be generated. The range of EPS1 should be wide enough to cover anticipated operating eccentricities.
8. BETA = Groove angle in degrees. BETA must be specified for the first region of the bearing (first value) and the second region of the bearing (second value). For a pump-in design, with grooving in the first region, and a smooth seal in the second region, BETA should be read in as an obtuse angle, the same value for BETA being read in for the second region as for the first region. For a pump out design, with grooving in the second region of the bearing and a seal in the first region, BETA should be read in as acute angle with the same value of BETA being read in for the first region as for the second region. Never set BETA = 0.
9. DEP = Groove recess ratios in the two regions of journal with the first value referring to the first region, etc.
 = δ/c , where δ = groove recess, in.
 and c = nominal, radial clearance, in.
 To impose the condition of a smooth bearing (no grooving) in either region, set DEP = 0 for that region.
10. ALPHA = Fractional groove width in the two regions of a journal with the first value referring to the first region = $a_g / (a_g + a_r)$, where a_g and a_r are the widths in inches in the groove and ridge portion respectively. To impose the condition of a smooth bearing in either region, set ALPHA = 0 for that region.
11. EPS2 = An array of three values of ϵ_2 for which outer bearing film data are to be generated. The range of EPS2 should be wide enough to cover anticipated operating eccentricity.

Case II: In the case of known film characteristics, only the namelisting "NGPUT" is required. In addition to that, 18 cards must be followed which contain the film data.

The content of namelisting "NGPUT" is essentially the same as those of Case I. provided INPRD must be equal to 1.

The inner film data appear first corresponding to three eccentricity ratios at three different inner film Reynolds numbers.

The data include (these symbols are defined below)

$$Re, e, \bar{T}_j, \bar{T}_B, S, \phi$$

which are punched on one card with the format of (1X, F8.1, F5.2, 4E13.6). The first three cards are for the same Reynolds number, the smallest of the three values. Each card refers to a different eccentricity ratio. Again, the order of the eccentricity ratio is ascending. The next three cards correspond to a higher Reynolds number but with the same set of eccentricity ratios. In total, there are 9 cards for the inner film.

Following the inner film data, there are 9 cards for outer film data arranged in an order similar to that for the inner film.

The six quantities used as input for the inner and outer film are defined below.

1. Re = Reynolds number

$$= \frac{(\omega_1 - \omega_2) R_1 C_1}{\nu} \quad (\text{for inner film})$$

$$= \frac{\omega_2 R_2 C_2}{\nu} \quad (\text{for outer film})$$

2. e = Eccentricity (see Fig. 3)

$$= e_1 / c_1 \quad (\text{for inner film})$$

$$= e_2 / c_2 \quad (\text{for outer film})$$

3. \bar{T}_j = Dimensionless Torque of Journal

$$= \frac{T_j}{WC_1} \quad (\text{for inner film}), \text{ where } W = \text{load, pounds}$$

$$= \frac{T_j}{WC_2} \quad (\text{for outer film})$$

Case II:

4. \bar{T}_B = Dimensionless Torque of Bearing

$$= \frac{T_B}{WC_1} \quad (\text{for inner film})$$

$$= \frac{T_B}{WC_2} \quad (\text{for outer film})$$

5. S = Sommerfeld Number

$$= \frac{LD_1 \mu (N_1 + N_2) \left(\frac{R_1}{C_1}\right)^2}{W} \quad (\text{for inner film})$$

$$= \frac{LD_2 \mu N_2 \left(\frac{R_2}{C_2}\right)^2}{W} \quad (\text{for outer film})$$

where N_1 and N_2 are speed of journal and ring in rev./sec., respectively.

6. ϕ = Attitude angle, degree (see Fig. 3)

$$= \phi_1 \quad (\text{for inner film})$$

$$= \phi_2 \quad (\text{for outer film})$$

Output

The output appears under the title of "Floating-Ring with herringbone journal".

1. Main program input: it prints out the title of "Main program input". Immediately, there follows the title of "Namelist NGPUT" and the entire contents in that namelist. At the end, it prints out "end namelist NGPUT".
2. Input for subroutine "HERNB": it prints out the title of "Herringbone Bearing Input" and a title of "Namelist INPUT". Then, the entire contents of that namelist are printed out. At the end, it prints out "end namelist INPUT".
3. Single film data
 - A. For Inner Film:

There are three eccentricity ratios at three different Reynolds numbers corresponding to three different speed ratios. The output starts with a title of "inner film data" and then the headings REYNOLDS NO., ECCENTRICITY, INNER TORQUE, OUTER TORQUE, SOMMERFELD

NO., ATT. ANGLE, FLOW, on one line. Immediately, there follows 9 lines of data. Each line contains seven quantities under the appropriate heading. The first six of these seven quantities are defined above in the input list for NGPUT, Case II. The flow is defined as

\bar{Q} -- dimensionless flow

$$= \frac{Q}{R_1^2 C_1 (N_1 + N_2)} \quad (\text{for inner film})$$

$$= \frac{Q}{R_2^2 C_2 N_2} \quad (\text{for outer film})$$

Q = Flow, cu. in./sec.

B. For Outer Film:

After the output of the inner film, there are a set of output referring to the outer film just like those for the inner film. The output comprises the title of "Outer Film Data", the heading and 9 lines of data.

4. Final performance characteristics of the floating ring bearing at the steady state equilibrium condition. Under the title of output, there are four values in a line. These are:

ECCENTR/C₁ = e/C₁ = the overall eccentricity of the journal at equilibrium position divided by the nominal clearance of the inner film (see Fig. 4).

N₂/N₁, C₂/C₁ and R₂/R₁ as previously explained.

Next, there is a table of output referring to the inner film, the outer film, and the overall bearing. There are seven values in a line and a total of 3 lines. Each line contains

$$\text{REYNOLDS NO.} = \frac{(\omega_1 - \omega_2) R_1 C_1}{\nu} \quad (\text{for inner film})$$

$$= \frac{\omega_2 R_2 C_2}{\nu} \quad (\text{for outer film})$$

$$= \frac{\omega_1 R_1 C_1}{\nu} \quad (\text{for overall})$$

$$\text{ECCENTRICITY} = e_1 / C_1 \quad (\text{for inner film}) = e_1$$

(see Figs. 3 and 4)

$$e_2 = e_2 / C_2 \quad (\text{for outer film})$$

$$e = e / C_1 + C_2 \quad (\text{for overall})$$

TORQUE = Dimensionless form defined as

$$= \left[\frac{T_A}{WC_1} \right] - \frac{1}{2} S_1 \epsilon_1 \bar{F}_{t1} \quad (\text{for inner film})$$

$$= \left[\frac{T_B}{WC_2} \right] + \frac{1}{2} S_2 \epsilon_2 \bar{F}_{t2} \quad (\text{for outer film})$$

$$= \left[\frac{T_A}{WC_1} \right] \quad (\text{for overall})$$

where \bar{F}_{t1} and \bar{F}_{t2} are defined on page 139.

SUPPLY PRES = Dimensionless supply pressure

$$= \frac{P}{\mu \left(\frac{R_1}{C_1} \right) (N_1 + N_2)} \quad (\text{for inner film})$$

$$= \frac{P}{\mu N_2 \left(\frac{R_2}{C_2}\right)^2} \quad (\text{for outer film})$$

$$= \frac{P}{\mu N_1 \left(\frac{R_1}{C_1}\right)^2} \quad (\text{for overall})$$

SOMMFD NO. = Sommerfeld Number

$$S_1 = \frac{LD_1 \mu (N_1 + N_2) \left(\frac{R_1}{C_1}\right)^2}{W} \quad (\text{for inner film})$$

$$S_2 = \frac{LD_2 \mu N_2 \left(\frac{R_2}{C_2}\right)^2}{W} \quad (\text{for outer film})$$

$$S = \frac{LD_1 \mu N_1 \left(\frac{R_1}{C_1}\right)^2}{W} \quad (\text{for overall})$$

ATT. ANGLE = Attitude angle in deg. (see Fig. 3)

= ϕ_1 (for inner film)

= ϕ_2 (for outer film)

= ϕ (for overall)

TANG. FORCE = Dimensionless form of tangential force

$$\bar{F}_{t1} = \frac{F_{t1}}{WS_1} \quad (\text{for inner film})$$

$$\bar{F}_{t2} = \frac{F_{t2}}{WS_2} \quad (\text{for outer film})$$

where F_{t1} = Tangential force of the inner film, pound

F_{t2} = Tangential force of the outer film, pound

A Fortran listing of program PN 406 is provided in the next few pages. Typical listings of input and output are also given.

03/04/69

MAIN - SYN SOURCE STATEMENT - IFN(5) -

C	FLOATING-RING IN CONJUNCTION WITH HERRINGBONE JOURNAL IN TURBULENT		
C	REGIME		
	DIMENSION P(6,3,3),Q(6,3,3),A(4,3,3),B(4,3,3),AP(4,3,3),BP(4,3,3)	53	
	DIMENSION REY(1),C2C1(1),EPIS(10),BA(6),BC(6),AA(4,3),BB(4,3)	54	
	DIMENSION AP1(4,3),BP1(4,3),A1(4,3),B1(4,3),SA(4),SB(4)	55	
	DIMENSION EPS1(3),BETA(3),DEP(3),ALPHA(3),PRES(3),EPS2(3)	56	
500	FORMAT(1X,F8.1,F5.2,4E12.6)	57	
525	FORMAT(6(1PE12.5))	58	
C	INPRO=1,CATA FOR HERRINGBONE BEARING READ IN	62	
	NAMLIST/NGPUT/INPRC,NEPS,NCASE,MN,R2R1, ANTT,DN,REY,	63	
	1EPIS,COR1,COR2,PRES/INPUT/RINSP,DELSP,BLOVD,I1,I2,N9,		
	1EPS1,BETA,DEP,ALPHA,EPS2	65	
52	NRE=1	66	
	GAM=0.0	67	
	EDOT=0.0	68	
	MUST=0		
	PHDOT=0.0	69	
	KDIAG=0	70	
	NSES1=0	71	
	NSES2=0	72	
	READ(5,NGPUT)	80	6
	IF(MUST.EQ.1) GO TO 53	73	
	KDIAG=1	74	
	NSES1=1	75	
	NSES2=1	76	
53	NCC=1	77	
	WRITE(6,505)	78	14
505	FORMAT(41H) FLOATING-RING WITH HERRINGBONE JOURNAL)		
	C2C1(1)=COR2/CCR1*R2R1	81	
	WRITE(6,210)	82	15
	FCS=PRES(2)	85	
210	FORMAT(20H MAIN PROGRAM INPUT)	84	
	WRITE(6,NGPUT)	85	16
	IF(INPRC.EQ.1) GO TO 202	86	
	READ(5,INPUT)	87	20
	WRITE(6,212)	88	21
212	FORMAT(27H HERRINGBONE BEARING INPUT)	89	
	WRITE(6,INPUT)	90	22
	MPAS=1	91	
	REQ=REY(1)	92	
	CALL HERRNB(BLCVD,COR1,COR2,PRES,I1,I2,N9,EDOT,PHDOT,EPS1,GAM,BETA,	93	
	1DEP,ALPHA,RINSP,REQ,R2R1,DELSP,MPAS,KDIAG)	94	25
	REWIND 9	95	26
	DO 1213 K=1,3	96	
	DO 1213 J=1,3	97	
	READ(9) (P(1,J,K),P(2,J,K),P(3,J,K),P(4,J,K),P(5,J,K),P(6,J,K))	98	31
ERRCR	MESSAGE NUMBER 1		
1213	CONTINUE	99	
	REWIND 9		41
	GO TO 304	100	
202	READ(5,500) ((P(1,J,K),P(2,J,K),P(3,J,K),P(4,J,K),P(5,J,K),P(6,J,K)	101	
	I1,J=1,3),K=1,3)	102	43
304	IF(MUST.EQ.1)WRITE(6,500)((P(1,J,K),P(2,J,K),P(3,J,K),P(4,J,K),P(5	103	
	1,J,K),P(6,J,K),J=1,3),K=1,3)	104	59

1	((C(1,J,K),Q(2,J,K),Q(3,J,K),Q(4,J,K),Q(5,J,K),C(6,J,K)	158	
	1,J=1,3),K=1,3)	159	165
209	IK=2	160	
	GO TC 2	161	
9	DO 201 IA=1,NRE	162	
	RE=REY(IA)	163	
	DO 201 IB=1,NCC	164	
	CC=C2C1(IB)	165	
	DO 201 IC=1,NEPS	166	
	EP=PIS(IC)	167	
	ANRT=ANTT	168	
	ND=J	169	
	NA=J	170	
50	RE1=RE*(1.-ANRT)	171	
	RE2=R2R1*CC*RE1/(1.0/ANRT-1.C)	172	
	C1=P(1,1,3)	173	
	IF(RE1-C1) 11,10,17	174	
10	KC=J	175	
	GO TC 14	176	
11	DO 13 K=2,3	177	
	C1=P(1,1,K)	178	
	IF(RE1-C1) 12,13,13	179	
12	KC=K	180	
	GO TC 14	181	
13	CONTINUE	182	
14	DO 18 I=1,4	183	
	DO 18 J=1,3	184	
	AR=AP(I,J,KC)	185	
	BR=BP(I,J,KC)	186	
	CR=P(I+2,J,KC)	187	
	XR=P(1,J,KC)	188	
	KL=KC-1	189	
	AL=AP(I,J,KL)	190	
	BL=BP(I,J,KL)	191	
	CL=P(I+2,J,KL)	192	
	XL=P(1,J,KL)	193	
	C1=RE1-XR	194	
	C1=CR+C1*(BR+C1*AR)	195	
	C2=RE1-XL	196	
	C2=CL+C2*(BL+C2*AL)	197	
	IF(KC=2)15,15,16	198	
15	C2=C1	199	
	GO TC 18	200	
16	IF(3-KC) 17,17,18	201	
17	C1=C2	202	
18	AA(I,J) = (C1+C2)/2.	203	
	IF(NSES2.NE.1) GO TO 88	204	
87	WRITE(6,525)((AA(I,J),J=1,3),I=1,4)	205	235
88	DO 19 I=1,4	206	
	AP1(I,1)=0.0	207	
	AP1(I,3)=0.0	208	
	BP1(I,3)=0.0	209	
	BP1(I,1)=0.0	210	
	X2=P(2,1,1)	211	
	X3=P(2,2,1)	212	
	IF(I=4)101,102,101	213	

03/04/69

MAIN	SFN	SOURCE STATEMENT	IFR(S)
101		Y2=AA(1,1)*X2	214
		Y3=AA(1,2)*X3	215
		GO TC 133	216
102		Y2=AA(1,1)	217
		Y3=AA(1,2)	218
103		DO 19 J=2,2	219
		Y1=Y2	220
		Y2=Y3	221
		X1=X2	222
		X2=X3	223
		X3=P(2,J+1,1)	224
		IF(I=4) 104,105,104	225
104		Y3=AA(1,J+1)*X3	226
		GO TC 106	227
105		Y3=AA(1,J+1)	228
106		DT1=X2-X1	229
		DT2=X3-X2	230
		C1=Y2-Y1	231
		C2=Y3-Y2	232
		C3=X3-X1	233
		C4=DT1/DT2	234
		C24=C2*C4	235
		AP1(I,J)=(C24-C1)/(DT1*C3)	236
		BP1(I,J)=(C24+C4/C4)/C3	237
19		CONTINUE	238
		C1=P(2,3,1)	239
		IF(EP-C1) 21,20,20	240
20		KA=3	241
		GO TC 24	242
21		DO 23 J=2,3	243
		C1=P(2,J,1)	244
		IF(EP-C1) 2,23,23	245
22		KA=J	246
		GO TC 24	247
23		CONTINUE	248
24		DO 109 I=1,4	249
		AR=AP1(I,KA)	250
		BR=BP1(I,KA)	251
		XR=P(2,KA,1)	252
		CR=AA(I,KA)	253
		IF(I=4) 131,132,132	254
131		CR=CR*XR	255
132		KB=KA-1	256
		AL=AP1(I,KB)	257
		BL=BP1(I,KB)	258
		XL=P(2,KB,1)	259
		CL=AA(I,KB)	260
		IF(I=4) 133,134,134	261
133		CL=CL*XL	262
134		C1=EP*XR	263
		C1=CR+C1*(BR+C1*AR)	264
		C2=EP*XL	265
		C2=CL+C2*(BL+C2*AL)	266
		IF(KA=2) 25,25,26	267
25		C2=C1	268
		GO TC 28	269

26	IF(3-KA) 27,27,28	270
27	C1=C2	271
28	IF(I=4) 107,108,107	272
107	SA(I)=(C1+C2)/(2.*EP)	273
	GO TC 109	274
108	SA(I)=(C1+C2)/2.	275
109	CONTINUE	276
	RF=SA(I)	277
	S1=SA(3)	278
	RCFN=(SA(1)+SA(2))/2.	279
	ATT1=SA(4)	280
	FT=(SA(1)-SA(2))/(EP+S1)	281
	C1=R2R1+3	282
	C2=CC*CC	283
	S2=S1*C1/(C2*(1.+1./ANRT1))	284
	C1=Q(1,1,3)	285
	IF(R22-C1) 31,30,33	286
30	JC=3	287
	GO TC 34	288
31	DO 33 K=2,3	289
	C1=Q(1,1,K)	290
	IF(R22-C1) 32,33,33	291
32	JC=K	292
	GO TC 34	293
33	CONTINUE	294
34	DO 38 I=1,4	295
	DO 38 J=1,3	296
	AR=A(I,J,JC)	297
	BR=B(I,J,JC)	298
	CR=Q(I+2,J,JC)	299
	XR=Q(1,J,JC)	300
	JL=JC-	301
	AL=A(I,J,JL)	302
	BL=B(I,J,JL)	303
	XL=Q(1,J,JL)	304
	CL=Q(I+2,J,JL)	305
	C1=R22*XR	306
	C1=CR+C1*(BR+CL*AR)	307
	C2=R22*XL	308
	C2=CL+C2*(BL+C2*AL)	309
	IF(JC=2) 35,35,36	310
35	C2=C1	311
	GO TC 38	312
36	IF(3-JC) 37,37,38	313
37	C1=C2	314
38	BB(I,J)=(C1+C2)/2.	315
	IF(NSES2.NE.1) GO TO 90	316
89	WRITE(6,525)((BB(I,J),J=1,3),I=1,4)	317
90	DO 59 J=1,3	318
	NB=4-J	319
	C3=Q(2,J,1)	320
	C1=C3*C3	321
	BC(NB)=C1/C1	322
	BA(NB)=BB(3,J)	323
59	CONTINUE	324
	A1(3,1)=C.J	325

358

A1(3,3)=C.0	326
B1(3,1)=C.0	327
B1(3,3)=0.0	328
X2=BA(1)	329
X3=BA(2)	330
Y2=BC(1)	331
Y3=BC(2)	332
DO 39 J=2,3	333
Y1=Y2	334
Y2=Y3	335
X1=X2	336
X2=X3	337
X3=BA(J+1)	338
Y3=BC(J+1)	339
DT1=X2-X1	340
DT2=X3-X2	341
C1=Y2-Y1	342
C2=Y3-Y2	343
C3=X3-X1	344
C4=DT1/DT2	345
C24=C2+C4	346
A1(3,J)=(C24-C1)/(DT1+C3)	347
B1(3,J)=(C24+C1/C4)/C3	348
39 CONTINUE	349
C1=BA(3)	350
IF(S2-C1) 41,40,40	351
40 NC=3	352
GO TC 44	353
41 DO 43 J=2,3	354
C1=BA(J)	355
IF(S2-C1) 42,43,43	356
42 NC=J	357
GO TC 44	358
43 CONTINUE	359
44 AR=A1(3,NC)	360
BR=B1(3,NC)	361
CR=BC(NC)	362
XR=BA(NC)	363
NL=NC-1	364
AL=A1(3,NL)	365
BL=B1(3,NL)	366
CL=BC(NL)	367
XL=BA(NL)	368
C1=S2-XR	369
C1=CR+C1*(BR+C1*AR)	370
C2=S2-XL	371
C2=CL+C2*(BL+C2*AL)	372
IF(NC=2) 45,45,46	373
45 C2=C1	374
GO TC 48	375
46 IF(3-NC) 47,47,48	376
47 C1=C2	377
48 C3=(C1+C2)/2.	378
C2=1./C3	379
EP2=.1*SQRT(C2)	380
DO 49 I=1,4	381

03/04/69

MAIN	- EFN	SOURCE STATEMENT	- IFR(SI)
		A1(I,1)=0.0	382
		A1(I,3)=0.0	383
		B1(I,1)=0.0	384
		B1(I,3)=0.0	385
		X2=Q(2,1,1)	386
		X3=Q(2,2,1)	387
		IF(I=4) 111,112,111	388
111		Y2=BB(I,1)*X2	389
		Y3=BB(I,2)*X3	390
		GO TC 113	391
112		Y2=BB(I,1)	392
		Y3=BB(I,2)	393
113		DO 49 J=2,2	394
		Y1=Y2	395
		Y2=Y3	396
		X1=X2	397
		X2=X3	398
		X3=Q(2,J+1,1)	399
		IF(I=4) 114,115,114	400
114		Y3=BB(I,J+1)*X3	401
		GO TC 116	402
115		Y3=BB(I,J+1)	403
116		DT1=X2-X1	404
		DT2=X3-X2	405
		C1=Y2-Y1	406
		C2=Y3-Y2	407
		C3=X3-X1	408
		C4=DT1/DT2	409
		C24=C2+C4	410
		A1(I,J)=(C24-C1)/(DT1+C3)	411
		B1(I,J)=(C24+C1/C4)/C3	412
49		CONTINUE	413
		C1=Q(2,3,1)	414
		IF(EP2-C1) 61,60,60	415
60		LC=3	416
		GO TC 64	417
61		DO 63 J=2,3	418
		C1=Q(2,J,1)	419
		IF(EP2-C1) 62,63,63	420
62		LC=J	421
		GO TC 64	422
63		CONTINUE	423
64		DO 120 I=1,4	424
		AR=A1(I,LC)	425
		BR=B1(I,LC)	426
		XR=Q(2,LC,1)	427
		CR=BB(I,LC)	428
		IF(I=4) 135,136,136	429
135		CR=CR*XR	430
136		LL=LC-1	431
		AL=A1(I,LL)	432
		BL=B1(I,LL)	433
		XL=Q(2,LL,1)	434
		CL=BR(I,LL)	435
		IF(I=4) 137,138,138	436
137		CL=CL*XL	437

MAIN		EFN	SOURCE STATEMENT	IFA(S)	03/04/69
138			C1=EP2-XR		438
			C1=CR+C1*(BR+C1*AR)		439
			C2=EP2-XL		440
			C2=CL+C2*(BL+C2*AL)		441
			IF(LC=2) 55,55,56		442
			C2=C1		443
			GO TO 58		444
56			PI=(PI-LC) 57,57,58		445
57			C1=C2		446
58			IF(I-4) 118,119,118		447
118			SB(I)=(C1+C2)/(2.*EP2)		448
			GO TO 120		449
119			SB(I)=(C1+ 2)/2.		450
120			CONTINUE		451
			ATT2=SB(4)		452
			PI=3.1415926536		453
			RAD=PI/180.		454
			C1=EP2*CC		455
			C2=180.-ATT1+ATT2		456
			IF(C2=90.) 150,150,151		457
151			C2= 180.-C2		458
			C2=C2*RAE		459
			CA=CCS(C2)		460
			GO TO 152		461
150			C2=C2*RAE		462
			CA=CCS(C2)		463
152			CSA=SIN(C2)		464
			EPP=SQR(EP*EP+C1*C1-2.*C1*EP*CA)		465
			CSB=C1*CSA/EPP		466
			CCB=SQR(1.-CSB*CSB)		467
			CTB=CSB/CCB		468
			TB=ATAN(CTB)		469
			TR=ATT1+RAD-TB		470
			TD=TR/RAC		471
			EPS=EPP/(1.+CC)		472
			RCF2=(SB(1)+SB(2))/2.		473
			FT2=(SB(1)-SB(2))/(S2*EP2)		474
			C1=(1.-ANRT)/(1.+ANRT)		475
			IF (INPRD.NE.1) C1=1.		476
			C2=RCFM*C1		477
			C1=S1*FT*EP/2.		478
			RCFI=C2-C1		479
			C1=EP2+S2*FT2/2.		480
			RCFD=RCF2+C1		481
			RID=RCFI/RCFD		482
			ER=RID-CC		483
			IF(INSES1.NE.1) GO TO 86		484
85			WRITE(6,525)RE1,RE2,ANRT,CC,EP		485
			WRITE(6,525)RCFI,RCFD,ER,S1,S2		486
			WRITE(6,525)EP2,FT,FT2,RCFM,RCF2		487
			WRITE(6,525) SB(1),SB(2),SB(3),SB(4),ATT1,ATT2		488
86			IF(NA=1) 70,71,72		489
70			O1=ER		490
			C1=ANRT		491
			ANRT=O1*CN		492
			NA=1		493

GO TO 50		
71 IF(D1=ER) 73,74,74	494	
73 NA=2	495	
Q3=ANRT	496	
D3=ER	497	
ANRT=(Q1+Q3)/2.	498	
GO TO 30	499	
74 C1=ANRT	500	
D1=ER	501	
ANRT=Q1+EN	502	
ND=ND+1	503	
IF (ND=NN) 50,700,700	504	
700 WRITE (6,702) NN		521
702 FORMAT (15H DIVERGED AFTER .15.6H TIMES)		
GO TO 201		
72 IF(NA=3) 76,75,79		
76 IF(D1=ER) 78,77,77	506	
77 C1=ANRT	507	
D1=ER	508	
NA=3	509	
ANRT=(Q1+Q3)/2.	510	
GO TO 50	511	
78 Q3=ANRT	512	
D3=ER	513	
ANRT=(Q1+Q3)/2.	514	
NA=3	515	
GO TO 50	516	
79 Q2=ANRT	517	
D2=ER	518	
NA=4	519	
DTA=Q3-C1	520	
C1=DTA*DTA	521	
C2=(C1+C3-2.*C2)*2./C1	522	
C3=(D3-C1)/DTA	523	
IF(C2) 80,81,80	524	
81 C4=-Q2/C3	525	
GO TO 82	526	
80 DTA=.5*C3/C2	527	
C4=SQRT(CTA*DTA-Q2/C2)	528	
IF(DTA) 83,84,84	529	538
83 C4=-C4	530	
84 C4=C4-DTA	531	
82 ANRT=Q2+C4	532	
GO TO 50	533	
79 S3=S1/(1.+ANRT)	534	
IF(PDS) 91,92,91	535	
92 PD1=0.0	536	
PD2=0.0	537	
GO TO 93	538	
91 PD1=PDS/(1.+ANRT)	539	
PD2=PDS*(CCR2/COR1)**2/ANRT	540	
93 WRITE(6,501)	541	
WRITE(6,508)	542	549
WRITE(6,600)EPP,ANRT,CC,R2R1	543	550
WRITE(6,502)	544	551
WRITE(6,522)REL,EP,RCFM,PD1,S1,ATT1,FT	545	552
	546	553

WRITE(6,924)R2,RP2,RCF1,PD2,92,ATT2,PT2	927	929
WRITE(6,925)R2,RP2,RCF1,PD2,92,ATT2,PT2	928	930
902 FORMAT(12X03H REYNOLDS NO ECCENTRIC TORQUE SUPPLY PRES 80MM	929	
IFD NO ATT. ANGLE TANG. FORCE)	930	
901 FORMAT(7+ OUTPUT)		
908 FORMAT(47H ECCENTR/C1 N2/W1 C2/C1 N2/W1)	931	
909 FORMAT(4(1X811.4))	932	
922 FORMAT(12H INNER RING ,7(1X811.4))	933	
924 FORMAT(12H OUTER RING ,7(1X811.4))	934	
926 FORMAT(12H OVERALL ,8(1X811.4))	935	
901 CONTINUE	936	
IF(CASE) 92,91,92	937	
91 STOP	938	
END	939	

HERA - EFN SOURCE STATEMENT - IFN(S) -

	SUBROUTINE HERNB(BLOVD,COR1,COR2,PRES,I1,I2,N4,EDOT,PHDOT,EPS1,GAM	1	
	1.BETA,DEP,ALPHA,RINSP,REQ,RZR1,DELSP,MPAS,KDIAG)	2	
C	HERRINGEGNE JOURNAL ,CORRECT FOR TORQUE IN CAVITATED REGION,	3	
C	1-16-68	4	
C	WITH LARGE ECCENTRICITY AND MISALIGNMENT	5	
C	IN TURBULENCE REGIME	6	
	COMMON MCIAG,CCLX,DELZ,DELZS,M,MS,MG1,MG2,N,NP(17,19),A1(2,5,1	7	
	19),B1(2,19),CC(2,19),AF1(17,19),AF2(17,19),AF3(17,19),AF4(17,19),A	8	
	2F6(17,19),AF7(17,19),AF5(17,19),PHI(17,19)	9	
	DIMENSICA BETA(3),CEP(3),ALPHA(3),PFI(3), QQQ(19),M9(17	10	
	1,19),QQCC(19),PP(17),PPP(17),PPX(17),PPPX(17),AX1(17,19),AX2(17,19	11	
	2),AX3(17,19),AX6(17,19),AX7(17,19),AX8(17,19),AX5(17,19),WS11(17,1	12	
	39),WS12(17,19),WS13(17,19),WS14(17,19),XX(17),AXL(2,19),CZ(2,19)	13	
	DIMENSICA EPS1(3),PRES(3)	14	
	DIMENSICA KUPY(17,19)	15	
	LOGICAL FPOUT,VENT,TORO	16	
	2 FORMAT(7E14.7)	17	
	4 FORMAT(10IX,F11.7)	18	
	3 FORMAT (89H REYNOLDS NC. ECCENTRICITY INNER TORQUE OUTER TORQUE	19	
	1 SOMMERFELD NO ATT. ANGLE FLOW)	20	
	6 FORMAT(33H SIN AND COS FORCE COMPONENTS = E14.7,2H, E14.7)	21	
	7 FORMAT(31H SIN AND COS MOMENTS ABOUT Z=0 E14.7,2H, E14.7)	22	
	9 FORMAT(29H FINAL PRESSURE DISTRIBUTION. //)	23	
	IF (KDIAG.EQ.1) WRITE (6,2) BLOVD,COR1,COR2,PRES(1),PRES(2),PRES(3	24	
	1), EDOT,PHDOT,EPS1(1),EPS1(2),EPS1(3),EPS1(4),EPS1(5),EPS1(6)	25	
	1,GAM,BETA(1),BETA(2),BETA(3),DEP(1),DEP(2),DEP(3),ALPHA(1),ALPHA(2	26	
	1),ALPHA(3),RINSP,REQ,RZR1,DELSP	27	2
	INDR=KDIAG	28	
	MDIAG=0	29	
	N=N4	30	
	MPAS=MPAS	31	
	IF (MPAS.EQ.1) WRITE(6,5)		8
	5 FORMAT (1H1)		
	IF (MPAS.EQ.1) WRITE (6,1)	32	10
	IF (MPAS.EQ.2) WRITE (6,10)	33	12
	1 FORMAT (15X17H INNER FILM DATA)	34	
	10 FORMAT (15X17H OUTER FILM DATA)	35	
	WRITE (6,3)	36	13
	GAMDOT=0.0	37	
	MD=0	38	
	MG1=I1-1	39	
	AMG=MG1	40	
	MS=I2-I1	41	
	VENT=.TRUE.	42	
	IF(VENT) GO TC 102	43	
	M=I2+I1-1	44	
	BMM1=M-1	45	
	MG2=MG1	46	
	GO TC 101	47	
102	M=I2	48	
	BMM1= M-1	49	
	BMM1=BMM1#2.	50	
	MG2=0	51	
101	IF(MPAS.EQ.2) GO TO 35	52	
	DO 20 I=1,M	53	

03/04/69

HERA	- EFA	SOURCE STATEMENT	- IFA(S)	-
		DO 20 J=1,N		54
		NP(I,J)=0		55
	20	CONTINUE		56
		DO 30 J=1,N		57
		NP(1,J)=1		58
		NP(M,J)=1		59
	30	CONTINUE		60
	35	KK=1		61
	100	AN=N		62
		PI=3.14159265258979		63
		DTHETA=2.*PI/AN		64
		DTHE2=0.5/DTHETA		65
		PFIX(1)=PRES(1)		66
		SPRITO=RINSP		67
		PFIX(3)=PRES(3)		68
		IF (MPASS.EQ.1) GO TO 105		69
		GO TO 108		70
	105	SPRITO=2.*DELSP+RINSP		71
		DELSI=CELSP		72
		GO TO 107		73
	108	DELSI=CELSP		74
	107	DO 599 L8=1,3		75
		IF(MPASS.EQ.2) GO TO 120		76
		ANM1=SPRITO-1.0		77
		ANP1=SPRITO+1.0		78
		COR=COR1		79
		SIGN=ANM1/ANP1		80
		PFIX(2)=PRES(2)*ANP1		81
		ALVD=BLCVD		82
		REN=RED*ANM1*(-1.)		83
		GO TO 130		84
	120	SIGN=-1.		85
		COR=COR2		86
		PFIX(2)=PRES(2)*(COR2/COR1) **2/SPRITO		87
		ALVD=BLCVD/R2R1		89
		REN=RED*(R2R1)**2*COR2/COR1*SPRITO		90
	130	ELVD=ALCVD		91
		RATLD=2.0*ALVC		93
		DO 592 L7=1,3		94
		EPS=EPS1(L7)		95
		TPS=2.*PI*SIGA		96
		CON1=6.*TPS		97
		RADIAN=.017493292519943		98
		GAI=GAM*RADIAN		99
		EDT=0.0		100
		CON2=CON1/REN		101
		TORQ=.FALSE.		102
		TPS1=TPS/8.0		103
		TRQ=TPS1*REN		104
		DELX=DTHETA		105
		DELZ=RATLD/BNP1		106
		TPS1=(2.*PI)**2*2.*ELVD		107
		AMS=MS		108
		DELZS=DELZ		109
		ANG=0.0		110
		PHMC=PHCOT=(1.-SIGN)*0.5		111

03/04/69

NCR - EFL SOURCE STATEMENT - 15A(1) -

IND=1	112	
EPQ2=1.	113	
L1=1	114	
L2=11	115	
38 DO 40 J=1,N	116	
CC(L1,J)=0.0	117	
AXL(L1,J)=0.	118	
CZ(L1,J)=0.	119	
A1(L1,2,J)=0.0	120	
A1(L1,3,J)=0.0	121	
40 AF7(L2,J)=0.0	122	
IF(IAD.EC.2)GC TO 48	123	
IF(VENT) GO TC 48	124	
L1=2	125	
L2=12	126	
IND=2	127	
GO TC 38	128	
48 NR=1	129	
PN=MG1	130	
MM=11	131	
ISS=1	132	
DEL=CELZ	133	
DZ=C.5/DELZ	134	
ZS=1	135	
Z=0.0	136	
00 BET=BETA(NR)*RACIAN	137	
DEPH=DEP(NR)	138	
ALPH=ALPHA(NR)	139	
ALM1=1.-ALPH	140	
ALTA1=ALPH*ALM1	141	
SINB=SIN(BET)	142	99
COSB=COS(BET)	143	100
SINB2=SINB*SINB	144	
COSB2=CCSB*CCSB	145	
COT2=COSB2/SINB2	146	
DLZ=DEL*CTHETA	147	
IF(TCRQ) GO TC 1001	148	
DU 2J00 I=IS,PM	149	
XX(I)=Z	150	
ZCOR=Z/CCR	151	
EPZGH=EPS+GA1*ZCOR	152	
EDZR=EDCY+GANCCT*ZCOR	153	
EPZG=EPZGH*PHIMC	154	
DO 2001 J=1,N	155	
S1=SIN(ANG)	156	109
CO=CCS(ANG)	157	110
H=1.+CO*EPZGH	158	
H9(I,J)=+	159	
H3=H*H*+	160	
HG=H+DEP+	161	
HGHR=HG/+	162	
AX9(I,J)=(EDZR+CO+EPZG*S1)*SINB*PI*24.0	163	
HG3=HG**3	164	
HGHR3=HG3/H3	165	
S1=1./SINB2	166	
S2=-COSB/SINB2	167	

03/04/69

HERA - EFN SOURCE STATEMENT - IFN(S) -

RENH=REN*H	168	
RENG=REN*HG	169	
GXR=GTCF(RENH)*12.	170	113
GXG=GTCF(RENG)*12.	171	114
GZR=GZCF(RENH)*12.	172	115
GZG=GZCF(RENG)*12.	173	116
S5=(GXR+GZR*CCT2)	174	
S6=(GXG+GZG*CCT2)	175	
S7=GZG*S2	176	
S8=GZR*S2	177	
S9=GZG*S1	178	
S10=GZR*S1	179	
S11=-S5/S6/HGR3	180	
S12=1.-S11*ALPH-ALPH	181	
S13=(S7-S8/HGR3)/S6/S12	182	
S14=RENH/HGR3/S12*(1.-HGR1)/S6	183	
ALH3=ALPH*HG3	184	
A1S=SINB*(ALH3*S6*S11-ALM1*S5*H3)/S12	185	
A2=-ALM1*(ALPH*S5*S13+S8)*H3	186	
A2=(A2+ALH3*(ALM1*S6*S12-S7))*SINB	187	
A3=ALTAL1*S14*(S6*HG3-S5*H3)/REN	188	
A3=CCN1*(A3*H*ALM1+HG*ALPH)*SINB	189	
DMY=H3*ALM1	190	
S7H=HGHR3*S7	191	
B1S=-H3/S12*(S8*ALM1-S7*ALPH*S11)*SINB	192	
B2=ALH3*(S9-S7*S13*ALM1)+DMY*(S10+ALPH*S8*S13)	193	
B3=CCN1*ALTAL1*S14*(S8-S7H)	194	
B2=-B2*SINB	195	
AX1(I,J)=A1S+A2*COSB	196	
B3=-B3*H3*SINB/REN	197	
AX2(I,J)=A2*SINB	198	
WS11(I,J)=S11/S12	199	
WS12(I,J)=1./S12	200	
WS13(I,J)=S13	201	
WS14(I,J)=S14	202	
AX3(I,J)=A3	203	
AX6(I,J)=B1S+B2*COSB	204	
AX7(I,J)=B2*SINB	205	
AX8(I,J)=B3	206	
IF(MC,NE,2) GO TO 2001	207	
IF(I.EQ.15.ANC.J.EQ.1)	208	
1 WRITE(6,2) AX1(I,J),AX2(I,J),AX3(I,J),AX6(I,J),AX7(I,J),AX8(I,J),AX9(I,J)	209	
2001 ANG=ANG+CTHETA	210	130
ANG=U.J	211	
IF(I.EQ.MM) GC TO 2000	212	
Z=Z+DEL	213	
2000 CONTINUE	214	
IF(NR.EQ.1) GC TO 2010	215	
IF(NR.EQ.3) GC TO 2014	216	
IF(VENT) GO TO 2014	217	
GO TO 2020	218	
2010 IK=1	219	
GO TO 3800	220	
2014 IK=MM	221	
GO TO 3800	222	
	223	

03/04/69

C	COMPUTE THE DIFFERENCES IN XS AND COEFFICIENT	224	
3800	IRIK	225	
	DO 4010 J=1,N	226	
	AF1(I,J)=0.0	227	
	AF2(I,J)=0.0	228	
	AF3(I,J)=0.0	229	
	AF4(I,J)=0.0	230	
	AF5(I,J)=0.0	231	
	AF6(I,J)=1.0	232	
	AF7(I,J)=PFIX(NR)	233	
4010	CONTINUE	234	
2020	IST=IS+1	235	
	MM1=MM-1	236	
	DO 4000 I=IST,MM1	237	
	IO=I-1	238	
	IR=I+1	239	
	DO 4000 J=1,N	240	
	DTH=DTHE2	241	
	IF(J.EQ.1.OR.J.EQ.N) GO TO 4004	242	
	JO=J-1	243	
	J1=J+1	244	
	GO TO 4008	245	
4004	IF(J.EQ.1) GO TO 4006	246	
	JO=N-1	247	
	J1=1	248	
	GO TO 4008	249	
4006	JO=N	250	
	J1=2	251	
4008	AF1(I,J)=SINB*AX7(I,J)	252	
	AF2(I,J)=(AX2(I,J1)-AX2(I,JO)+COSB*(AX7(I,J1)-AX7(I,JO)))*DTH	253	
	+SINB*(AX7(I7,J)-AX7(I0,J))*DZ	254	
	AF3(I,J)=AX2(I,J)+COSB*AX7(I,J)+SINB*AX6(I,J)	255	
	AF4(I,J)=(AX1(I,J1)-AX1(I,JO)+COSB*(AX6(I,J1)-AX6(I,JO)))*DTH	256	
	+SINB*(AX6(I7,J)-AX6(I0,J))*DZ	257	
	AF5(I,J)=AX1(I,J)+COSB*AX6(I,J)	258	
	AF6(I,J)=0.0	259	
	AF7(I,J)=(AX3(I,J1)-AX3(I,JO)+COSB*(AX8(I,J1)-AX8(I,JO)))*DTH	260	
	+SINB*(AX8(I7,J1)-AX8(I0,J1))*DZ+AX9(I,J)	261	
	IF (NO.EQ.2 .AND. J. EQ. 1)	262	
	WRITE(6,2) AF1(I,J),AF2(I,J),AF3(I,J),AF4(I,J),AF5(I,J),AF7(I,J)	263	
	264	228	
4000	CONTINUE	265	
	IF(NR.EC.1) GC TO 4020	266	
	IF(NR.EC.2) GC TO 4040	267	
	II=2	268	
	IE=12	269	
	GO TO 4090	270	
4020	II=1	271	
	IE=MM	272	
	GO TO 4090	273	
4040	II=1	274	
	IE=IS	275	
4090	DO 4100 J=1,N	276	
	A1(II,1,J)=0.0	277	
	A1(II,5,J)=0.0	278	
	TRS=AX7(IE,J)	279	

TRSZ=TRZ+DZ+2.0	280	
A1(II,4,J)=TRSZ	281	
A1(II,2,J)=A1(II,2,J)-TRSZ*ERO2	282	
DDT=AX6(IE,J)*CTHE2	283	
CC(II,J)=CZ(II,J)-CCT	284	
CZ(II,J)=CCT	285	
B1(II,J)=CC(II,J)	286	
A1(II,3,J)=A1(II,3,J)+TRSZ	287	
AF7(IE,J)=AXL(II,J)-AXB(IE,J)	288	
AXL(II,J)=AXE(IE,J)	289	
AF1(IE,J)=0.0	290	
AF2(IE,J)=0.0	291	
AF3(IE,J)=0.0	292	
AF4(IE,J)=0.0	293	
AF5(IE,J)=0.0	294	
AF6(IE,J)=0.0	295	
IF(MC.EQ.2.AND.J.EQ.N)	296	
1 WRITE(6,2) A1(II,2,J),A1(II,4,J),A1(II,3,J),B1(II,J)	297	
1,CC(II,J),AF7(IE,J)	298	280
4100 CONTINUE	299	
IF(NR.EC.1) GO TO 4102	300	
GO TC 4150	301	
4102 IS=11	302	
NR=2	303	
MM=12	304	
ERO2=0.	305	
DEL=DELZS	306	
CZ=0.5/DELZS	307	
GO TC 200	308	
4180 IF(VENT) GO TC 4190	309	
IF(KK.EC.1) GO TO 4180	310	
IS=12	311	
MM=M	312	
NR=3	313	
ERO2=0.	314	
DEL=DELZ	315	
CZ=0.5/DELZ	316	
GO TC 200	317	
4180 IE=12	318	
ERO2=1.	319	
KK=2	320	
II=2	321	
GO TC 4090	322	
4150 IF(NR.EC.2) GO TO 4160	323	
4190 MTSR=MD	324	
MD =>TSR	325	
CALL CICI (MC)	326	319
MC=0	327	
PPOUT=.FALSE.	328	
IF (KDIAG.NE.1) GO TO 571	329	
IF(IND3.EQ.1.CR.INC3.EQ.2) PPOUT=.TRUE.	330	
IF(PPOUT) WRITE(6,9)	331	327
571 DO 575 I=1,M	332	
IF(PPOUT) WRITE(6,4)(PHI(I,J),J=1,N)	333	332
DO 575 J=1,N	334	
KUPT(I,J)=0	335	

HERN - EFN SOURCE STATEMENT - IFR(S) -

	IF(PHI(I,J).GE.0.0) GC TO 575	336
	PHI(I,J)=0.0	337
	KUPT(I,J)=1	338
575	CONTINUE	339
C	DIMENSIONLESS FLOW	340
	IP=I-1	341
4204	AFLOW=J.C	342
	DO 4200 J=1,N	343
	IF(J.EQ.1.OR.J.EQ.N) GO TO 4220	344
	YF1=(PHI(IP,J+1)-PHI(IP,J-1))*DTHE2	345
4210	AFLOW=(YF1+AX6(IP,J)+AX8(IP,J)+AX7(IP,J)*(PHI(IP+1,J)-PHI(IP-1,J)))*DZ+AFLOW	346
	IF(MCIAG.EQ.2) WRITE(6,2)YF1,AFLOW	348
	GO TO 4200	349
4220	IF(J.EQ.N) GC TO 4230	350
	YF1=(PHI(IP,2)-PHI(IP,N))*DTHE2	351
	GO TO 4210	352
4230	YF1=(PHI(IP,1)-PHI(IP,N-1))*CTHE2	353
	GO TO 4210	354
4200	CONTINUE	355
	AFLOW=AFLOW+DTHE2TA/12.	356
C	TORQUE CIVIDEC BY MUXNXXRXXR/C	357
	NR=1	358
	TORQ=.TRLE.	359
	TQ=.0	360
	IT1=1	361
	IT2=11	362
	TCI=C.0	363
	GO TO 200	364
1001	DO 1000 I=IT1,IT2	365
	DO 1000 J=1,N	366
	IF(KUPT(I,J).EQ.1) GC TO 1000	367
	IF(I.EQ.IT1.OR.I.EQ.IT2) GO TO 1800	368
	DPDZ=(PHI(I+1,J)-PHI(I-1,J))/DZ	369
	AFTR=1.0	370
1200	IF(J.EQ.1.OR.J.EQ.N) GO TO 1600	371
	DPDT=(PHI(I,J+1)-PHI(I,J-1))*DTHE2	372
1240	H=H9(I,J)	373
	BQ=H*ALTA1*CEPH	374
	AQ=(-BQ*COSB*WS13(I,J)+ALPH1*WS12(I,J)-ALPH*WS11(I,J)*(H+CEPH))*	375
	10PDT	376
	AQ=AC+BC*(-CCN2*WS14(I,J)-WS13(I,J)*DPDZ+SINB)	377
	TQ=TC+AC*DLZ*C.5*AFTR	378
	GO TO 1010	379
1600	IF(J.EQ.N) GC TO 1610	380
	DPDT=(PHI(I,2)-PHI(I,N))*DTHE2	381
	GO TO 1240	382
1610	DPDT=(PHI(I,1)-PHI(I,N-1))*CTHE2	383
	GO TO 1240	384
1800	AFTR=.5	385
	IF(I.EQ.IT2) GC TO 1810	386
	DPDZ=(PHI(IT1+1,J)-PHI(IT1,J))/DELZ	387
	GO TO 1200	388
1810	DPDZ=(PHI(IT2,J)-PHI(IT2-1,J))/DELZ	389
	GO TO 1200	390
1010	RE=REN*H	391

03/04/69

HERA - EFN SOURCE STATEMENT - IFN(S) -			
	TCC=TCC1FE1+ALP1	392	432
	RE=REN*(1+DEPH)	393	
	TC1=TC1*(TC2+TCC(RE)+ALPH)*TRQ*DLZ+AFTR	394	433
	IF (J,AE,1) GO TO 1000	395	
	IF(MC.EC,2,AND,I,EQ,IT1)	396	
	1 WRITE(6,2)AQ,TQ,RE,TC1,TC2	397	431
1000	CONTINUE	398	
	IF(MC.EC,2)WRITE(6,2)WS11(I,J),WS12(I,J),WS13(I,J),WS14(I,J)	399	442
	IF(NR.EC,1) GC TO 1400	400	
	IF(NR.EC,2) GC TO 1410	401	
	GO TC 578	402	
1400	NR=2	403	
	IT1=11	404	
	IT2=12	405	
	GO TC 200	406	
1410	IF(VENT) GO TC 578	407	
	NR=3	408	
	IT1=12	409	
	IT2=M	410	
	GO TC 200	411	
578	TQO=(TQ+TC1)	412	
	THE=0.0	413	
	DO 380 J=1,N	414	
	QQQ(J)=SIN(THE)	415	468
	COQQ(J)=COS(THE)	416	470
580	THE=CTHETA+THE	417	
	DO 590 I=1,M	418	
	PP(I)=0.0	419	
	PPP(I)=0.0	420	
	DO 600 J=1,N	421	
	CUM=PHI(I,J)	422	
	PP(I)=PP(I)+CCC(J)*CUM	423	
600	PPP(I)=PPP(I)+CGQQ(J)*CUM	424	
	PP(I)=PP(I)*CTHETA	425	
	PPP(I)=PPP(I)*CTHETA	426	
	PPX(I)=PP(I)*XX(I)	427	
590	PPPX(I)=PPP(I)*XX(I)	428	
	FSIN=SUM(PP,M,DELZ)	429	501
	FCOS=SUM(PPP,M,DELZ)	430	502
	FMSIN=SUM(PPX,M,DELZ)	431	503
	FMCOS=SUM(PPPX,M,DELZ)	432	504
	FCOS=-FCCS		
	FMCOS=-FMCOS		
	IF (KDIAG.NE.1) GO TC 594	433	
	WRITE(6,6)FSIN,FCOS	434	507
	WRITE(6,7)FMSIN,FMCOS	435	508
594	WLOAD=FCCS**2+FSIN**2	436	
	WLOAD=ABS(WLCAC)	437	
	WLOAD=SQR(WLCAD)	438	510
	SOMER=2.00*ELVC/WLOAD		
	PHEE=ATAN2(FSIN,FCOS)	440	511
	PHEE=PHEE/RADIAN	441	
	TQO=TQO/WLOAD	445	
	TQ1=TQO*EPS*FSIN/WLOAD	446	
	WRITE(6,2)REN,EPS,TQ1,TQO,SOMER,PHEE,AFLOW	447	512
	IF(IMPAS.EQ.1) GO TO 593	448	

03/04/69

WRITE(10) REN, EPS, TQI, TQO, SOMER, PHEE	449	515
GO TO 591	450	
593 WRITE(9) REN, EPS, TQI, TQO, SOMER, PHEE	451	517
591 INDS=ING3+KCIAG	452	
592 CONTINUE	453	
599 SPRITO=SPRITO+DELSI	454	
RETURN	455	
END	456	

03/04/69

CICI. - EFN SOURCE STATEMENT - IFN(S) -

SUBROUTINE CICI(MD)	2
COMMON MCIAC,CELX,CELZ,DELZS,H,MS,MG1,MG2,N,MP(17,19),A1(2,5,1	3
19),B1(2,19),CC(2,19),AF1(17,19),AF2(17,19),AF3(17,19),AF4(17,19),A	4
2F6(17,19),AF7(17,19),AF5(17,19),PHI(17,19)	5
DIMENSION A(17,17),B(17,17),C(17,17),D(17,17),F(20,17),AK(17,17),G	6
1N(17,17),S(20,17),AFJ(17),BC(17,17),BF(17),DD(17,17),DS(17),G(17,	7
217),GI(17,17),E(17,17)	8
AM=1.0/CELX	9
NC=0	10
M=MS+MG1+MG2+1	11
MN1=MG1+1	12
MN2=MN1+MS	13
DX1=AM*0.5	14
DX2=AM*2	15
203 DO 205 I=1,M	16
DO 204 II=1,M	17
E(I,II)=0.	18
204 D(I,II)=C.	19
F(I,II)=C.	20
205 D(I,II)=1.	21
DO 300 J=1,N	22
WRITE(7)((E(I,II),D(I,II),I=1,M),II=1,M)	23 23
IF(MD.EQ.2) GO TO 240	24
WRITE(6,103) AF1(1,J),AF2(1,J),AF3(1,J),AF4(1,J),AF5(1,J),AF6(1,J	25
1),AF7(1,J)	26 34
WRITE(6,103)	27
1 A1(1,1,J),A1(1,2,J),A1(1,3,J),A1(1,4,J),A1(1,5,J),B1(MN1,	28
1J),CC(MN1,J)	29 42
WRITE(6,103)	30
1 A1(2,1,J),A1(2,2,J),A1(2,3,J),A1(2,4,J),A1(2,5,J),	31
B1(MN2,J),CC(MN2,J)	32 50
240 DZ1=0.5/(CELZ)	33
DZ2=1.7/(CELZ)**2	34
241 DD242 I=1,M	35
DO 242 II=1,M	36
B(I,II)=S.	37
A(I,II)=0.	38
242 C(I,II)=C.	39
DO 250 I=1,M	40
206 IF(I-MG1=1) 212,210,212	41
209 AFJ(I)=AF7(I,J)	42
A(I,1)=1.	43
GO TO 250	44
210 IF(MS) 211,212,211	45
211 DZ1=0.5/CELZS	46
DZ2=1.7/(CELZS)**2	47
IF(NP(I,J)) 209,232,209	48
232 IF(MG1) 233,212,233	49
233 IF(NC.EQ.2) GO TO 600	50
A(I,I-2)=A1(1,1,J)	51
A(I,I-1)=A1(1,2,J)	52
A(I,I)=A1(1,3,J)	53
A(I,I+1)=A1(1,4,J)	54
A(I,I+2)=A1(1,5,J)	55
B(I,1)=B1(1,J)	56

03/04/69

C(I,1)=CC(I,J)	57
600 AFJI(I)=-AF7(I,J)	58
GO TC 25C	59
212 IF(NP(I,J))209,234,209	60
234 IF(I-MG1=MS-1) 215,213,215	61
213 IF(MS) 214,215,214	62
214 CZ1=0.5/CELZ	63
DZ2=(1./CELZ)**2	64
IF(NC.EC.2) GO TO 301	65
A(I,1-2)=A1(2,1,J)	66
A(I,1-1)=A1(2,2,J)	67
A(I,1)=A1(2,3,J)	68
A(I,1+1)=A1(2,4,J)	69
A(I,1+2)=A1(2,5,J)	70
B(I,1)=B1(2,J)	71
C(I,1)=CC(2,J)	72
601 AFJI(I)=-AF7(I,J)	73
GO TC 25C	74
215 IF(NC.EC.2) GO TO 602	75
B(I,1-1)=AF3(I,J)*CX1*CZ1	76
B(I,1)=AF5(I,J)*DX2-AF-(I,J)*DX1	77
B(I,1+1)=-AF3(I,J)*DX1*CZ1	78
A(I,1-1)=AF1(I,J)*CZ2-AF2(I,J)*CZ1	79
A(I,1)=AF6(I,J)-2.5*(AF1(I,J)*CZ2 +AF5(I,J)*DX2)	80
A(I,1+1)=AF1(I,J)*CZ2+AF2(I,J)*DZ1	81
C(I,1-1)=-AF3(I,J)*DX1*CZ1	82
C(I,1)=AF4(I,J)*CX1+AF5(I,J)*DX2	83
C(I,1+1)=AF3(I,J)*CX1*CZ1	84
602 AFJI(I)=-AF7(I,J)	85
25C CONTINUE	86
IF(NC.EC.2) GO TO 503	87
DO 260 I=1,M	88
DO 260 II=1,M	89
AK(I,II)=A(I,II)	90
DO 260 III=1,M	91
260 AK(I,II)=AK(I,II)+B(I,III)*E(III,II)	92
IF(MCIAG.LT.2) GO TO 262	93
WRITE(5,101)J	94 188
DO 261 I=1,M	95
261 WRITE(6,102) (AK(I,II),II=1,M)	96 191
262 CALL MATINV(AK,M,CUM,C,CUM1)	97 198
603 CONTINUE	98
DO 404 I=1,M	99
BF(I)=AFJI(I)	100
F(J+1,I)=0.	101
DO 404 II=1,M	102
E(I,II)=C.	103
BD(I,II)=0.	104
DO 403 III=1,M	105
E(I,II)=F(I,II)-AK(I,III)*C(III,II)	106
403 BD(I,II)=BD(I,II)+E(I,III)*C(III,II)	107
404 BF(I)=BF(I)-E(I,II)*F(J,II)	108
DO 406 I=1,M	109
DO 406 II=1,M	110
D(I,II)=0.	111
DO 405 III=1,M	112

CICI.	EFN	SOURCE STATEMENT	IFN(S)	
405		D(I,II)=C(I,II)-A*(I,III)*D(III,II)	113	
405		F(J+1,I)=F(J+1,I)+A*(I,II)*B*(II)	114	
300		CONTINUE	115	
		DO 505 I=1,M	116	
		CO 504 II=1,M	117	
504		DD(I,II)=-D(I,II)	118	
505		DD(I,II)=1.+DD(I,II)	119	
		IF(MDIAG.LT.2) GO TO 264	120	
		WRITE (6,101)	121	267
		DO 263 I=1,M	122	
263		WRITE (6,100) (D(I,II),II=1,M)	123	271
264		CALL MATINV(CC,M,DUM,C,CUM1)	124	279
		DO 507 I=1,M	125	
		S(N,I)=0.	126	
		DO 507 II=1,M	127	
		GN(I,II)=0.	128	
		DO 506 III=1,M	129	
		GN(I,II)=GN(I,II)+D(I,III)*E(III,II)	130	
506		G(I,II)=GN(I,II)	131	
507		S(N,I)=S(N,I)+D(I,II)*F(N+1,II)	132	
		J=N+1	133	
		DO 512 K=2,N	134	
		WRITE(8) ((G(I,II),I=1,M),II=1,M)	135	309
		BACKSPACE 7	136	317
		READ(7) ((E(I,II),D(I,II),I=1,M),II=1,M)	137	318
		BACKSPACE 7	138	327
		IF(MDIAG.EQ.2) WRITE(6,100) ((E(I,II),D(I,II),I=1,M),II=1,M)	139	328
		J=J-1	140	
		DO 309 I=1,M	141	
		S(J-1,I)=F(J,I)	142	
		DO 509 II=1,M	143	
		GI(I,II)=0.	144	
		DO 508 III=1,M	145	
		GI(I,II)=GI(I,II)+D(I,III)*GN(III,II)+E(III,II)*G(III,II)	146	
		IF(MDIAG.NE.2) GO TO 502	147	
508		CONTINUE	148	
509		S(J-1,I)=S(J-1,I)+E(I,II)*S(J,II)+D(I,II)*S(N,II)	149	
		DO 512 I=1,M	150	
		CO 512 II=1,M	151	
512		G(I,II)=GI(I,II)	152	
280		DO 511 I=1,M	153	
		CO 510 II=1,M	154	
510		DD(I,II)=-G(I,II)	155	
511		DD(I,II)=1.+DD(I,II)	156	
		IF(MDIAG.LT.2) GO TO 266	157	
		WRITE (6,101)	158	396
		DO 265 I=1,M	159	
265		WRITE (6,100) (D(I,II),II=1,M)	160	400
266		CALL MATINV(CC,M,DUM,C,CUM1)	161	408
		IF(MDIAG.LT.2) GO TO 270	162	
		I=0	163	
		WRITE (6,101)	164	413
		DO 273 I=1,M	165	
273		WRITE (6,100) (D(I,II),II=1,M)	166	417
270		DO 513 I=1,M	167	
		I+I(I,1)=0	168	

05704709

CIC1. - EFN SOURCE STATEMENT - IFN(S) -

DO 515 II=1,M	169	
515 PHI(I,1)=DD(I,II)*S(I,II)+PH-I(I,1)	170	
DO 516 J=2,N	171	
BACK SPACE 8	172	441
READ(8) ((G(I,II),I=1,M),II=1,M)	173	442
BACKSPACE 8	174	450
DO 516 I=1,M	175	
PHI(I,J)=S(J,I)	176	
DO 516 II=1,M	177	
516 PHI(I,J)=PHI(I,J)+G(I,II)*PH-I(II,1)	178	
REWIND 7	179	465
REWIND 8	180	466
IF (MC.EQ.2) GC TC 110	181	
IF(MDIAG.LT.2) GO TO 268	182	
110 WRITE (6,102)	183	473
DO 267 I=1,M	184	
267 WRITE (6,100) (PHI(I,J),J=1,N)	185	477
268 RETURN	186	
100 FORMAT(1X,1P10E11.4)	187	
101 FORMAT(5P0CIC1,15)	188	
102 FORMAT(1P0,30X10HPINAL PHI /1HO)	189	
103 FORMAT (1X,1P7E11.4)	190	
END	191	

03/04/69

MATN. - EFN SOURCE STATEMENT - IFA(S) -

	SUBROUTINE MATINV(A,N,B,M,DETER)	2
C	MATRIX INVERSION WITH ACCOMPANYING SOLUTION OF LINEAR EQUATIONS	3
	DIMENSION IPIVC(17),A(17,17),B(17,1),INDEX(17,2),PIVOT(17)	4
	EQUIVALENCE (IROW,JROW), (ICCLU ,JCOLU), (AMAX, T, SWAP)	5
C	INITIALIZATION	6
C		7
	10 DETER =1.0	8
	15 DO 20 J=1,N	9
	20 IPIVC (J)=0	10
	30 DO 550 I=1,N	11
C		12
C	SEARCH FOR PIVOT ELEMENT	13
C		14
	40 AMAX=0.0	15
	45 DO 105 J=1,N	16
	50 IF (IPIVC (J)-1) 60, 105, 60	17
	60 DO 100 K=1,N	18
	70 IF (IPIVC (K)-1) 80, 100, 740	19
	80 IF (ABS (AMAX)-ABS (A(J,K))) 85, 100, 100	20
	85 IROW=J	21
	90 ICOLU =K	22
	95 AMAX=A(J,K)	23
	100 CONTINUE	24
	105 CONTINUE	25
	110 IPIVC (ICOLU)=IPIVC (ICOLU)+1	26
C		27
C	INTERCHANGE ROWS TO PUT PIVOT ELEMENT ON DIAGONAL	28
C		29
	130 IF (IROW-ICOLU) 140, 260, 140	30
	140 DETER =-DETER	31
	150 DO 200 L=1,N	32
	160 SWAP=A(IROW,L)	33
	170 A(IROW,L)=A(ICCLU ,L)	34
	200 A(ICCLU ,L)=SWAP	35
	205 IF(M) 260, 260, 210	36
	210 DO 250 L=1, M	37
	220 SWAP=B(IROW,L)	38
	230 B(IROW,L)=B(ICCLU ,L)	39
	250 B(ICCLU ,L)=SWAP	40
	260 INDEX(I,1)=IROW	41
	270 INDEX(I,2)=ICCLU	42
	310 PIVOT(I)=A(ICCLU ,ICOLU)	43
	320 DETER =DETER *PIVOT(I)	44
C		45
C	DIVIDE PIVOT ROW BY PIVOT ELEMENT	46
C		47
	330 A(ICCLU ,ICOLU)=1.0	48
	340 DO 350 L=1,N	49
	350 A(ICCLU ,L)=A(ICOLU ,L)/PIVOT(I)	50
	355 IF(M) 380, 380, 360	51
	360 DO 370 L=1,M	52
	370 B(ICCLU ,L)=B(ICOLU ,L)/PIVOT(I)	53
C		54
C	REDUCE NON-PIVOT ROWS	55
C		56

MATN.	- EFN	SOURCE STATEMENT	- IFN(S)
390	DO	550 L1=1,N	57
390	IF	(L1-ICCLU) 400, 550, 400	58
400	T=A	(L1,ICLU)	59
420	A	(L1,ICLU)=0.0	60
430	DO	450 L=1,N	61
450	A	(L1,L)=A(L1,L)-A(ICLU ,L)*T	62
455	IF	(M) 550, 550, 460	63
460	DO	500 L=1,M	64
500	B	(L1,L)=B(L1,L)-B(ICLU ,L)*T	65
550	CONTINUE		66
C			67
C	INTERCHANGE	COLUMNS	68
C			69
600	DO	710 I=1,N	70
610	L=N+1-I		71
620	IF	(INDEX(L,1)-INDEX(L,2)) 630, 710, 630	72
630	JROW=INDEX	(L,1)	73
640	JCOLU =INDEX	(L,2)	74
650	DO	705 K=1,N	75
660	SWAP=A	(K,JROW)	76
670	A	(K,JROW)=A(K,JCOLU)	77
700	A	(K,JCOLU)=SWAP	78
705	CONTINUE		79
710	CONTINUE		80
740	RETURN		81
	END		82

03/04/69

GTCF. - FFA SOURCE STATEMENT - IFRIS: -

FUNCTION GTCF(REYN)	2	
RE=REYN	3	
IF(RE.LE.70.0)GO TO 20	4	
IF((RE.GT.70.0).AND.(RE.LE.2000.0)) GO TO 30	5	
10 IF((RE.GT.2000.0).AND.(RE.LE.5.5E+03))GO TO 40	6	
IF((RE.GT.5500.0).AND.(RE.LE.2.0E+04)) GO TO 50	7	
GTCF=20.5/(RE)**0.784	8	14
RETURN	9	
20 GTCF=1.0/12.0	10	
RETURN	11	
30 GTCF=.619E-08*(RE)**2-3.465E-05*RE+.08565	12	
RETURN	13	
40 GTCF=4.90/(RE)**.628	14	18
RETURN	15	
50 GTCF=10.35/(RE)**.716	16	20
RETURN	17	
END	18	

GZCF. - EFN SOURCE STATEMENT - (FN(S) -

03/04/69

FUNCTION GZCF(REYN)	2	
RE=REYN	3	
IF(RE.LE.70.0)GO TO 20	4	
IF((RE.GT.70.0).AND.(RE.LE.4000.0))GO TO 30	5	
10 IF((RE.GT.4000.0).AND.(RE.LE.7.0E+03)) GO TO 40	6	
IF((RE.GT.7000.0).AND.(RE.LE.2.0E+04)) GO TO 50	7	
GZCF=25.6/(RE)**.756	8	14
RETURN	9	
20 GZCF=1.0/12.0	10	
RETURN	11	
30 GZCF=1.858 E-09*(RE)**2-1.876E-05*RE+.0846	12	
RETURN	13	
40 GZCF=9.62/(RE)**.652	14	18
RETURN	15	
50 GZCF=11.3/(RE)**.674	16	20
RETURN	17	
END	18	

03/04/69

SUM. - EFN SOURCE STATEMENT - IFN(S) -

FUNCTION SUM(F,M,DX)	2
DIMENSION P(17)	3
K=2	4
KK=M-1	5
KKK=2	6
SUM=0.0	7
10 DO 20 I=K, KK, KKK	8
20 SUM=SUM+P(I)	9
GO TC (30,40,50),K	10
30 SUM=SUM*CX/3.C	11
RETURN	12
40 K=3	13
45 SUM=SUM*2.0	14
GO TC 10	15
50 K=1	16
KK=M	17
KKK=M-1	18
GO TC 45	19
END	20

03/04/66

TCC.	- EFN	SOURCE STATEMENT	- IFN(S)	-
		FUNCTION TCC(RE)		2
		IF(RE.GT.100.0) GO TO 10		3
		TCC=.8/RE		4
		GO TC 100		5
10		IF(RE.GT.400.0) GO TO 20		6
		TCC=.175/(RE)**.86		7
		GO TC 100		8
20		IF(RE.GT.1000.0) GO TO 30		9
		TCC=.547/(RE)**.521		10
		GO TC 100		11
30		IF(RE.GT.4000.0) GO TC 40		12
		TCC=.342/(RE)**.453		13
		GO TC 100		14
40		TCC=.064/(RE)**.25		15
100		RETURN		16
		END		17

FLICATING-RING WITH HERRINGBONE JOURNAL
DATA PROGRAM INPUT

* INPUT

INPRC =	0.				
NEPR =	3.				
NCASE =	1.				
NH =	10.				
R2R1 =	0.1200000E 01.				
ANTY =	C.2500000E-00.				
DN =	C.0999999E-00.				
REY =	C.0999999E 02.				
EP15 =	C.2000000E-00.	0.3000000E-00.	0.5000000E 00.	-0.0000000E-19.	-0.0000000E-19.
	-C.0000000E-19.	-0.0000000E-19.	-0.0000000E-19.	-0.0000000E-19.	-0.0000000E-19.
COM1 =	C.9999999E-03.				
COM2 =	C.9999999E-03.				
PRE3 =	C.	0.4199999E 01.	-0.		

* END
HERRINGBONE BEARING INPUT

* INPUT

RIRSP =	C.2500000E-00.		
DELSP =	C.0999999E-00.		
BLDVC =	C.0999999E 01.		
I1 =	3.		
I2 =	7.		
N9 =	12.		
EP31 =	C.2000000E-00.	0.3000000E-00.	0.5000000E 00.
BETA =	C.1490000E 03.	0.3059999E 02.	0.0999999E 01.
DEP =	0.	0.1399999E 01.	0.
ALPHA =	-0.	0.9500000E 00.	0.
EP32 =	0.5000000E 00.	0.5999999E 00.	0.0000000E 00.

* END

INNER FILM DATA

REYNCLDS	NO.	ECCENTRICITY	INNER TORQUE	OUTER TORQUE	SOMMERFELD	NO	ATT.	ANGLE	FLOW
0.5500000E	01	0.2000000E-00	-0.1273566E	02-0.1265375E	02	0.2129888E	01	0.3618759E	02-0.7218548E 01
0.5500000E	01	0.3000000E-00	-0.8305493E	01-0.8483987E	01	0.1369939E	01	0.3651181E	02-0.7565410E 01
0.5500000E	01	0.5000000E-00	-0.4678258E	01-0.4985645E	01	0.7334086E	00	0.3793541E	02-0.8679913E 01
0.6500000E	01	0.2000000E-00	-0.1537007E	02-0.1548261E	02	0.1993225E	01	0.3424303E	02-0.6979188E 01
0.6500000E	01	0.3000000E-00	-0.1001766E	02-0.1018751E	02	0.1279345E	01	0.3448471E	02-0.7299742E 01
0.6500000E	01	0.5000000E-00	-0.5635432E	01-0.5920835E	01	0.6808451E	00	0.3564804E	02-0.8330470E 01
0.7500000E	01	0.2000000E-00	-0.1795031E	02-0.1825662E	02	0.1847429E	01	0.3211124E	02-0.6772657E 01
0.7500000E	01	0.3000000E-00	-0.1168741E	02-0.1184764E	02	0.1183250E	01	0.3228307E	02-0.7066473E 01
0.7500000E	01	0.5000000E-00	-0.6565635E	01-0.6839612E	01	0.6259599E	00	0.3322680E	02-0.8012116E 01

OUTER FILM DATA

REYNCLDS	NO.	ECCENTRICITY	INNER TORQUE	OUTER TORQUE	SOMMERFELD	NO	ATT.	ANGLE	FLOW
0.3600000E	01	0.5000000E-00	-0.6054526E	01-0.6116465E	01	0.3480382E-00	00	0.938564E	01-0.2802687E 02
0.3600000E	01	0.6000000E-00	-0.5024480E	01-0.5134692E	01	0.2722008E-00	00	0.1058461E	02-0.3048566E 02
0.3600000E	01	0.8000000E-00	-0.4138659E	01-0.4349845E	01	0.1781508E-00	00	0.1530646E	02-0.3678925E 02
0.5040000E	01	0.5000000E-00	-0.7135547E	01-0.7250334E	01	0.4060655E-00	00	0.1280149E	02-0.2057270E 02
0.5040000E	01	0.6000000E-00	-0.5880299E	01-0.6025070E	01	0.3147292E-00	00	0.1396234E	02-0.2231984E 02
0.5040000E	01	0.8000000E-00	-0.4703731E	01-0.4960753E	01	0.2008538E-00	00	0.1874024E	02-0.2681073E 02
0.6480000E	01	0.5000000E-00	-0.7911438E	01-0.8042833E	01	0.4465474E-00	00	0.1523563E	02-0.1643149E 02
0.6480000E	01	0.6000000E-00	-0.6468842E	01-0.6637570E	01	0.3439290E-00	00	0.1633265E	02-0.1778327E 02
0.6480000E	01	0.8000000E-00	-0.5074263E	01-0.5361702E	01	0.2157208E-00	00	0.2104944E	02-0.2126711E 02

OUTPUT

ECCENTR/C1	N2/N1	C2/C1	R2/R1	REYNCLDS	NO	ECCENTRIC	TORQUE	SUPPLY PRES	SOMMFD	NO	ATT.	ANGLE	TANG.	FORCE
0.6001E	00	0.3941E-00	0.1200E 01	0.1200E	01									
INNER RING	0.6359E	01	0.2000E-00	-0.1427E	02	0.3012E	01	0.2055E	01	0.3512E	02	0.2800E-00		
OUTER RING	0.5076E	01	0.3411E-00	-0.1201E	02	0.1066E	02	0.6970E	00	0.1390E	02	0.5694E 00		
OVERALL	0.1000E	02	0.2728E-00	-0.1421E	02	0.4200E	01	0.1474E	01	0.2083E	02			

OUTPUT

ECCENTR/C1	N2/N1	C2/C1	R2/R1	REYNCLDS	NO	ECCENTRIC	TORQUE	SUPPLY PRES	SOMMFD	NO	ATT.	ANGLE	TANG.	FORCE
0.8641E	00	0.3947E-00	0.1200E 01	0.1200E	01									
INNER RING	0.6053E	01	0.3000E-00	-0.9344E	01	0.3011E	01	0.1321E	01	0.3541E	02	0.4388E-00		
OUTER RING	0.5684E	01	0.4817E-00	-0.7517E	01	0.1064E	02	0.4485E-00	00	0.1389E	02	0.5425E 00		
OVERALL	0.1000E	02	0.3928E-00	-0.9257E	01	0.4000E	01	0.9468E	00	0.2121E	02			

OUTPUT

ECCENTR/C1	N2/N1	C2/C1	R2/R1	REYNCLDS	NO	ECCENTRIC	TORQUE	SUPPLY PRES	SOMMFD	NO	ATT.	ANGLE	TANG.	FORCE
0.1404E	01	0.3597E-00	0.1200E 01	0.1200E	01									
INNER RING	0.6403E	01	0.5000E-00	-0.5694E	01	0.3065E	01	0.6661E	00	0.3588E	02	0.8542E 00		
OUTER RING	0.5180E	01	0.7664E-00	-0.4987E	01	0.1168E	02	0.2178E-00	00	0.1798E	02	0.1432E 01		
OVERALL	0.1000E	02	0.6362E-00	-0.5548E	01	0.4200E	01	0.5046E	00	0.2426E	02			

REFERENCES

1. Vohr, J.H. and Chow, C.Y., "Characteristics of Herringbone-Grooved, Gas-Lubricated Journal Bearings," Trans. of ASME, Journal of Basic Engineering, Vol. 87, Series D, Number 3, (64-Lub-15), September, 1965.
2. Hirs, G.G., "Load Capacity and Stability Characteristics of Hydrodynamic Grooved Journal Bearings," Transactions of the American Society of Lubrication Engineers, Vol. 8, No. 3, July 1965.
3. Malanoski, S.B., "Experiments on an Ultrastable Gas Journal Bearing," Trans. of the ASME, Journal of Lubrication Technology, Vol. 89, Series F, No. 4, October, 1967.
4. Ng, Chung-Wah and Pan, C.H.T., "A Linearized Turbulent Lubrication Theory," Trans. of the ASME, Journal of Basic Engineering, Vol. 87, Series D, No. 3 (64-Lub-29), September, 1965.
5. Elrod, H.G., and Ng, C.W., "A Theory for Turbulent Fluid Films and Its Application to Bearings," Trans. of the ASME, Journal of Lubrication Technology Vol. 89, Series F, No. 3, (66-Lub-12), July, 1967.
6. Castelli, V. and Shapiro, W., "Improved Method for Numerical Solutions of the General Incompressible Fluid Film Lubrication Problem," Trans. of the ASME, Journal of Lubrication Technology, Vol. 89, Series F, No. 2, (66-Lub-14), April, 1967.
7. Castelli, V. and Pirvics, J., "Equilibrium Characteristics of Axial-Groove Gas-Lubricated Bearings," Trans. of the ASME, Journal of Lubrication Technology, Vol. 89, Series F, No. 2, (65-Lub-16), April, 1967.
8. Smalley, A.J., Lloyd, T., Horsnell, R. and McCallion, H., "Steadily Loaded Journal Bearings - A Comparison of Performance Predictions," Proc. Lubrication and Wear Convention, Instn. Mech. Engrs, London, May, 1966.
9. Lund, J.W., "Rotor-Bearing Dynamics Design Technology - Part V: Computer Program Manual for Rotor Response and Stability," Technical Report AFAPL-TR-65-45, Part V, Air Force Aero Propulsion Laboratory, Research and Technology Division, Air Force Systems Command, Wright-Patterson Air Force Base, Ohio.
10. IBM 7090/7094 IBSYS Operating System Version 13, Fortran IV Language, IBM System Reference Library.

UNCLASSIFIED

Security Classification

DOCUMENT CONTROL DATA - R & D		
<i>(Security classification of title, body of abstract and indexing annotation must be entered when the overall report is classified)</i>		
1. ORIGINATING ACTIVITY (Corporate author) Mechanical Technology Incorporated 968 Albany Shaker Road ✓ Latham, New York 12110		2a. REPORT SECURITY CLASSIFICATION UNCLASSIFIED
		2b. GROUP N/A
3. REPORT TITLE Rotor-Bearing Dynamics Design Technology PART VIII: Spiral Grooved Floating Ring Journal Bearing		
4. DESCRIPTIVE NOTES (Type of report and inclusive dates) Final Report for Period 1 May 1967 to 1 May 1968.		
5. AUTHOR(S) (First name, middle initial, last name) J. H. Vohr & C. Y. Chow		
6. REPORT DATE September 1968	7a. TOTAL NO. OF PAGES 181	7b. NO. OF REFS 10
8a. CONTRACT OR GRANT NO. ✓ AF33 (615)-3238	8b. ORIGINATOR'S REPORT NUMBER(S) MTI-68TR16 - <i>PC-6</i>	
8c. PROJECT NO. 3048		
8d. Task Nr: 304806	9b. OTHER REPORT NO(S) (Any other numbers that may be assigned this report) <i>PC-7</i> AFAPL-TR-65-45, PART VIII	
10. DISTRIBUTION STATEMENT This document is subject to special export controls and each transmittal to foreign governments or foreign nationals may be made only with prior approval of the Air Force Aero Propulsion Laboratory.		
11. SUPPLEMENTARY NOTES None	12. SPONSORING MILITARY ACTIVITY Air Force Aero Propulsion Laboratory Wright-Patterson AFB, Ohio 45433	
13. ABSTRACT In this volume is presented an analysis of the static and dynamic characteristics of the spiral-grooved journal bearing operating with incompressible lubricant in both laminar and turbulent regimes. Both single film and floating ring bearing configurations are considered. Extensive design data are presented giving load capacity, attitude angle, bearing torque, bearing flow rate, stiffness and damping coefficients and critical rotor mass for limit of stable operation. In addition, two computer programs accompany the volume, and instructions and listings of the programs are included. These programs may be used to obtain data for cases not covered by the presented design data.		

DD FORM 1 NOV 68 1473

UNCLASSIFIED

Security Classification

UNCLASSIFIED

Security Classification

14. KEY WORDS	LINK A		LINK B		LINK C	
	ROLE	WT	ROLE	WT	ROLE	WT
Bearings						
Lubrication						
Floating Ring						
Fluid Film						
Hydrodynamic						
Hydrostatic						
Rotor-Bearing Dynamics						
Stability						
Critical Speed						

UNCLASSIFIED

Security Classification